

2

**REPAIR, EVALUATION, MAINTENANCE, AND
REHABILITATION RESEARCH PROGRAM**

AD-A234 566

TECHNICAL REPORT REMR-GT-15

**PLASTIC CONCRETE CUTOFF WALLS
FOR EARTH DAMS**

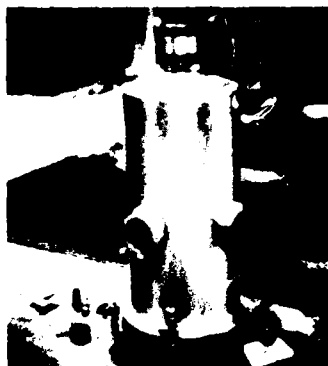
by

Thomas W. Kahl, Joseph L. Kauschinger, Edward B. Perry

Geotechnical Laboratory

DEPARTMENT OF THE ARMY

Waterways Experiment Station, Corps of Engineers
3909 Halls Ferry Road, Vicksburg, Mississippi 39180-6199



DTIC
SELECTE
APR 30 1991
S **D**
C



March 1991

Final Report

Approved For Public Release; Distribution Unlimited

DTIC FILE COPY

Prepared for DEPARTMENT OF THE ARMY
US Army Corps of Engineers
Washington, DC 20314-1000

91 4 29 009

The following two letters used as part of the number designating technical reports of research published under the Repair, Evaluation, Maintenance, and Rehabilitation (REMR) Research Program identify the problem area under which the report was prepared:

<u>Problem Area</u>		<u>Problem Area</u>	
CS	Concrete and Steel Structures	EM	Electrical and Mechanical
GT	Geotechnical	EI	Environmental Impacts
HY	Hydraulics	OM	Operations Management
CO	Coastal		

Destroy this report when no longer needed. Do not return it to the originator.

The findings in this report are not to be construed as an official Department of the Army position unless so designated by other authorized documents.

The contents of this report are not to be used for advertising, publication, or promotional purposes. Citation of trade names does not constitute an official endorsement or approval of the use of such commercial products.

COVER PHOTOS:

TOP — Placing plastic concrete in triaxial mold.

MIDDLE — Plastic concrete test specimen.

BOTTOM — Triaxial compression test chamber.

REPORT DOCUMENTATION PAGE			Form Approved OMB No. 0704-0188	
Public reporting burden for this collection of information is estimated to average 1 hour per response, including the time for reviewing instructions, searching existing data sources, gathering and maintaining the data needed, and completing and reviewing the collection of information. Send comments regarding this burden estimate or any other aspect of this collection of information, including suggestions for reducing this burden, to Washington Headquarters Services, Directorate for Information Operations and Reports, 1215 Jefferson Davis Highway, Suite 1204, Arlington, VA 22202-4302, and to the Office of Management and Budget, Paperwork Reduction Project (0704-0188), Washington, DC 20503.				
1. AGENCY USE ONLY (Leave blank)	2. REPORT DATE March 1991	3. REPORT TYPE AND DATES COVERED Final report		
4. TITLE AND SUBTITLE Plastic Concrete Cutoff Walls for Earth Dams			5. FUNDING NUMBERS WU 32310	
6. AUTHOR(S) Thomas W. Kahl Joseph L. Kauschinger Edward B. Perry			8. PERFORMING ORGANIZATION REPORT NUMBER Technical Report REMR-GT-15	
7. PERFORMING ORGANIZATION NAME(S) AND ADDRESS(ES) US Army Engineer Waterways Experiment Station Geotechnical Laboratory 3909 Halls Ferry Road, Vicksburg, MS 39180-6199			10. SPONSORING/MONITORING AGENCY REPORT NUMBER	
9. SPONSORING/MONITORING AGENCY NAME(S) AND ADDRESS(ES) US Army Corps of Engineers, Washington, DC 20314-1000			10. SPONSORING/MONITORING AGENCY REPORT NUMBER	
11. SUPPLEMENTARY NOTES A report of the Geotechnical problem area of the Repair, Evaluation, Maintenance, and Rehabilitation (REMR) Research Program. Available from National Technical Information Service, 5285 Port Royal Road, Springfield, VA 22161.				
12a. DISTRIBUTION/AVAILABILITY STATEMENT Approved for Public Release, Distribution Unlimited			12b. DISTRIBUTION CODE	
13. ABSTRACT (Maximum 200 words) Remedial seepage control of earth dams is a critical problem. A concrete cutoff wall may be used as a remedial measure in some situations. Since the wall in its simplest structural form is a rigid diaphragm, deformations of earth embankment due to increase in reservoir level or seismic activity could cause its rupture which would greatly decrease the flow efficiency of the cutoff wall and jeopardize the safety of the dam. In response to this dilemma, engineers in Europe, Asia, and South America have used plastic concrete, which has deformation characteristics similar to the earth dam, to construct cutoff walls. Plastic concrete consists of aggregate, cement, water, and bentonite clay mixed at a high water-cement ratio to produce a ductile material. Geotechnical engineers in the United States have been reluctant to specify the use of plastic concrete <p style="text-align: right;">(Continued)</p>				
14. SUBJECT TERMS Cutoff wall Ductile behavior Plastic concrete Diaphragm wall Earth dam Remedial seepage control			15. NUMBER OF PAGES 186	
17. SECURITY CLASSIFICATION OF REPORT Unclassified			16. PRICE CODE	
18. SECURITY CLASSIFICATION OF THIS PAGE Unclassified	19. SECURITY CLASSIFICATION OF ABSTRACT Unclassified	20. LIMITATION OF ABSTRACT		

13. (Concluded).

for cutoff walls due to limited documentation of field performance of existing cutoff walls and lack of laboratory test data on plastic concrete under test conditions which approximate field behavior.

This research was conducted to quantify the stress-strain-strength behavior and permeability of plastic concrete, and to develop design data for specifying plastic concrete for use in a diaphragm cutoff wall for an earth dam. The results of this research indicate that the addition of bentonite clay to conventional concrete significantly increases the ductility and plastic deformation of the concrete while simultaneously reducing its shear strength. The permeability of plastic concrete was found to be the same or less than conventional concrete, and it decreased significantly with consolidation. A design method is given for determining the mix design of a plastic concrete cutoff wall based upon the unconfined compressive strength and/or modulus of the embankment soil.

PREFACE

The work described in this report was authorized by Headquarters, US Army Corps of Engineers (HQUSACE), as part of the Geotechnical (Soil) Problem Area of the Repair, Evaluation, Maintenance, and Rehabilitation (REMR) Research Program from October 1987 to November 1989. The work was performed under Work Unit 32310, "Remedial Cutoff and Control Methods for Adverse Seepage Conditions in Embankment Dams and Soil Foundations," for which Dr. Edward P. Perry was the Principal Investigator. Mr. Arthur H. Walz, HQUSACE, was the REMR Technical Monitor for this work.

Mr. Jesse A. Pfeiffer, Jr. (CERD-C) was the REMR Coordinator at the Directorate of Research and Development, HQUSACE; Mr. James E. Crews (CECW-OM) and Dr. Tony C. Liu (CECW-EG) served as the REMR Overview Committee; Mr. William F. McCleese (CEWES-SC-A), US Army Engineer Waterways Experiment Station (WES) was the REMR Program Manager. Mr. Gene P. Hale, Soil and Rock Mechanics Division (S&RMD), Geotechnical Laboratory (GL), was the Problem Area Leader.

This report was prepared by Mr. Thomas W. Kahl, former graduate student at Tufts University working as a contract student to WES, and presently with GEI Consultants, Inc., Winchester, MA; Dr. Joseph L. Kauschinger, former Assistant Professor of Civil Engineering at Tufts University working under the Intergovernment Personnel Act to WES, and presently Technical Director, Ground Engineering Services, Hooksett, NH; and Dr. Perry, S&RMD, WES. General supervision was provided by Dr. Don C. Banks, Chief, S&RMD, and Dr. William F. Marcuson III, Chief, GL. Senior technical reviewer of this report was Dr. Paul F. Hadala, Assistant Chief, GL. Ms. Odell F. Allen, Visual Production Center, Information Technology Laboratory, edited the report.

COL Larry B. Fulton, EN, was Commander and Director of WES during the preparation and publication of this report. Dr. Robert W. Whalin was Technical Director.



Accession For	
NTIS GRA&I	<input checked="" type="checkbox"/>
DTIC TAB	<input type="checkbox"/>
Unannounced	<input type="checkbox"/>
Justification	
By	
Distribution/	
Availability Codes	
Avail and/or	
Dist	Special
A-1	

CONTENTS

	<u>Page</u>
PREFACE.....	1
CONVERSION FACTORS, NON-SI TO SI (METRIC)	
UNITS OF MEASUREMENT.....	4
PART I: INTRODUCTION.....	5
Purpose.....	5
Scope of Work.....	6
PART II: LITERATURE REVIEW.....	10
General Observations of Recent Plastic Concrete Research.....	10
Major Plastic Concrete Research Programs.....	13
Plastic Concrete Cutoff Wall Field Case Studies.....	17
PART III: LABORATORY TESTING TECHNIQUE.....	24
Materials.....	24
General Concrete Fabrication Procedure.....	25
Unconfined Compression Test Procedure.....	31
Brazilian Splitting Tensile Test Procedure.....	41
Flexural Beam Test Procedure.....	42
Erodability Test Procedure.....	43
Triaxial Testing Equipment.....	46
Q Test Procedure.....	53
CIUC Test Sample Setup and Consolidation Procedure.....	55
Permeability Test Procedure.....	62
CIUC Shear Test.....	66
PART IV: UNCONFINED TEST RESULTS.....	67
Unconfined Compression Test Data Analysis.....	67
Results of Unconfined Compression Test Series.....	70
Error Analysis of Unconfined Compression Tests.....	73
Conclusions from Unconfined Compression Tests.....	74
Results of Other Unconfined Tests.....	75
PART V: TRIAXIAL AND PERMEABILITY TEST RESULTS.....	78
Results of CIUC Tests.....	79
Results of Unconsolidated Undrained Compression Tests.....	81
Results of Permeability Tests.....	83
PART VI: ANALYSIS AND DISCUSSION.....	85
Relationship of Unconfined Compressive Strength and Splitting Tensile Strength to Cement Factor and Water-Cement Ratio.....	85
Relationship of Elastic Modulus and Strain at Failure to Unconfined Compressive Strength.....	91
Relationship Between Unconfined Compressive Strength and Splitting Tensile Strength.....	92
Effect of Curing Age and Bentonite Content on Unconfined Compressive Strength.....	93
Effect of Consolidation on Cement Factor and Water-Cement Ratio.....	95

	<u>Page</u>
Effect of Bentonite Content on Pore Pressure Generation and Stress Path.....	96
Relationship Between Triaxial Stress-Strain-Strength Behavior and Unconfined Stress-Strain-Strength Behavior.....	103
Comparison of a CIUC Test and a Q Test Having the Same Cement Factor, Bentonite Content, and Water-Cement Ratio Tested at the Same Age.....	107
Influence of Bentonite Content, Confining Stress, Consolidation, and Age on Triaxial Stress-Strain-Strength Behavior of Plastic Concrete.....	108
Permeability of Plastic Concrete.....	113
PART VII: SUMMARY AND RECOMMENDATIONS.....	115
Summary.....	115
Recommendations.....	116
REFERENCES.....	118
APPENDIX A: DETAILED TEST DATA FROM COLBUN MAIN DAM LABORATORY PROGRAM AND MUD MOUNTAIN DAM LABORATORY PROGRAM.....	A1
APPENDIX B: CHEMICAL ANALYSIS OF CEMENT AND BENTONITE FINE AND COARSE AGGREGATE GRAIN SIZE DISTRIBUTION AND BATCH DESIGN EXAMPLE.....	B1
APPENDIX C: CALIBRATIONS OF RIEHLE TESTING MACHINE AND 1,000 LB BEAM BALANCE SCALE.....	C1
APPENDIX D: SUMMARY TABLES OF UNCONFINED COMPRESSION TESTS (PHASES I AND II), BRAZILIAN TENSILE TESTS (PHASES I AND II), AND FLEXURAL BEAM TESTS.....	D1
APPENDIX E: PHASE II CIUC, Q, AND UC STRESS-STRAIN CURVES BY BATCH.....	E1
APPENDIX F: SUMMARY TABLES OF PERMEABILITY TESTS.....	F1

CONVERSION FACTORS, NON-SI TO SI (METRIC)
UNITS OF MEASUREMENT

Non-SI units of measurement used in this report can be converted to SI (metric) units as follows:

<u>Multiply</u>	<u>By</u>	<u>To Obtain</u>
cubic feet	0.02831685	cubic metres
cubic yards	0.7645549	cubic metres
Fahrenheit degrees	5/9	Celsius degrees or Kelvins*
feet	0.3048	Metres
gallons (US dry)	0.004404884	cubic decimetres
gallons (US liquid)	3.785412	cubic decimetres
inches	2.54	centimetres
kips (force) per square inch	6.894757	megapascals
pounds (force) per square inch	6.894757	kilopascals
pounds (mass)	0.4535924	kilograms
pounds (mass) per cubic foot	16.01846	kilograms per cubic metres
pounds (mass) per cubic yard	0.5932764	kilograms per cubic metres
square inches	6.4515999	square centimetres

* To obtain Celsius (C) temperature readings from Fahrenheit (F) readings, use the following formula: $C = (5/9)(F - 32)$. To obtain Kelvin (K) readings, use $K = (5/9)(F - 32) + 273.15$.

PLASTIC CONCRETE CUTOFF WALLS FOR EARTH DAMS

PART I: INTRODUCTION

Purpose

1. This research program was to evaluate the mechanical properties of plastic concrete for use as a remedial diaphragm cutoff wall material in earth dams to control seepage. Many of the earth dams in the United States were constructed during the Depression Era of the 1930's and immediately after World War II. Today, many of these dams are over 50 years old, and a few have severe leakage problems due to the erosion of core material. The potential catastrophic failure of one of these dams due to piping creates a need for effective and practical remedial seepage control solutions. One solution is to install a deep, relatively thin concrete diaphragm wall along the axis of an earth dam using the slurry trench method. This type of cutoff is usually quite effective in controlling seepage. Examples of this type have been done at Clemson Lower Diversion Dam, Mud Mountain Dam, Navajo Dam, and Fontenelle Dam. Problems can arise, however, when conventional concrete is used as a cutoff trench backfill material because of its inherent brittleness. Deformations of earth embankments due to fluctuations in impounded reservoir levels or seismic activity can cause concrete cutoffs to develop cracks. New leakage problems may then develop through these cracks, producing an inefficient cutoff.

2. In response to this dilemma, engineers in Europe, Asia, and South America have used plastic concrete to construct cutoff walls which have deformation characteristics similar to dam embankment soils. Plastic concrete consists of aggregate, cement, water, and bentonite clay mixed at high water-cement ratios to produce a material more ductile than conventional structural concrete. Geotechnical engineers in the United States, however, have been reluctant to specify the use of plastic concrete for cutoff walls due to the limited and/or poorly documented field performance data for plastic concrete cutoffs. Thus, this research was conducted to quantify factors which influence the stress-strain-strength behavior and permeability of plastic concrete, and to develop design data for specifying plastic concrete.

Scope of Work

3. This research program was conducted in two phases. Phase I consisted of evaluating the unconfined compression, tensile, and flexural behavior of plastic concrete as a function of cement and bentonite content versus age. The data was used to supplement and replicate previous testing done by the North Pacific Division of the US Army Corps of Engineers (NPDEN) and to provide a data base for selection of mix designs for Phase II triaxial testing. In addition, the data from the unconfined compression tests were used to develop a design procedure for relating cement factor and water-cement ratio to compressive strength and Young's modulus.

4. All the mix designs tested in this research program were proportioned to produce 8-in.* slump concrete, as required for tremie placement in a slurry trench. In addition, the recommended tremie concrete fine/coarse aggregate ratio (by weight) of approximately one was used for all batches (Tamaro 1988). For ease of comparison with NPDEN data, the following batch design parameters were adopted to quantify all mix constituents (see paragraph 46 for definitions of these parameters):

- a. Cement factor equals pounds of cement plus bentonite per cubic yard of plastic concrete.
- b. Percent bentonite equals percentage of cement factor, by weight, which is bentonite.
- c. Water-cement ratio is the ratio of water to cement plus bentonite, by weight.

5. Given these parameters, the required weights of the fine and coarse aggregate per cubic yard of concrete can be back calculated by volume. This method has the advantage of describing the mix design of a given batch with only three parameters, eliminating the need to include all batch constituents in the analysis.

6. The scope of Phase I tests was as follows:

- 251 unconfined compression (UC) test
cement factors 230 to 450 lb/cu yd
bentonite contents of 0, 10, 20, 40, and 60 percent
ages of 3 to 660 days
- 45 splitting tensile (Brazilian) tests
cement factors 240 to 360 lb/cu yd

* A table of factors for converting non-SI units of measurement to SI (metric) units is presented on page 4.

bentonite contents of 0, 20, and 60 percent
ages of 3 to 90 days

6 flexural beam tests

2 erodability tests (high velocity pinhole type)

7. Phase II was conducted to examine the influence of consolidation and horizontal confinement on the stress-strain characteristics, strength behavior, and permeability of plastic concrete to simulate the stress and drainage conditions plastic concrete would be subjected to at the bottom of a tremie placement in a deep trench. Plastic concrete cutoff walls for remedial seepage control are constructed in panels through the embankment (and foundation if required) and keyed into an aquiclude. During excavation, the panel is filled with a bentonite slurry which penetrates the adjacent soil and forms a filter cake on the sides of the excavation ($k_{\text{filter cake}} = 10^{-7}$ to 10^{-9} cm/sec depending on the depth within the cutoff trench and the thickness of the filter cake (EM 1110-2-1901, Figure 9-9)). At the completion of the excavation, plastic concrete with a 8-in. slump is tremied into the excavation, from the bottom upward, displacing the bentonite slurry to form the panel. As the surface of the tremie plastic concrete rises, it may remove the filter cake from the sides of the excavation. However, the relatively low permeability of the adjacent soil, which was penetrated with bentonite slurry, will prevent the free (unabsorbed) water in the plastic concrete panel from draining laterally. The water will be free to migrate upward through the plastic concrete. The plastic concrete begins to set as soon as it is placed in the excavation with stiffening occurring from the bottom of the panel upward. The set of the panel will occur within a few hours, generally less than 1 day (retarding admixtures can be used to prolong the set). Consolidation of the plastic concrete panel under the vertical stress imposed by the weight of the overlying plastic concrete (some of this stress will be taken by arching if the sides of the excavation move laterally) will be completed in a matter of days, the exact time depending on the depth of the plastic concrete cutoff wall. After consolidation, the permeability of the plastic concrete will be $k_{\text{plastic concrete}} = 10^{-8}$ to 10^{-9} cm/sec (measured in this study). The plastic concrete will continue to cure and gain strength following consolidation. Due to the low permeability of the plastic concrete, very little migration of water will occur within the plastic concrete cutoff wall after consolidation.

8. The laboratory stress-strain characteristics and strength behavior, permeability, and erodability should be obtained under test conditions which approximate, as closely as possible, those which exist in the field. It was not feasible (for this study) to form, consolidate, and test tensile strength samples (Brazilian and Flexural Beam Test) and erodability samples (pinhole type test) under conditions which would duplicate those existing in the field. However, for permeability and compressive strength testing, this was feasible, and plastic concrete specimens were formed in the triaxial chamber after mixing, isotropically consolidated in the triaxial chamber with vertical drainage, and cured in the triaxial chamber under effective confining pressures typical for existing cutoff walls (50 to 300 psi). Permeability tests were conducted in the triaxial device during the curing phase (once gas generation within the sample had ceased). Following the permeability test, the pore water pressure in the sample was given time to equalize, and the sample was sheared under undrained conditions. In addition to the consolidated-isotropic undrained compression (CIUC) triaxial tests described above, unconsolidated-undrained triaxial compression (Q) tests were conducted to determine the effects of consolidation on the stress-strain characteristics and strength behavior of plastic concrete (previous investigators had suggested that the effects of consolidation could be simulated by forming a Q test sample at the cement factor and water-content ratio a CIUC test sample would have at the end of consolidation). Unconfined compression tests were conducted to correlate with the more time-consuming and expensive CIUC tests.

9. The scope of Phase II tests was as follows:

20 CIUC Tests

6-in.-diam 12-in.-high sample size
cement factor of 300 lb/cu yd
bentonite contents of 0, 20, and 40 percent
effective confining pressures of 50, 100, 200, and 300 psi
ages of 3, 7, and 14 days
permeability tests

20 Q Tests

6-in.-diam 12-in.-high sample size
cement factor of 300 lb/cu yd
bentonite contents of 0, 20, and 40 percent
total confining pressures of 50, 100, 200, and 300 psi
ages of 3, 7, and 14 days

10. As a control, two unconfined compression tests and a splitting tensile test were performed on the same material molded for each pair of CIUC and Q tests. The UC companion tests were used to ensure:

- a. Repeatability with a batch, i.e. to ensure uniform mixing of constituents.
- b. Consistency with Phase I UC results for the same batch design and age.
- c. Comparability of Phase I UC tests and Phase II triaxial tests for development of design procedure.

PART II: LITERATURE REVIEW

11. Although plastic concrete has been used to produce cutoff walls with greater ductility than conventional concrete, relatively little published research has been done to develop a comprehensive design procedure. This is because most previous plastic concrete research was done by contractors and is therefore proprietary. In addition, most previous plastic concrete research programs were conducted in conjunction with dam construction and were generally limited in scope and site specific.

12. Part II contains a comparison and summary of major published works on plastic concrete since 1968. General observations on the scope and types of tests performed in the body of literature are presented first. A summary of each test program is then presented containing relevant mix design, stress-strain-strength data, and conclusions. Finally, performance data for constructed plastic concrete cutoff walls are presented.

General Observations of Recent Plastic Concrete Research

13. Table 1 was constructed in order to compare mix designs and scopes of work of various test programs. Different methods of describing plastic concrete batch designs are used throughout the literature. To make comparisons of mix design possible, all of the mix design parameters of the research programs listed in Table 1 were converted to cement factor, percentage bentonite, and water-cement ratio as previously defined. In addition, all the reported confining stresses were converted into units of pounds per square inch.

14. For each test program listed in Table 1, mix design parameters percentage bentonite, cement factor, and water-cement ratio are presented first along with slump and fine-coarse aggregate ratio. The scope of each testing program is then summarized according to the type of tests performed, number of tests performed, curing ages tested, and, if applicable, the range of confining stresses examined.

15. The body of work lacks critical data necessary to evaluate the range of behavior possible in plastic concrete for design in a cutoff wall. The most glaring deficiency is the lack of CIUC testing. CIUC tests are

Table 1

Summary of Plastic Concrete Test Programs

Test Program	Mix Design					UC			UU/Q			Tests Performed			Other				
	BEN %	CF pcv	W/C	S in.	F/C	No.	Age day	No.	Age day	No.	Age day	No.	Age day	No.	Age day	σ_3 psi	k 10^{-8} cm/s	T	FL
Habib, 1977	63	409	1.7	6	1	--	--	4	?	?	25-42	--	--	--	--	--	--	--	--
Woodard-Clyde, 1981, (Colbun Dam)	12-38	135-265	2.9-6.3*	6	0.1-1**	?	7-90	11	14	14	14-71	--	--	--	--	--	4-40	--	--
Fenoux, 1985	27	289	2.4	8	1	?	10-1000	?	?	?	1-15	--	--	--	--	--	0.1-1	--	--
Tamaro, 1986	8	308	1.1	8	0.8	4	7-90	--	--	--	--	--	--	--	--	--	0.01-10	--	--
Evans, 1987	25-50	288-580	1.0-2.1	6-8	1.4-1.7	--	--	3	14	?	?	--	--	--	--	--	5-35	--	--
US Army, 1987 (Mud Mountain Dam)	0-80	300	1.2-3.5	8	1	40	3-365	9	28	28	50-200	3†	28	200	200	--	--	--	YES
Present Study	0-60	230-450	1.0-2.8	8	1	251	3-660	20††	3-14	3-14	50-300	20††	3-14	50-300	50-300	0.1-10	0.1-10	YES	YES

* Bentonite and water mixed as slurry prior to batching.

** Includes some silty material.

† Samples consolidated in pressure cylinder, removed and then cured under atmospheric pressure.

†† Cement factor 300 lb/cu yd, bentonite content to 40 percent.

KEY TO ABBREVIATIONS

- UC unconfined compression test ($\sigma_3 = 0$)
- UU/Q unconsolidated, undrained compression test
- CF water-cement ratio
- W/C water-cement ratio
- CIUC consolidated-isotropic-undrained compression test
- S slump
- k permeability
- F/C fine-coarse aggregate ratio
- T splitting tensile test
- σ_3 total confining stress
- FL flexural beam test
- BEN percent bentonite

essential to understanding the behavior of plastic concrete in a deep tremie placement. None of the test programs listed in Table 1 prior to the Mud Mountain Dam (MMD) test program consolidated wet (8-in. slump) plastic concrete under constant confining pressure.

16. A second deficiency shown in Table 1 is the lack of any high pressure triaxial testing. Although several test programs included Q tests, the maximum total confining stress evaluated, with the exception of the MMD tests program, was 71 psi. The stress is inadequate to simulate the high confining stresses present at the bottom of remedial cutoff wall during a tremie placement. Typically, a remedial cutoff is placed through both embankment and foundation soil and can be up to 400 ft deep. During a tremie placement, the stress an element of concrete is subjected to is a function of the head of wet concrete above that element. Since pressure in a fluid equals the unit weight of the fluid times the depth of the fluid, the pressure exerted by wet concrete (unit weight approximately equal to 140 lb/cu ft) can be approximated as 1 ft concrete equals 1 psi. Therefore, in order to correctly simulate the possible range of in-situ cutoff wall confinement stress, confining stresses up to 300 to 400 psi must be examined.

17. Many of the prior research programs listed in Table 1 lack sufficient scope to design with any measure of confidence. Few long-term (more than 1 year) tests were performed to establish the effects of curing age on the stress-strain-strength behavior of plastic concrete. Most of the programs tested only one specimen at a given age and mix design. Thus, there is no way to gage the accuracy of the results of a particular test. Also limited are the ranges of cement and bentonite contents evaluated. There is a lack of control mixes with no bentonite to use as a basis for evaluating the influence of the addition of bentonite on stress-strain-strength behavior.

18. In addition, many of the problems with the existing literature discussed in this section are compounded by poorly documented testing procedures. In particular, it was difficult to ascertain, for some test programs, the exact type and number of triaxial tests that were performed due to the proprietary nature of these prior research programs.

Major Plastic Concrete Research Programs

19. This section contains summaries of each of the major plastic concrete research programs listed in Table 1. Some of the programs described consisted of laboratory testing only. Other programs were conducted to develop mix designs for specific earth dam cutoff walls. In addition, some of the programs also examined the influence of adding other materials to concrete.

Comparison of grout mixes and plastic concrete presented at the 9th conference of the ICSMFE*

20. This research program (Habib 1977) consisted of comparing the triaxial stress-strain-strength and permeability characteristics of grouts and a plastic concrete for use as a cutoff wall material. The grout mix design consisted of cement, clay, and water mixed at a ratio of 20:13:67 (percent by weight). The plastic concrete mix design examined was:

Cement factor	409 lb/cu yd
Percent bentonite	63%
Water-cement ratio	1.7
Fine-coarse aggregate ratio	1.0
Slump	6 in.

21. The stress-strain curves of unconfined and triaxial tests performed on this mix are shown in Figure 1. Figure 1 shows that the deviator stress at failure increases with confining stress. The permeability of both the grout mix and plastic concrete mix was to range between 0.5 and 2.1×10^{-6} cm/sec.

Other major conclusions were:

- a. Plastic concrete has significantly greater strain at failure than grout.
- b. Coarser aggregate reduces the strain at failure of plastic concrete.
- c. The permeability of grout and plastic concrete are of the same order of magnitude.
- d. Recommended applications:
 - (1) Grouts--shallow or temporary cutoffs, excavation protection.

* ICSMFE = International Conference on Soil Mechanics and Foundation Engineering.

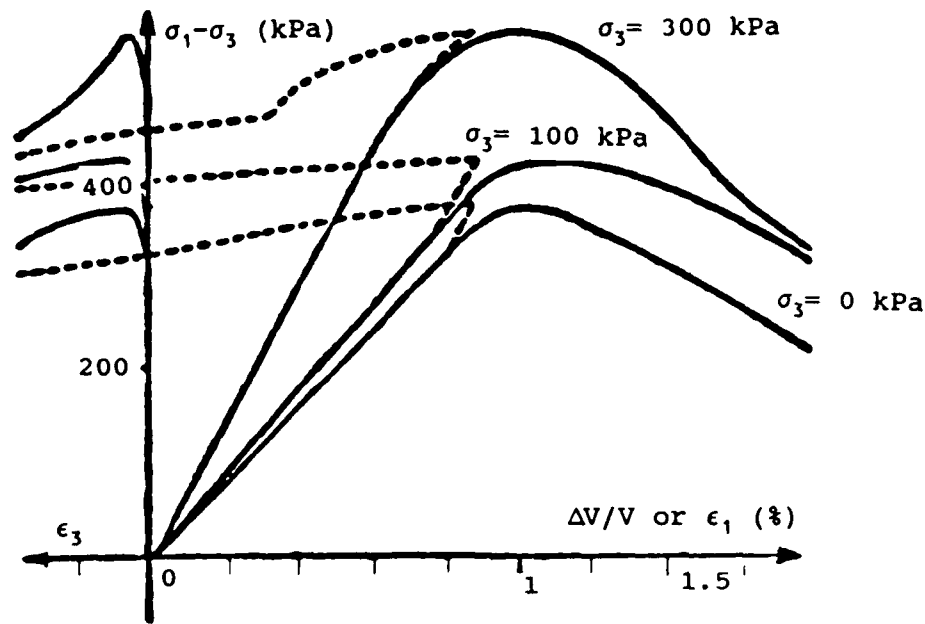


Figure 1. Influence of confining stress on the stress-strain behavior of plastic concrete (Habib 1977)

- (2) Plastic concrete--deep cutoffs, high dams, in seismic zones.

Colbun Dam research program

22. This research program (Woodward-Clyde Consultants 1981) evaluated the six plastic concrete mix designs for use in the Colbun Main Dam cutoff wall (paragraph 34). The proportions of these mix designs are summarized in Appendix A, Table A1. The mix designs were essentially mortar mixes made up of water, bentonite, cement, silty clay, and sand (sand plus silty clay equals 65 percent). These constituents reflected the types of materials readily available for use at the Colbun site.

23. The laboratory testing program consisted of UC tests, triaxial permeability tests, and CIUC tests. A summary of these tests is presented in Appendix A, Tables A2 and A3. The results in Tables A2 and A3 indicate that peak deviator stress, strain at failure, and modulus of elasticity increase with increases in confining stress. It does not appear, however, that the triaxial samples listed in Tables A2 and A3 as "CIUC" tests were consolidated wet (i.e. consolidated in triaxial chamber immediately after mixing the plastic concrete). The published procedure (Woodward-Clyde Consultants 1981) states that the CIUC samples were consolidated after curing in cylinder molds for 7 to 10 days. The results of constant head permeability tests on the mix

designs in Table A1 are summarized in Tables A4 through A6. The permeability of the mix designs tested was $4-40 \times 10^{-8}$. Other major conclusions were:

- a. Permeability is independent of gradient and no significant piping occurred at gradients up to 280.
- b. The shear strength and initial tangent modulus increase as the water-cement ratio decreases and as the effective consolidation stress increases.
- c. Strain at failure increases as consolidation stress increases.

Design procedure presented in
International conference on large dams

24. This report summarizes the criteria and design philosophy that should be used in plastic concrete diaphragm construction (Fenoux 1985).

These include:

- a. Permeability should be approximately 10^{-7} to 10^{-8} cm/sec.
- b. Deformability should be values of Young's modulus 4 to 5 times greater than surrounding soil that is acceptable for strain compatibility between surrounding soil and diaphragm wall. In addition, plastic concrete should have a high strain at failure (greater than 1 percent).
- c. Plastic concrete should have as low a compressive strength as possible, but strong enough to support the weight of the diaphragm wall, support earth pressures at depth, and resist erosion and hydraulic fracturing.
- d. Plastic concrete should be able to resist loss of integrity due to piping and chemical attack.
- e. Plastic concrete should meet workability requirements of tremie placement.

25. In addition general guidelines are given for developing plastic concrete batch designs, and graphs of triaxial, unconfined and permeability testing are presented. However, the report does not include a generalized design procedure relating mix parameters to strength and modulus data over a large range.

Bucknell University research program

26. This research program (Evans, Stahl, and Drooff 1987) was conducted to evaluate plastic concrete as a cutoff wall material for sealing landfills. Permeability and shear tests were performed on samples from nine different mix designs of plastic concrete. Table 2 summarizes each mix design and its corresponding permeability, shear strength, and strain at failure. Six of these batches contained either fly ash or bottom ash in addition to the

Table 2
Summary of Batches Designs and Corresponding Shear Strength
and Strain Data from Bucknell University Research
Program (Evans 1987)

<u>Mix Proportion</u> (by wgt)	<u>Plastic Concrete Mix No.</u>									
	1	2	3	4	5	6	7	8	9	0
Bentonite Content (%)	4.1	4.2	4.1	4.1	4.1	4.1	4.1	4.1	4.1	4.0
Fine Aggregate(%)	41.6	41.6	41.6	41.4	41.5	41.3	41.5	41.1	40.4	
Coarse Aggregate(%)	33.2	29.1	24.9	29.0	29.1	29.9	29.0	28.8	28.3	
Cement Content (%)	4.1	8.3	12.4	6.6	4.1	2.5	6.6	4.1	2.4	
Bottom Ash Content (%)	0	0	0	0	0	0	1.7	4.1	5.7	
Fly Ash Content (%)	0	0	0	1.7	4.1	5.7	0	0	0	
Bentonite Water ratio	0.24	0.25	0.24	0.24	0.24	0.24	0.24	0.23	0.21	
Cement Water ratio	0.24	0.49	0.73	0.38	0.24	0.14	0.39	0.23	0.12	
<u>Properties</u>										
Hydraulic Conductivity ($\times 10^{-7}$ cm/sec)	3.5	1.1	0.5	0.8	1.2	2.0	3.2	1.8	1.7	
Shear Strength (kPa)	400	338	3427	1455	1214	903	1110	545	76	
Axial Strain at failure (%)	2.0	3.7	10.0	5.5	9.8	5.4	12.2	16.8	9.6	

standard plastic concrete constituents. For the conditions tested (see Table 2), the major conclusions were:

- a. The permeability of plastic concrete ranged between 10^{-7} and 10^{-8} cm/sec.
- b. The permeability of plastic concrete is at least an order of magnitude lower than for cement bentonite (about 10^{-6} cm/sec, see Tamaro 1988).
- c. The permeability of plastic concrete decreases slightly with time.
- d. Plastic concrete may offer greater resistance to contaminant attack than either soil bentonite or cement-bentonite.

Mud Mountain Dam
(MMD) research program

27. This research program was conducted in conjunction with the rehabilitation of MMD by the United States Army Corps of Engineers. MMD is a 425-ft high earth and rockfill flood control dam located on the White River near Enumclaw, WA. In 1982 piezometric studies conducted at the deepest point

of the center of the dam's clay core showed that the water level within the core responded very quickly to changes in elevation of the impounded reservoir. These observations suggested zones of deterioration within the core. Subsequent borings confirmed zones of soft and loose material having the potential to allow excessive seepage (Peck 1986). The Corps then conducted a research program to evaluate the possibility of installing a plastic concrete diaphragm cutoff wall in the core as a seepage barrier. Table A7 in Appendix A contains a summary of the plastic concrete mix designs examined and the results of unconfined compression, flexural beam, Q, pressure, and erodability tests (US Army Engineer Division, North Pacific 1987). The pressure tests were nonstandard tests conducted in lieu of CIUC tests to evaluate the influence of consolidation on the stress-strain-strength behavior of plastic concrete. Wet samples were formed in open ended steel cylinders, and pressure was applied to the samples with a hydraulic loading device. Water was allowed to drain from the samples through vertical slots in the steel cylinder. When drainage ended (25 to 45 min), the pressure was removed, and the samples were cured under atmospheric pressure and later tested in a triaxial chamber.

28. Important general conclusions from the tests series are:

- a. Unconfined compressive strength, flexural strength, and elastic modulus decrease dramatically with the addition of bentonite.
- b. Strain at failure increases dramatically with the addition of bentonite.
- c. Maximum deviator stress and elastic modulus increase with confinement.
- d. Maximum deviator stress increases with consolidation.

Plastic Concrete Cutoff Wall Field Case Studies

29. Several plastic concrete diaphragm walls have already been installed in earth dams, both as remedial seepage control measures and as foundation cutoffs in new dams. This section contains five representative case studies presented in chronological order. Mix designs and, where possible, measurements of the hydraulic effectiveness of the cutoff are included in the discussions.

Balderhead Dam

30. Balderhead Dam (Bennie and Partners 1968), completed in 1965, is a 48-m high earth embankment dam located on the Balder River in Yorkshire

England. The shell is crushed shale and the central core is composed of compacted boulder clay. The core is connected to the foundation bedrock by a conventional concrete cutoff. A profile of the dam is shown in Figure 2.

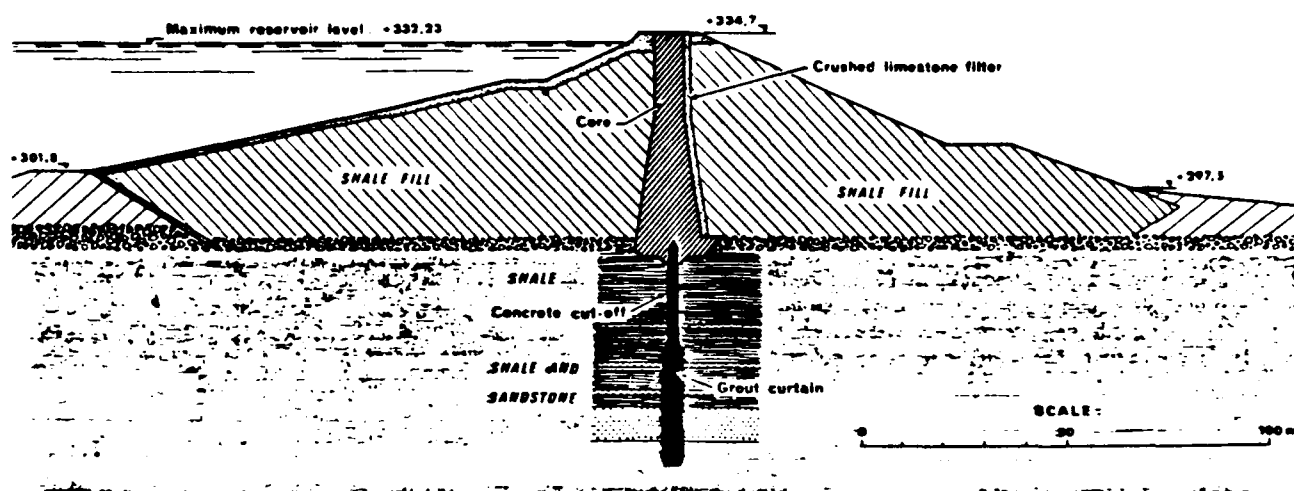


Figure 2. Profile of Balderhead Dam
(Binnie and Partners 1968)

31. Severe leakage problems developed in 1966-67 during the first reservoir impounding. When silty seepage water was observed downstream of the dam and 2.5-m deep swallow-holes opened along its crest, it was concluded that the leakage was due to extensive and continuing erosion of the clay core. The remedial solution adopted consisted of grouting the entire core and installing a plastic concrete diaphragm wall in the most damaged core zone. Plastic concrete was chosen because it would prevent cracking of diaphragm wall due to any additional future embankment settlements (dam was only 2 years old), and it was felt that grouting alone could not ensure an impermeable cutoff.

32. The final diaphragm wall was 200 m long, 43 m deep, and 0.6 m thick. The mix design used was as follows:

Cement factor	400 lb/cu yd
Percent bentonite	18 %
Water-cement ratio	1.7
Fine-coarse aggregate ratio	1.0

Subsequent studies showed seepage through the core was reduced from 60 l/sec to 5 l/sec.

Convento Viejo Dam

33. Convento Viejo Dam (Alvarez and Mahave 1982) is a 38-m high earth embankment dam located on the Tinguiririca River in Chile's central valley

constructed in 1977. Figure 3 shows an upstream elevation view of the dam. The original design called for a 14-m deep compacted clay cutoff to be installed beneath the embankment to control underseepage. During construction of the cutoff, however, it was discovered that underseepage occurred to a depth of 57 m. To remedy this, a continuous plastic concrete cutoff was installed to bedrock in front of the clay cutoff. The mix design used was as follows:

Cement factor	320 lb/cu yd
Percent bentonite	55 %
Water-cement ratio	1.7
Fine-coarse aggregate ratio	1.0

Subsequent pump test have determined seepage across the dam to be 29.1 l/sec, and the hydraulic efficiency of the plastic concrete cutoff to be 93.5 percent.

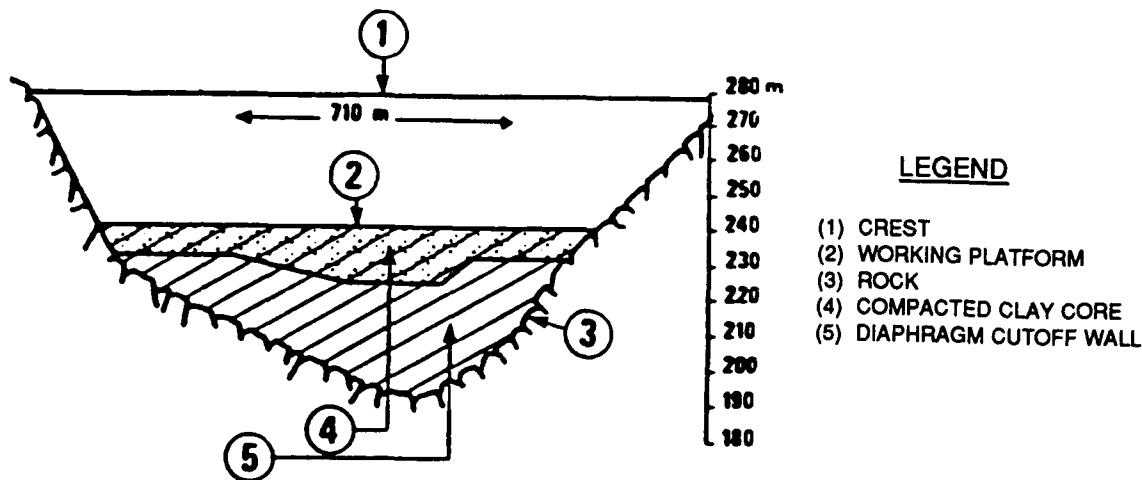
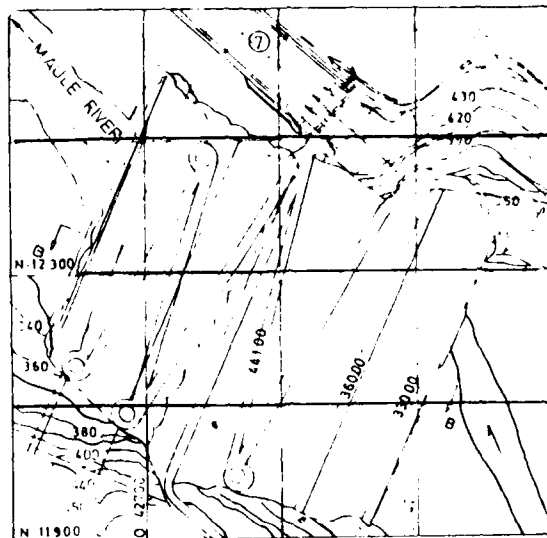


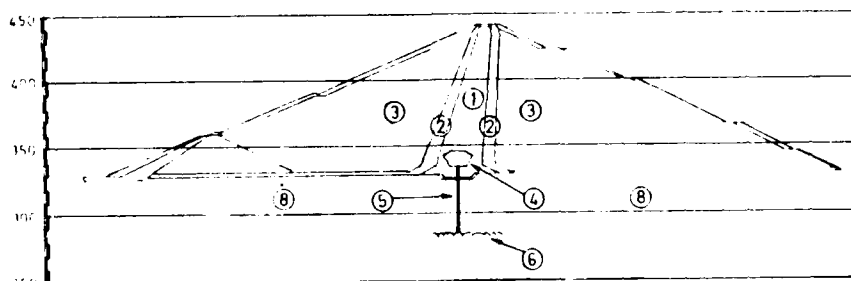
Figure 3. Elevation of Convento Viejo Dam (Hankour 1979)

Colbun Main Dam

34. The Colbun Dam (Noguera 1985) is a 116-m high zoned earth-gravel filled dam constructed in 1984 as part of Chile's Colbun-Machicura hydro-electric project. Figure 4 shows plan and section views of the dam. A 68-m deep plastic concrete cutoff wall was installed during construction through pervious alluvium to connect the core to bedrock. Plastic concrete was chosen to prevent the cutoff from cracking due to embankment settlement and potential seismic activity. An extensive laboratory testing program was conducted to



PLAN OF DAM
PLAN DU BARRAGE



SECTION - B
COUPE - B

LEGEND

- (1) CLAY CORE
- (2) FILTER ZONE
- (3) EARTH-GRAVEL FILL
- (4) CONCRETE CUTOFF CAP
- (5) PLASTIC CONCRETE CUTOFF WALL
- (6) BEDROCK
- (8) PERVIOUS ALLUVIUM

Figure 4. Plan and section of Colbun Main Dam (Pablo and Cruz 1985)

select the best mix design to meet these criteria (see paragraph 22). The mix design selected was as follows:

Cement factor	150 lb/cu yd
Percent bentonite	20 %
Water-cement ratio	4.5
Fine-coarse aggregate ratio	1.0
Slump	6-8 in.

35. Figure 5 shows unconfined stress-strain data from plastic concrete samples taken during construction of the cutoff. Comparison of triaxial test results to post-construction measurements indicate that the plastic concrete cutoff and foundation alluvium have similar deformation characteristics (Table 3).

Verney Dam

36. The Verney Dam (Tardieu and Costaz 1987) is a 42-m high earth embankment dam on the Eau D'Olle constructed in 1982 that creates the downstream reservoir for the pump/turbine station at Grand-Maison, France. A profile of the dam is shown in Figure 6. A 50-m deep plastic concrete diaphragm wall was installed in the foundation alluvium along the upstream toe as part of a waterproofing system that also included an asphalt coating on the upstream face. Gaps were left in the cutoff to allow for natural recharge of the downstream aquifer. The mix design used was as follows:

Cement factor	277 lb/cu yd
Percent bentonite	71 %
Water-cement ratio	1.9
Fine-coarse aggregate ratio	1.5

37. Stress-strain curves from triaxial tests on samples of the mix design are shown in Figure 7. Figure 7 indicates that peak deviator stress, elastic modulus, and strain at failure all increase with increases in confining stress. The permeability of the mix design is about 1×10^{-9} cm/sec, measured in the laboratory.

Mud Mountain Dam (MMD)

38. MMD (US Army Engineer Division, North Pacific 1987) is a 425-ft high earth and rockfill flood control dam located on the White River in Enumclaw, WA. The United States Army Corps of Engineers considered installing a plastic concrete diaphragm wall in the core as part of a remedial seepage control program (see Paragraph 27). Instead, a conventional concrete cutoff was installed.

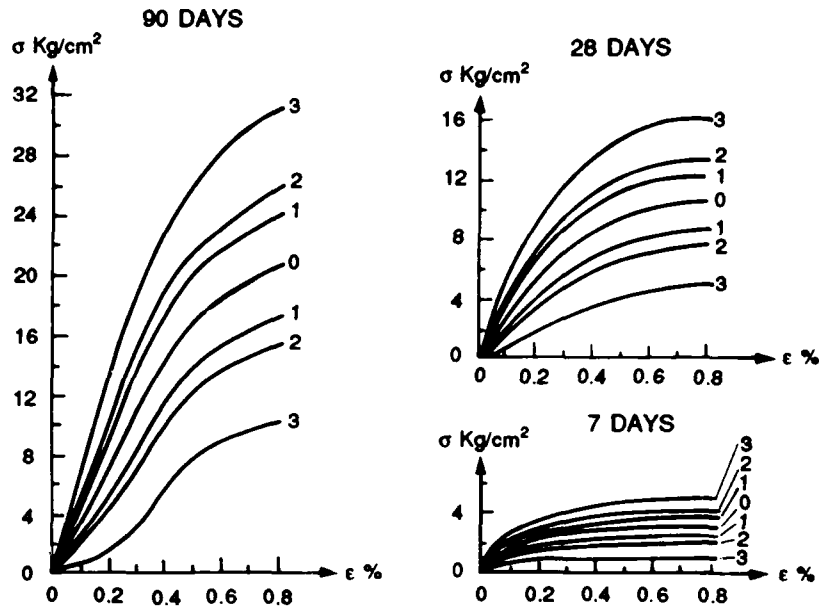


Figure 5. Unconfined compression tests on samples taken during construction of Colbun Main Dam (Noguera 1985)

Table 3

Comparison of the Behavior of Colbun Main Dam Plastic Concrete Diaphragm Wall with the Behavior of Foundation Soil Prior to Impounding of Reservoir (Noguera 1985)

Diaphragm cutoff wall	
Triaxial test	"Values in situ"
ϵ Failure - 4.15 %	$\epsilon = 0.30-0.60$ %
F Failure - 579 kg/cm ²	F = 3,200-5,500 kg/cm ²
F 75 % - 2,800 kg/cm ²	
F initial - 6,400 kg/cm ²	

Foundation alluviums	
Triaxial test	"Values in situ"
ϵ Failure - 4.17 %	$\epsilon = 0.20-0.90$ %
F Failure - 500 kg/cm ²	F = 2,000-5,000 kg/cm ²
F 75 % - 920 kg/cm ²	
F initial - 3,500 kg/cm ²	

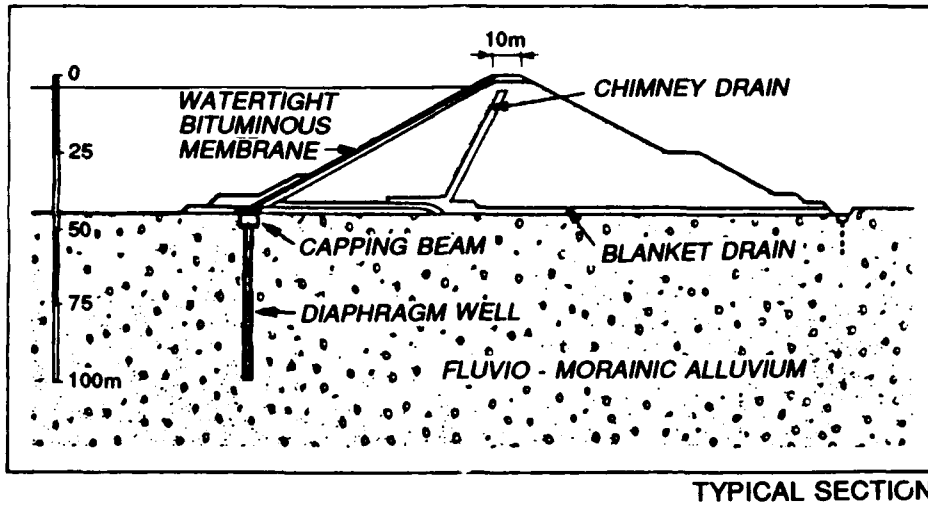


Figure 6. Profile of Verney Dam (Tardieu 1987)

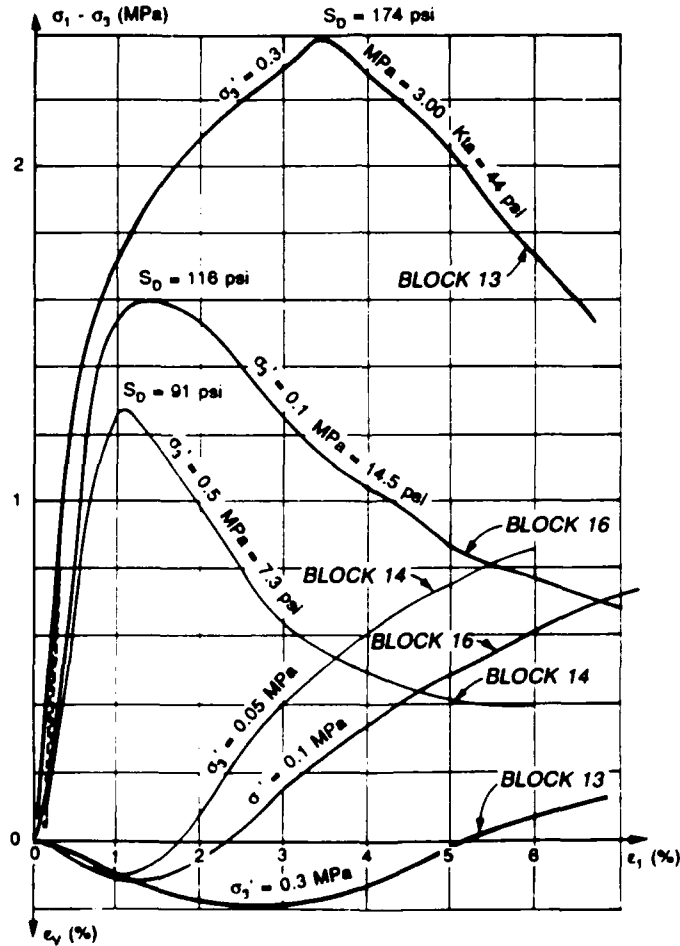


Figure 7. Triaxial drained tests, plastic concrete, Verney Dam (Tardieu and Costaz 1987)

PART III: LABORATORY TESTING TECHNIQUE

39. Throughout the research program, established American Society for Testing and Materials (ASTM) standards were used wherever possible to ensure quality and consistency. However, difficulties encountered when trying to consolidate wet 8-in. slump plastic concrete for the CIUC tests required the development of some nonstandard procedures. In the following sections the procedure for each type of tests performed in the research is described, and where applicable, references to ASTM standards are given. In addition, where nonstandard test procedures are described, any related ASTM standards are referenced. Descriptions of the materials used to make the plastic concrete specimens are presented first. A summary of the general fabrication and curing procedure used to make the unconfined compression, splitting tensile, flexural beam, and Q test specimens is then presented followed by descriptions and summaries of unconfined compression, splitting tensile, and flexural beam test equipment and procedures. Finally, descriptions of Q, CIUC, and permeability test equipment and procedures are presented.

Materials

40. The choice of materials was driven by two main considerations:
- a. Results of testing program had possible application in design of the Mud Mountain Dam cutoff wall. Therefore, material should match as closely as possible those used by NPDEN for their preliminary plastic concrete test program. A comparison between the grain size curves of the NPDEN aggregate and grain size curves of the aggregates used in this research program is shown in Appendix B, Table B1. Table B1 shows that there is no significant difference between the groups of aggregates.
 - b. Materials should represent types commonly available throughout most of the United States.

Descriptions of the actual materials used are discussed below.

Cement

41. Ironclad brand type I portland cement was used throughout the test program. Chemical analysis performed by the US Army Engineer Waterways Experiment Station (WES) confirmed that this cement conformed to ASTM designation C-150 (Appendix B, Table B2). For batch design, the specific gravity of solids (G_s) was taken as 3.15.

Bentonite

42. Volclay brand low yield (90 barrel*), untreated Wyoming grade sodium montmorillonite was used throughout the test program. This is the same material typically used for cutoff wall trench slurry. The results of a chemical analysis performed by WES are located in Appendix B, Table B3. Index properties are:

$$\begin{aligned}G_s &= 2.75 \\LL &= 530 \% \\PL &= 41 \% \\PI &= 489 \%\end{aligned}$$

Aggregates

43. Masonry sand (SP) and minus 3/4 in. well rounded gravel (GP) were used. Phase I aggregate was obtained from Lakeville Crushing, South Carver, MA. Phase II aggregate was obtained from Boston Sand and Gravel, Boston, MA. The grain size distribution of both sets of aggregates conformed to ASTM specification C 33-86 and are shown in Appendix B, Figures B1 through B4. Comparison of Figures B1 and B2 to Figures B3 and B4 shows very little difference between the grain size distributions of the two sets of aggregate.

Water

44. Potable tap water from the Geotechnical Laboratory at Tufts University was used for all batches.

General Concrete Fabrication Procedure

45. One of the primary criteria for tremie placement of plastic concrete in a slurry trench is flowability. In order to prevent clogging of tremie pipes, and to provide for uniform plastic concrete distribution along trench bottoms, an 8-in. slump is recommended (Tamaro 1988). In light of this, all of the plastic concrete batches produced in this research were designed for a nominal 8-in. slump. This section describes the procedures used for batching, mixing, and wet testing of all of the concrete batches

* One ton of clay will yield 90 barrels (42 gallons-US petroleum) of material with a dynamic viscosity of 15 centipoise.

produced in this research program. The fabrication and curing procedures for conventional test cylinders and flexural beams are also included.

Batch design

46. All batches were proportioned by the absolute volume method described in ACI Standard 211.1-81 (CRD-C 99-82). Consistent with this method, the following batch proportion parameters were used to describe the plastic concrete batches:

Cement factor - The cement factor was defined as the total amount, by weight, of cement and bentonite in a cubic yard of plastic concrete:

$$\text{cement factor} = (\text{weight cement} + \text{weight bentonite}) \text{ per cubic yard}$$

Bentonite content - Percentage of cement factor, by weight, which is bentonite. The bentonite content is calculated using the following equation:

$$\text{bentonite content, \%} = \frac{\text{weight of bentonite}}{\text{cement factor}} * 100$$

Water-cement ratio - The weight equivalency method was used to describe the amount of water in a batch:

$$\text{water-cement ratio} = \frac{\text{weight of water}}{\text{weight of cement} + \text{bentonite}}$$

Coarse-fine aggregate ratio - In order to produce tremie plastic concrete (Tamaro 1988), the ratio by weight of fine to coarse aggregate (ratio of sand to gravel) for all batches was approximately 1.1. In addition, since the sand and gravel used both had measured specific gravities of 2.65, the coarse to fine ratio by volume was also 1.

47. For a given cement factor and percent bentonite, a water-cement ratio was estimated from previous experience that would produce an 8-in. slump. The actual weights and volumes of cement, bentonite, and water required to produce a cubic yard of concrete were then calculated. The required volume of fine and coarse aggregate was then taken as the difference between a cubic yard and the sum of the volumes of cement, bentonite, and water. The weight of fine and coarse aggregate was then back calculated from

their volumes. The weights of all the constituents were then corrected for hygroscopic moisture content and scaled to produce the desired batch volume. After the batch was made, the cement factor and water-cement ratio were corrected for any additional water added during mixing (see Paragraph 48). An illustrative batch design example can be found in Appendix B, Table B4.

Plastic concrete mixing procedure

48. All plastic concrete batches were mixed at 25 revolutions/min in a stone brand six cubic foot power concrete mixer. The procedure which was generally followed corresponded to ASTM specification C 192-81, paragraph 6.1.2 (CRD-C 10-81). The modified procedure used is as follows:

- a. Water content tests were performed on cement, bentonite, sand and gravel to determine hygroscopic moisture. Figure 8 shows typical quantities of materials used for water content test.
- b. The bentonite and the cement were mixed together dry in a 5-gal bucket.
- c. Approximately one-half of the sand, gravel, and water were added to the mixer and mixed for approximately 15 sec.
- d. Approximately one-half of the cement-bentonite mix was added to the turning mixer.
- e. The remaining sand, gravel, and cement-bentonite mix was added to the turning mixer, along with enough of the remaining water to produce an 8-in. slump upon visual inspection.
- f. Batches containing bentonite tended to "stiffen" in the mixer over time as the bentonite absorbed water. To counter this, the remaining water and, if necessary, additional water was added approximately every 10 min to maintain an 8-in. slump. Additional water was added until the mix no longer "stiffened," generally about 45 min.
- g. Total mix time was approximately 10 min for batches with 0 percent bentonite and 45 min for batches with 10 to 60 percent bentonite.

49. An attempt was made to premix the bentonite and water in a bucket to form a slurry, as is commonly done in slurry trench field operations. This was unsuccessful due to balling of the bentonite. A special colloidal mixer would have been necessary to overcome this problem, but was deemed beyond the scope of this project. Therefore, the bentonite was dry mixed with the cement before being added to the mixer (as described above) to help ensure uniformity of the mix. In addition, the water content required for pumpable slurry is approximately twice the liquid limit, or 100 percent for the bentonite used in this research program. Based on estimated water-cement ratios, the use of



Figure 8. Samples of sand, gravel, bentonite, and cement (clockwise, from right) for water content tests to determine hygroscopic moisture

such a high water content would have limited the bentonite contents evaluated to 10 percent and less.

50. Because the hydration of bentonite in a mixer is time dependent, it was necessary to continue to add water to a mix until there was no longer a loss of slump with increased mixing. Trial batches reached this point after approximately 45 min, but more or less time may be taken if visual inspection determines that slump loss has ended. Any water added in addition to that specified in the batch design during this time period was figured into the recalculation of the batch design (see batch design example, Table B4).

Concrete fabrication equipment

51. All scales hand tools and mix pans used for concrete fabrication conformed to ASTM specification C 192-81 (CRD-C 10-81). Calibrations of the scales are presented in Appendix C, Figure C1.

Tests performed on wet concrete

52. The following tests were performed:

- a. Slump -- Tests were performed according to ASTM specification C 143-78 (CRD-C 5-86). Typical values ranged between 7-1/2 and 8-1/2 in.
- b. Unit weight -- For Phase I batches ASTM standard C 138-81 was followed using the air content test sample bowl as a measuring

container. For Phase II batches, the actual concrete cylinder specimens were used as measuring containers. This method allowed for multiple independent unit weight calculations (as many calculations as specimens formed), and therefore provided a measure of batch consistency. Typical values ranged between 125 and 145 lb/cu ft. Unit weight decreases with increasing bentonite content because water comprises a larger fraction of total batch weight as bentonite content increases.

- c. Air content -- Air content tests conformed to ASTM specification C 231-82 (CRD-C 41-84) for a type B air content meter. Typical air content values ranged between 0.2 percent and 2 percent.
- d. Water content -- Oven-dry water content tests were performed on wet concrete to develop a correlation between calculated water content and oven dry water content. Calculated water content is the ratio of weight of water to combined weight of other materials (cement, bentonite, and aggregate) used to form the batch. Oven dry water content tests were performed in accordance with ASTM standard D 2216 for soils. Typical values of oven dry water content ranged between 8 percent and 22 percent and the ratio of oven-dry to calculated water content ranged from 0.53 to 0.92 and averaged 0.74. This ratio can be used for field quality control to estimate the wet water content of tremie concrete from a sample taken from the top opening of the tremie pipe.
- e. pH -- The pH of wet concrete was determined for some Phase II batches with quantitative pH paper to ensure the proper suspension of bentonite in the mix. Typical values ranged between 11 and 12 (pH range for suspension of bentonite = 9.5 to 12) (Sliwinski and Fleming 1975).
- f. Temperature -- Temperature measurement of wet concrete conformed to ASTM specification C 1064-88 (CRD-C 3-87). Temperature was usually measured by inserting a thermometer into the concrete mound left by a slump test. Typical values ranged between 64 and 70° F.

Fabrication of conventional plastic concrete test cylinders

53. The formation of 6- by 12-in. cylindrical tests specimens for all unconfined compression, splitting tensile, and unconsolidated undrained compression (Q) tests conformed to ASTM C 192-81 (CRD-C 10-81). Specimens were formed using standard 6-in. diam by 12-in. high molds in three layers of approximately 4 in. thick. Each layer was rodded 25 to 30 times and vibrated by hand to ensure proper consolidation. Figure 9 shows test cylinders being formed.



Figure 9. Six in. by twelve in. plastic concrete cylinders being formed

54. Initially, cylinder molds made of plastic were used to form all specimens in Phase I. However, scarification problems were encountered when extracting the first high bentonite content (BEN = 40 and 60 percent) specimens from the plastic molds after the recommended ASTM period of 2 days. Thereafter, ASTM approved peel-off wax coated cardboard cylinder molds were used for all high bentonite specimens formed in Phase I. Due to general ease of use and better specimen quality, it was subsequently decided to use the cardboard molds exclusively for all Phase II specimens.

Fabrication of flexural beam specimens

55. All flexural beam specimens were formed in 6-in.-wide by 6-in.-high by 24-in.-long rectangular steel molds in accordance with ASTM specification C 192-81 (CRD-C 10-81).

Curing of concrete test specimens

56. All plastic concrete test specimens were cured in either a wet room or cure box environment. Figures 10 and 11 show specimens in the wet room and cure box, respectively. The wet room lacked temperature control, but humidity control was provided by an air/water mist system. During Phase I testing, specimens from the same batches were stored in both locations to evaluate their performance. Comparison of unconfined compression test results showed that curing location had no effect on the mechanical properties of the cylinders, as shown in Figure 12. Each data point represents cylinders of the same age and batch composition.

57. Monitoring of both locations over 60 days produced the following performance criteria:

a. Wet room:

Temperature range: (measured with min-max thermometer)	62 - 72° F
Humidity: (measured with wet-dry bulb thermometer)	>95%
Free water:	often observed on surface of specimens

b. Cure box:

Temperature range:	68 - 72° F
Humidity:	>95%
Free water:	some observed

These criteria conform to ASTM specification C 192-81 (CRD-C 10-81) except for temperature range (73 +/- 3° F). In addition, all specimens were stripped from their molds 20 to 48 hr after fabrication, as required by ASTM C 192-81.

Unconfined Compression Test Procedure

58. Twenty-one batches of plastic concrete were formed for unconfined compression testing during Phase I. A summary of the nominal mix design for each batch is presented in Table 4. For most batches, fifteen 6- by 12-in. cylinders were formed and broken in groups of three at nominal ages of 3, 7, 28, 90, and 365 or more days. Three cylinders were tested at each age to ensure statistical accuracy, as recommended in ASTM designation C 192-81. In



Figure 10. Six in. by twelve in. plastic concrete cylinders curing in wet room

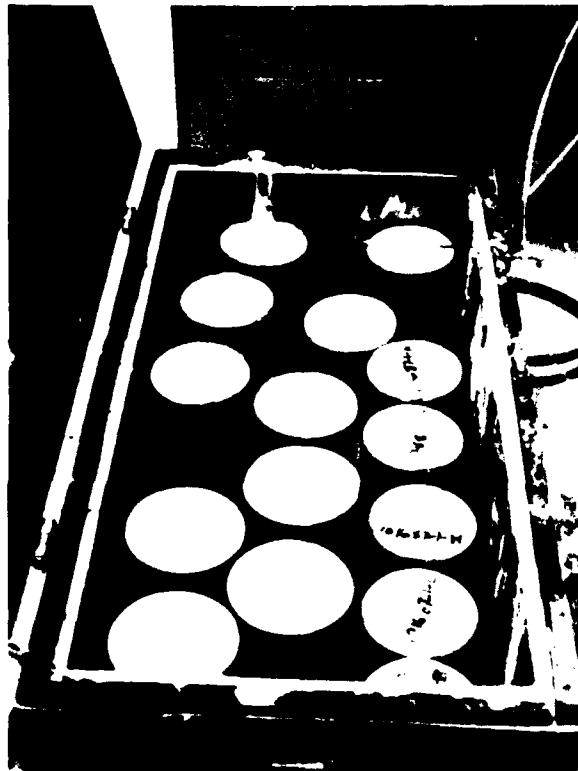


Figure 11. Six in. by twelve in. plastic concrete cylinders curing in cure box

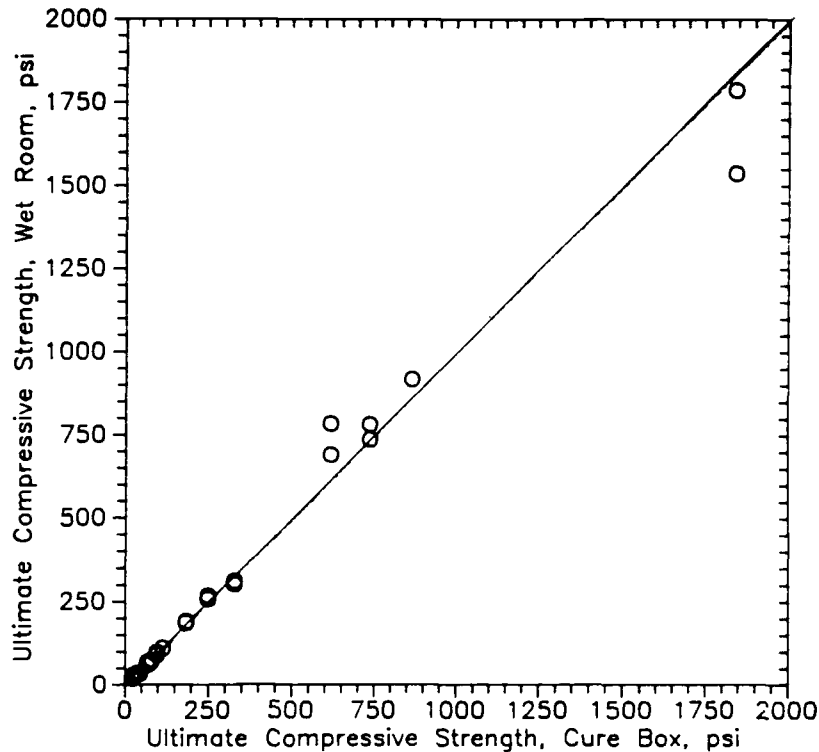


Figure 12. Ultimate compressive strength of samples cured in the wet room versus ultimate compressive strength of samples cured in the cure box

addition, two companion unconfined compressions were performed for each of the 20 CIUC batch designs tested in Phase II.

59. For all of the 291 unconfined compression tests performed in both phases, continuous load and deformation readings were recorded in order to evaluate the stress, strain, and strength characteristics of each specimen. A compilation of the data is presented in Appendix D, Table D1 and will be discussed more fully in Part IV. All tests were performed using ASTM C 39-86 (CRD-C 14-87) and ASTM C 469-83 (CRD-C 19-87) as guidelines, but some procedure and equipment modifications were made as noted. All tests were performed at a deformation rate of 0.05 in./min +/- 0.005 in./min.

Measurement of unconfined compression test samples

60. After curing in either the cure box or wet room for a specified amount of time, samples were removed and examined for signs of damage. Specimens too damaged to cap were discarded. Typically, the high bentonite content (BEN = 40%, 60%) specimens were most likely to be damaged during mold

Table 4

Summary of Nominal Batch Designs for Phase I Unconfined Compression Tests

<u>Batch ID*</u>	<u>Nominal Cement Factor, lb/cu yd</u>	<u>Percent Bentonite</u>	<u>Nominal Water/ Cement+Bentonite</u>
060387-1	300	0	0.8
060487-1	300	20	1.4
060587-1	300	20	2.0
061087-1	300	40	1.6
061287-1	300	60	2.6
061687-1	400	0	1.0
061887-1	400	20	1.2
061887-2	400	40	2.0
062387-1	400	60	2.0
071387-1	250	0	1.0
071487-1	250	20	1.6
072187-1	250	40	2.2
072787-1	250	60	2.2
102387-1	290	0	1.4
102687-1	290	20	1.8
110387-1	240	10	1.9
110387-2	280	10	1.8
110387-3	320	10	1.6
111087-1	360	10	1.4
111387-1	330	0	1.2
111387-2	260	20	2.1

* Batches listed in chronological order of fabrication. Batch ID = date of fabrication.

stripping and handling because of their low strength. Any loose aggregate on the sample ends was removed.

61. The length and the diameter of samples were measured as follows:

- a. Length: All Phase I samples were measured with a 12-in. vernier, precise to ± 0.0005 in. All Phase II samples were placed vertically on a piece of plate glass and measured with a 24-in. machine scale, precise to ± 0.008 in.
- b. Diameter: All Phase I samples were measured at top, middle, and bottom with a 6-in. micrometer, precise to ± 0.0005 in. All Phase II samples were measured at top, middle, and bottom with a double carpenters scale, precise to ± 0.008 in.

End capping of unconfined compression samples

62. Test specimens were capped with sulfur capping compound in order to assure the planeness and perpendicularity required by ASTM specification C 39-86 (CRD-C 14-87). The sulfur compound used has a rated strength of 14,000 psi. The capping procedure was performed in accordance with ASTM specification C 617-85b (CRD-C 29-86). The end capping fixture used and an example of a capped cylinder are shown in Figures 13, 14, and 15.

63. In an attempt to make end capping quicker and eliminate exposure to toxic sulphur fumes, some Phase I specimens were tested with a neoprene capping system developed by the New York Department of Transportation (Amsler and Grygill 1977). The neoprene system proved unsatisfactory for low strength samples because of spalling of sample ends during compression due to shear stresses developed at the neoprene-specimen interface. The spalling caused reduction in area and, in turn, lower loads at failure than a comparable sulfur-capped specimen. In addition, the samples tested with neoprene end caps failed by vertical splitting, rather than the diagonal cracking typical of specimens with sulphur end caps.

64. Twenty Phase I specimens were tested with the neoprene capping system before its use was discontinued. These tests are identified in the unconfined test summary (Table D1) by the designation NEOP in the "strain" column. In order to use the data from these tests in the general analysis of the unconfined compression tests, a correction procedure was developed and is described in Paragraph 148.



Figure 13. End capping and sulphur warming pot under ventilation hood



Figure 14. Sample being capped in fixture



Figure 15. Example of capped plastic concrete cylinder

Measurement of axial load
for unconfined compression tests

65. All unconfined compression tests were performed with a constant rate of deformation Riehle Model FS-300 testing machine. This machine has a screw-driven loading platen with a minimum deformation rate of 0.04 in./min and a maximum load capacity of 300,000 lb. Loads are measured internally with a beam-type reaction system and displayed on a large analog dial gage. The dial gage has six loading ranges:

<u>Range, lb</u>	<u>Precision, lb</u>
0-3,000	5
0-15,000	25
0-30,000	50
0-60,000	100
0-150,000	250
0-300,000	500

66. Figures 16 and 17 show the Riehle testing machine and a close up of its load head crushing a 6- by 12-in. sample. Calibrations of the Riehle testing machine are located in Appendix C, Figures C2 and C3.

67. Loads were read manually by the operator of the Riehle testing machine and hand recorded. Corresponding deflections were read manually by an assistant from a dial gage attached to the test specimen and hand recorded. Accurate reading of peak loads was ensured by a dial pointer follower. In order to develop complete stress-strain curves, deflection readings were taken at least six loads prior to peak load and, in most cases, at least two loads after peak.

Measurement of deflection
for unconfined compression tests

68. During Phase I, strain was initially calculated from the gross deflection of the load head of the testing machine as measured by a dial gage rigidly mounted to the loading platform. This gage had a precision of +/- 0.0005 in. Midway through Phase I, a compressometer conforming to ASTM specification C 469-83 (CRD-C 19-87) was purchased for measurement of deflection. The gage mounted on the compressometer had a precision of +/-0.0005 in. Schematic diagrams of the gross deflection system and compressometer are shown in Figures 18 and 19.

69. Subsequent Phase I tests were performed using both the gross deflection method and the compressometer method to establish the

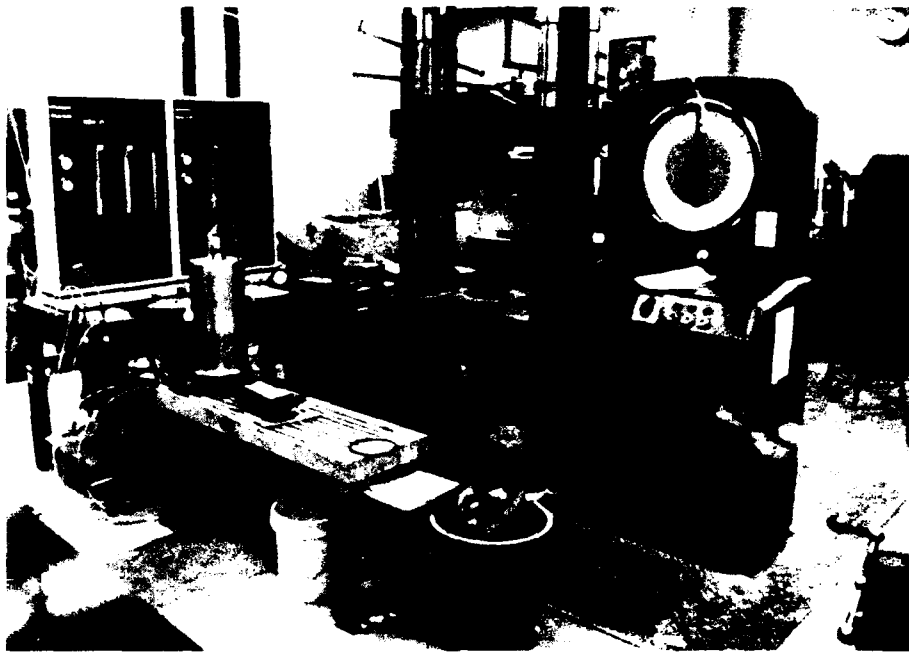


Figure 16. Riehle testing machine and general testing equipment setup



Figure 17. Load head of Riehle testing machine crushing 6- by 12-in. sample (no deflection measurement shown)

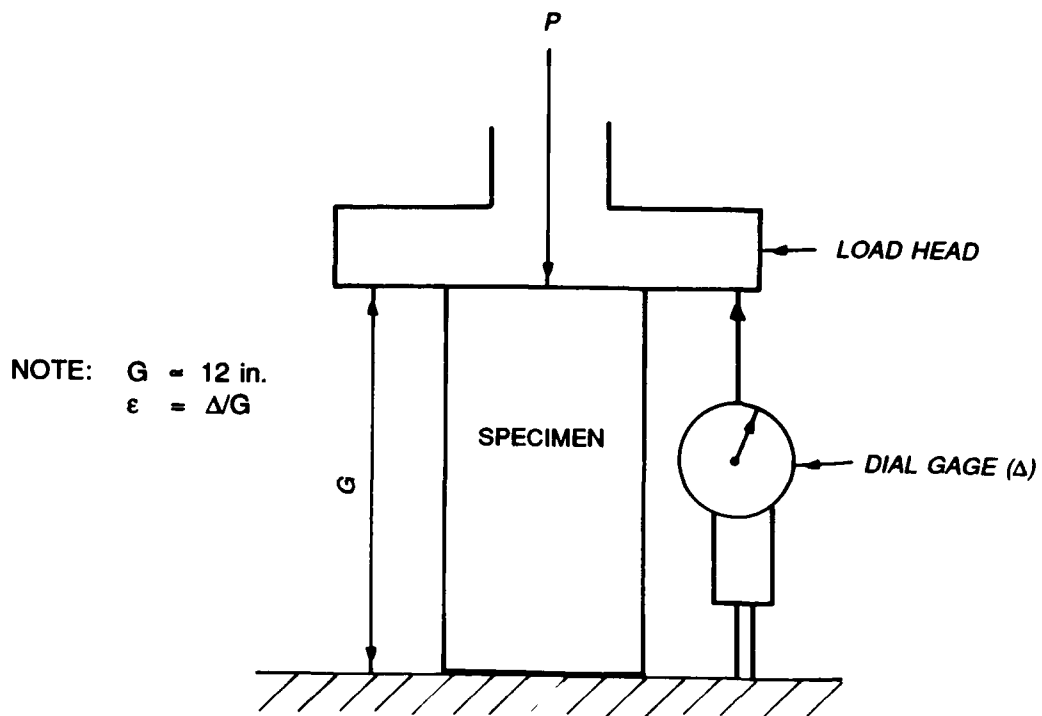


Figure 18. Schematic diagram of gross deflection system

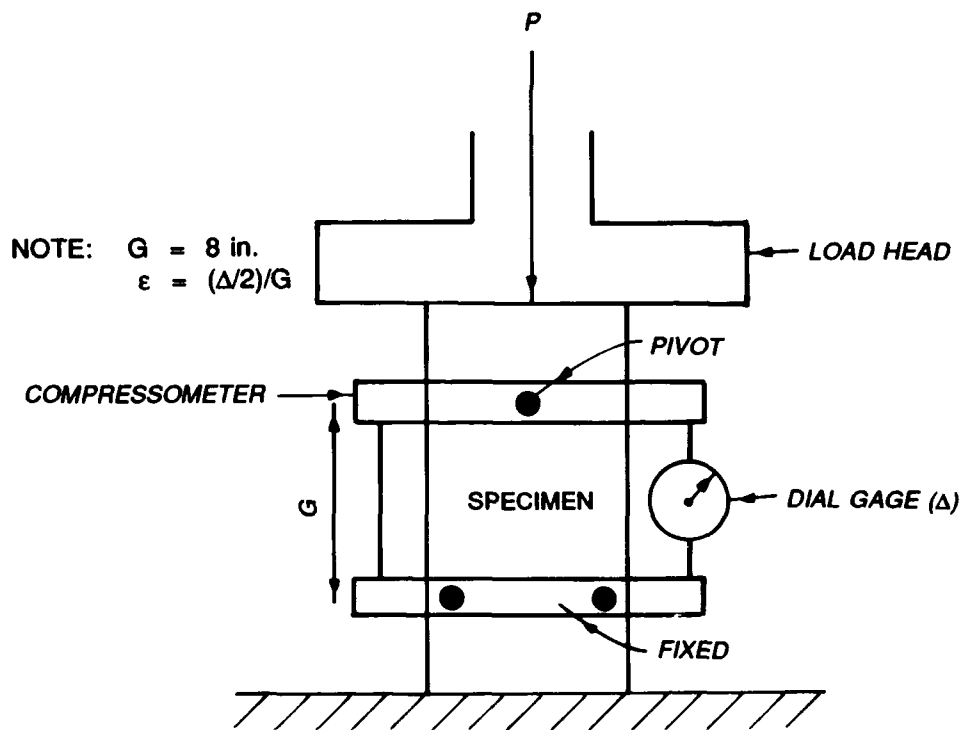


Figure 19. Schematic diagram of compressometer system

relationship between the two. For a given batch design and age, three samples were typically broken to ensure statistical confidence. Two of these samples were tested using the gross deflection method, and one sample was tested using the compressometer. If less than three cylinders were available for a given batch design and age, at least one test was performed using the compressometer.

70. A comparison of the strain at failure of specimens of the same age and batch design calculated with gross deflection and compressometer data is shown in Figure 20. Figure 20 shows that the scatter in strain at failure data is greater than any difference caused by the different deflection measurement systems. Only the compressometer was used to measure the deflections of unconfined compression tests performed in Phase II.

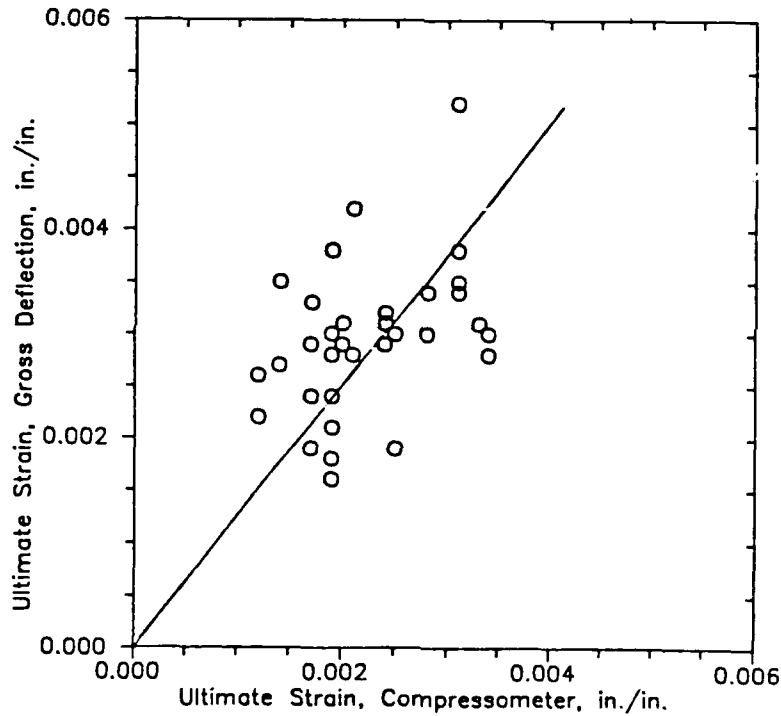


Figure 20. Ultimate strain measured with compressometer versus ultimate strain measured by gross deflection

Post-failure water content tests on unconfined compression tests

71. Post-failure water content tests were conducted on some unconfined compression tests to evaluate the relationship between water content at mixing and water content after curing. This was done as part of a separate, concurrent research program and is not part of the scope of this study.

72. After compression testing, one cylinder from each test group of the same age and batch design was broken into pieces less than 1 in. in size, and a water content was performed on pieces taken from the core. Standard oven-dry soils testing water content test procedure (ASTM D 2216) was used.

Brazilian Splitting Tensile Test Procedure

73. Brazilian splitting tensile tests were performed on 45 specimens from six batches of plastic concrete to evaluate the effect of bentonite content, cement factor, and age on splitting tensile strength. The nominal mix designs and test ages for each batch area listed in Table 5. The results of the tests are discussed in Paragraph 114. In addition, one companion Brazilian splitting tensile test was performed for each of the 20 CIUC tests performed in Phase II.

74. All splitting tensile tests were performed in accordance with ASTM specification C 496-85 (CRD-C 77-85). All tests were performed with the Riehle testing machine at a deformation rate of 0.05 in./min +/- 0.005 in./min.

Table 5

Summary of Nominal Batch Design for Phase I Splitting Tensile Test (Brazilian) and Flexural Beam Test

<u>Batch ID*</u>	<u>Nominal Cement Factor, lb/cu yd</u>	<u>Percent Bentonite</u>	<u>Nominal Water/Cement+Bentonite</u>
053088-1	250	0	1.5
060288-1	340	0	1.2
060288-2	260	20	2.0
061988-1	340	20	1.7
062288-1	260	60	2.4
062288-2	340	60	2.3

* Batches listed in chronological order of fabrication. Batch ID = date of fabrication.

Measurement of Brazilian splitting tensile test specimen

75. After the specified curing time, test samples were examined, cleaned, and measured as described in Paragraph 60. Two diametrical lines in

the same plane were then drawn across both sample ends to use as guides to align the specimen with the test apparatus.

Positioning of Brazilian splitting tensile test specimen

76. A 1-in. wide by 1/8-in. high by 12-in. long plywood strip was placed across the lower bearing block. The test cylinder was then placed horizontally on the plywood strip so that the lines marked on the ends of the cylinder were vertical and centered over the plywood strip. A second plywood strip was then placed lengthwise across the top of the cylinder and centered on the lines marked on the ends of the cylinder. A supplementary bearing bar, as described in ASTM specification C 496-85, was then placed on top of the upper plywood strip. The load head was then brought into contact with the supplementary bearing bar.

Measurement of load for Brazilian splitting tensile test

77. The peak load was read manually by the operator of the Riehle testing machine from the dial pointer follower and hand recorded. Splitting tensile strengths were then calculated as described in ASTM standard C 496-85. Post-test water content tests were performed as described in Paragraph 71.

Flexural Beam Test Procedure

78. One 6-in. wide by 6-in. high by 24-in. long flexural beam was cast in a steel mold for each preliminary Brazilian tensile test batch and tested in single-point simply supported flexure at an age of 28 days, in accordance with ASTM specification C 293-79 (CRD-C 17-80). All tests were performed with the Riehle testing machine at a deformation rate of 0.05 in./min. +/- 0.005 in./min.

Measurement of flexural test sample

79. After curing, the length, width at center, and thickness at center were measured to a precision of +/- 0.008 in. Post test measurements of the width and thickness of the beam at the point of rupture were taken and, if different from the initial measurements, recorded for use in calculation of the modulus of rupture.

80. The span length was then calculated using the equation:

where

L - Span length

D - Beam thickness

Support point marks were then drawn on the beam at distances of L/2 from the beam center line. A line was also drawn at the center line to locate the single center point load.

Positioning of flexural test
sample and measurement of load

81. Test beams were placed on the simple supports such that each support was lined up with a span mark on the beam, and the center point load block was lined up with the center line of the beam and the center line of the load head. Beams were then loaded and the peak load was manually recorded by the testing machine operator. Modulus of rupture was then calculated as described in ASTM standard C 293-79.

Erodability Test Procedure

82. Two tests were performed to measure the resistance of plastic concrete to erosion by seepage through cracks. Both tests were performed according to a nonstandard procedure originally developed by the NPDEN W.O. No. 87-C-329 for their preliminary plastic concrete testing program. Crack conditions were simulated by casting a 3/16-in. hole through each sample and flowing water through it at a velocity of 17 ft/sec. One test had a bentonite content of 0 percent and the other had a bentonite content of 60 percent. Both tests had cement factors of 300 lb/cu yd, and erosion measurements were taken continuously between ages 3 and 8 days with a No. 200 sieve.

Description of mold used
to cast erodability specimens

83. Erodability test specimens were formed using a modified 6- by 12-in. cardboard cylinder mold (Figure 21). Modification procedures were as follows:

- a. A 1/4-in. Swagelok bulkhead fitting (inside diameter: 3/16 in.) was installed in a hole drilled in the center of the metal bottom of the cardboard mold. Buna O-rings were used to seal the joint.

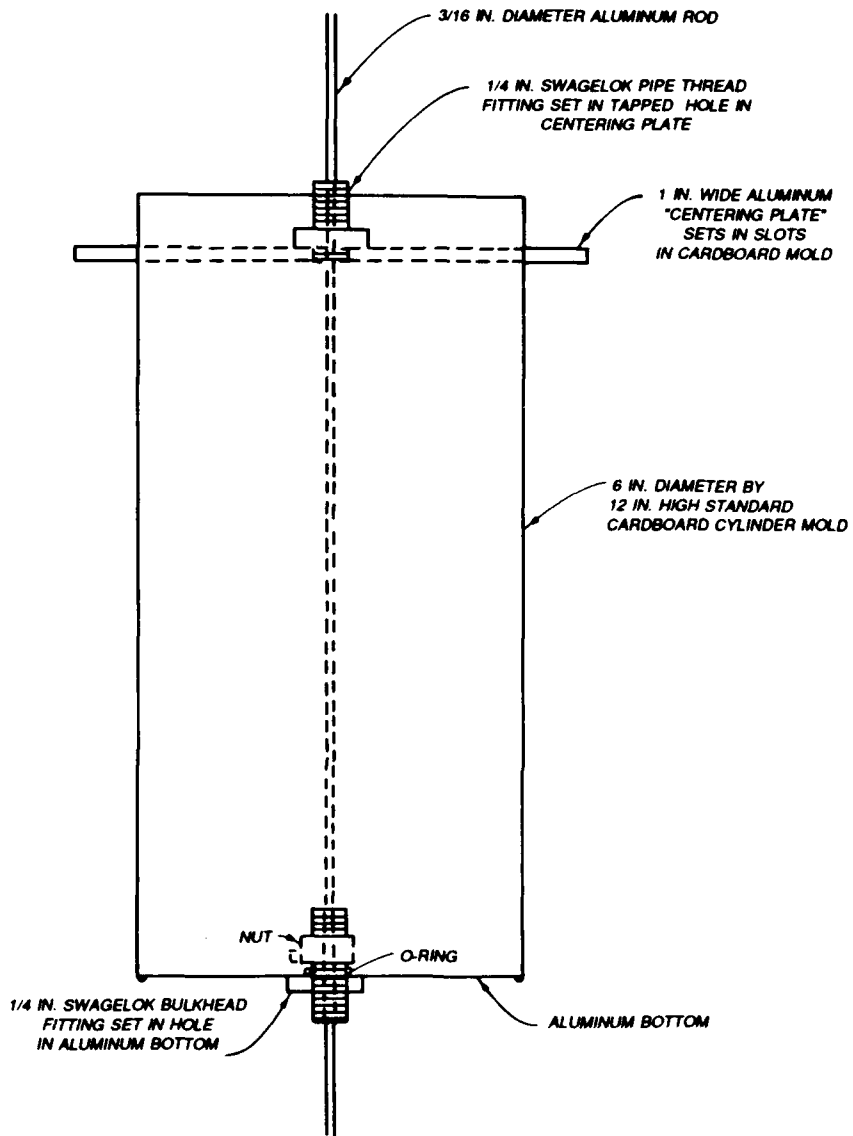


Figure 21. Schematic diagram of modified 6 by 12-in. erosion test cylinder

- b. A 1/4-in. Swagelok pipe thread fitting was installed in a hole drilled in a 1- by 8- by 1/4-in. piece of aluminum.
- c. The piece of aluminum with the pipe thread fitting was then installed into 1/4-in. slots cut into opposite sides near the top of the mold. The piece of aluminum was adjusted until both fittings were on the same axis.
- d. A 3/16-in. aluminum rod was then inserted through both fittings. The rod was coated with vacuum grease to help seal the bottom fitting and make later removal of the rod easier.

Sample set-up and erodibility measurement

84. A schematic diagram of the general erosion test setup is shown in Figure 22. The sample setup for testing procedures was as follows:

- a. The modified cylinder was filled with wet concrete using the same procedure as for unconfined compression cylinders as discussed in Paragraph 53. Care was taken so as not to cover the threads of the top fitting.

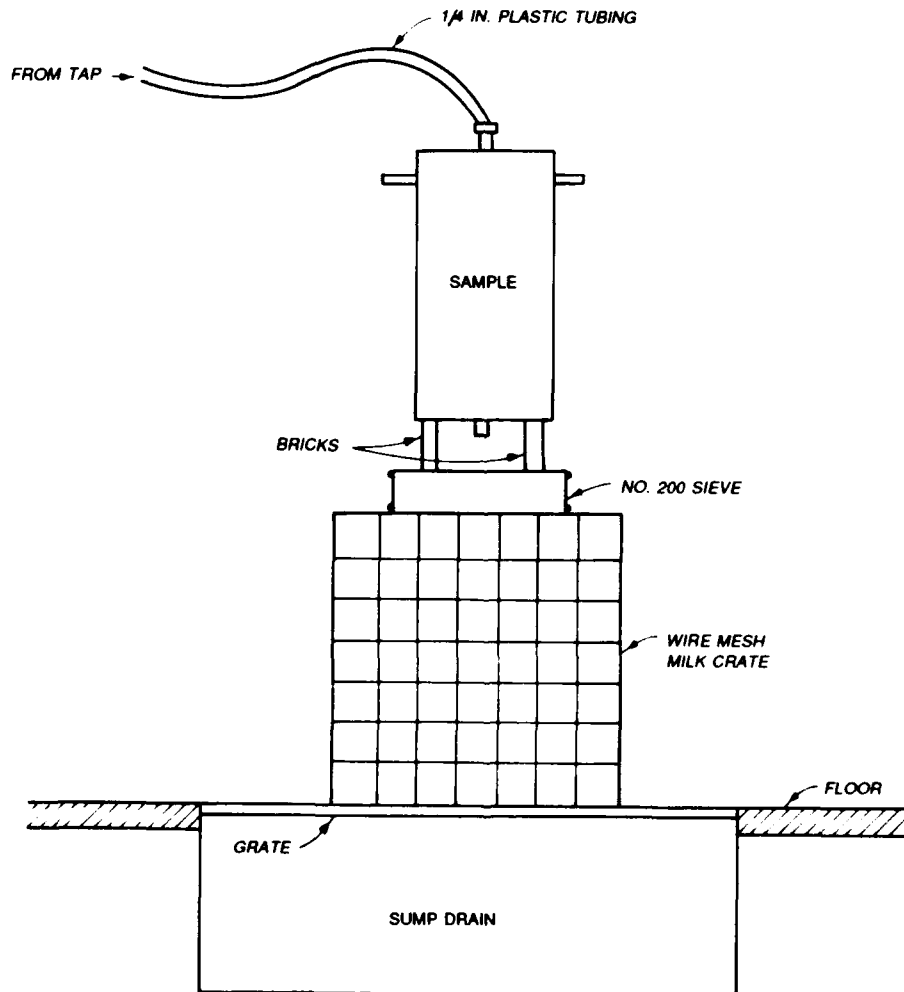


Figure 22. Schematic diagram of general erosion test setup

- b. The cylinder was allowed to cure in the open laboratory, for fear that moving the specimen might cause excessive cracking, To prevent drying of the specimen, the mold was left on so that the entire curing period and the top would keep moist. The aluminum rod was gently rotated periodically to prevent it from adhering to the concrete.
- c. At the required age, the mold was stripped and the aluminum rod removed. A 1/4-in.-diam hose carrying city water at 75 psi was then attached to the top fitting and a No. 200 sieve was placed beneath the bottom fitting.
- d. The water was turned on and flow rate calculated.
- e. The No. 200 sieve was periodically checked for eroded material. If significant material was observed, the test was stopped and the material weighed.
- f. The test was continued until it was determined that there was not change in the erosion rate.

Triaxial Testing Equipment

85. Most of the equipment used in the triaxial test program was standard soils testing equipment. Some pieces of equipment, however, were special made for this test program.

Triaxial cell and accessories

86. The following contains a listing of equipment used in the tests.

- a. Triaxial cell. Two Geotest brand model S5050 high pressure triaxial cells were used to perform all tests. A photograph and schematic diagram of one of the triaxial cells are shown in Figures 23 and 24. Extensive modification was done to the control valve system in order to make it simpler to operate and to accommodate pressure transducers. A schematic representation of the final valve scheme is included in Figure 24. All deflection measurements were corrected for the machine deflection of the triaxial cells. Critical features of the cells are:

Standard sample size	6-by 12-in. cylinder
Maximum cell pressure	400 psi
Maximum axial load	85,000 lb/ft
Piston bearing	low friction teflon sleeve
Drainage platens	dual-outlet flush through top cap and pedestal
Valve control	positive on-off brass Whitey ball valves



Figure 23. Geotest triaxial cell

Deflection measurement	0.0001-in. dial gage rigidly mounted to piston
------------------------	--

- b. Porous stones. A number of 6-in.-diam 1/8-in.-thick bronze stones were used (corundum stones were used in early tests but could not withstand the high stresses).
- c. Filter paper. Standard 6-in.-diam medium filter paper was used for all tests.
- d. Membranes. 6-in.-diam, 18-in.-long, 0.025-in.-thick latex rubber membranes were used for all tests. For most tests, two membranes were used (double membranes) with a layer of vacuum grease between them to reduce any membrane leakage.
- e. Sealing rings. 5-1/4-in.-diam, 3/16-in.-thick buna rubber O-rings were used to seal membranes against top cap and pedestal.
- f. Sealing grease. Dow Corning brand high vacuum grease was used to help seal all O-ring joints, membrane top cap/pedestal connections, and double membranes.
- g. CIUC sample mold (consolidometer). A 6-in.-diam (inside) 14-in.-long aluminum split-mold which attaches to pedestal was used to facilitate the forming of wet concrete samples inside the membrane. The device was made from stock aluminum tube cut in halves axially and machined inside to fit over membrane when

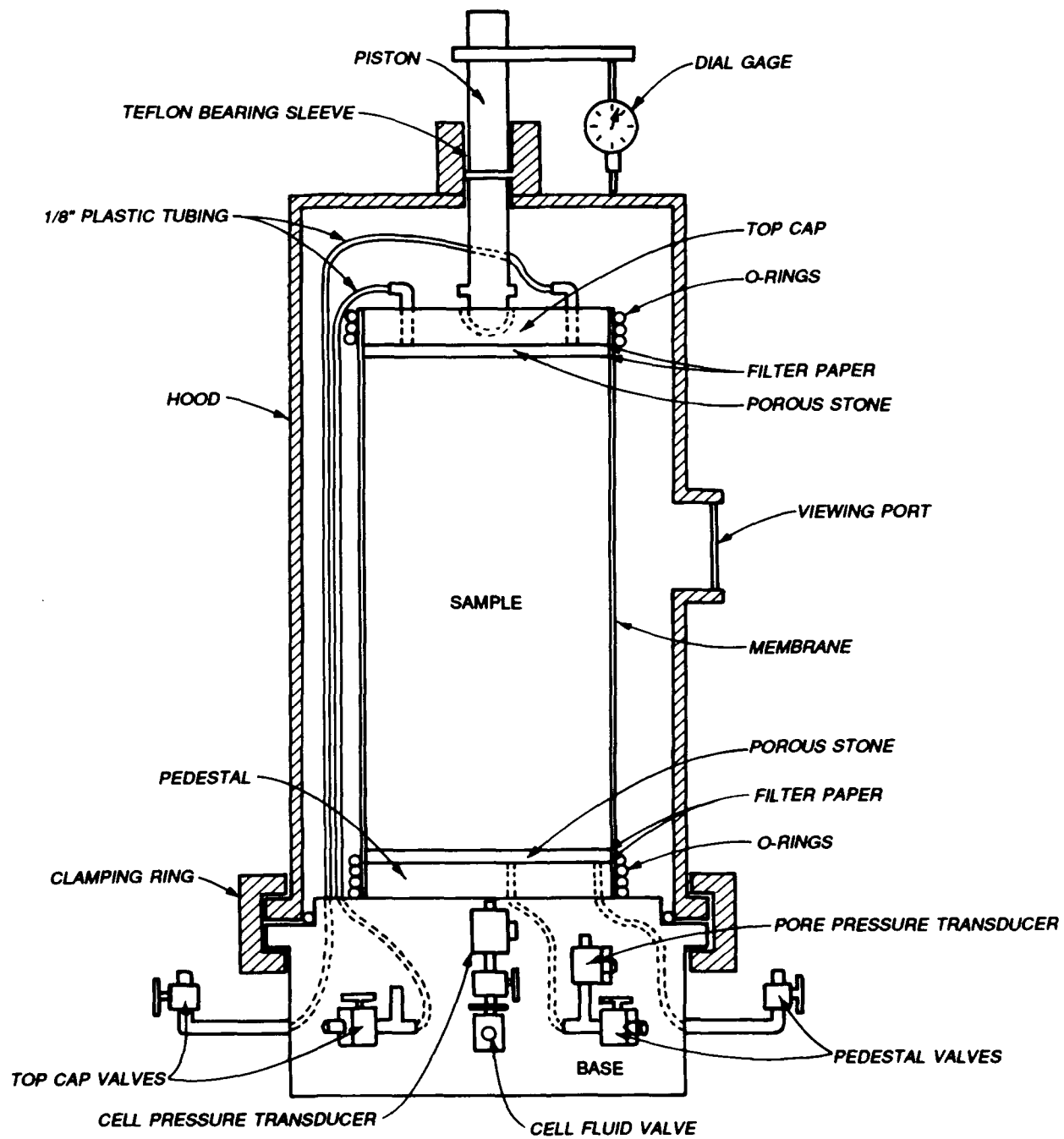


Figure 24. Schematic diagram on Geotest triaxial chamber with 6- by 12-in. sample inside

mounted on the pedestal. Halves were held together during tests by standard duct tape. Swagelok fittings were attached to each half to permit application of vacuum to hold the membrane to inner wall during sample formation.

- h. Pore pressure transducers. Validyne brand model DP15 variable reluctance differential pressure transducers were used to measure cell pressure and head difference during permeability testing for all CIUC tests. Voltage output was read by a multimeter. Transducers were calibrated, on average, every other test using a Refinery Supply Company model 35260-4 dead weight tester. The dead weight tester was calibrated annually.

Triaxial back pressure and consolidation fluid control

87. For all CIUC triaxial tests, back pressure consolidation was controlled by a Brainard-Kilman pressure control panel. A photograph and schematic diagram of the panel are shown in Figures 25 and 26. During consolidation, two accumulators were used for each triaxial cell, one controlling the top cap and the other controlling the pedestal. Each accumulator consists of 25 ml graduated pipette, precise to ± 0.05 ml, and a 100 ml (approximately) ungraduated annulus. The annulus and pipette can be used to measure volume change either alone or together, depending on flow requirements and order of precision required.

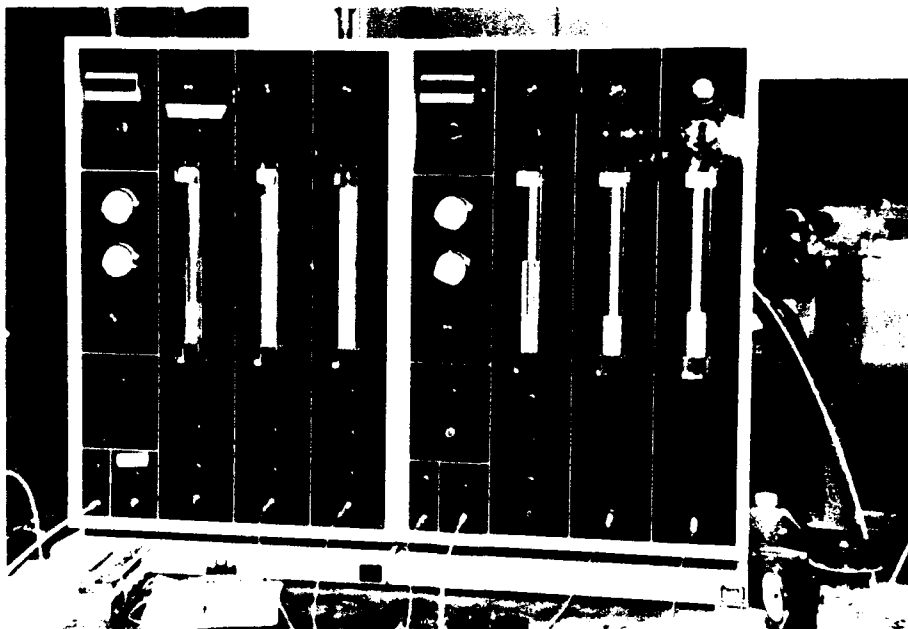


Figure 25. Two Brainard-Kilman panel boards

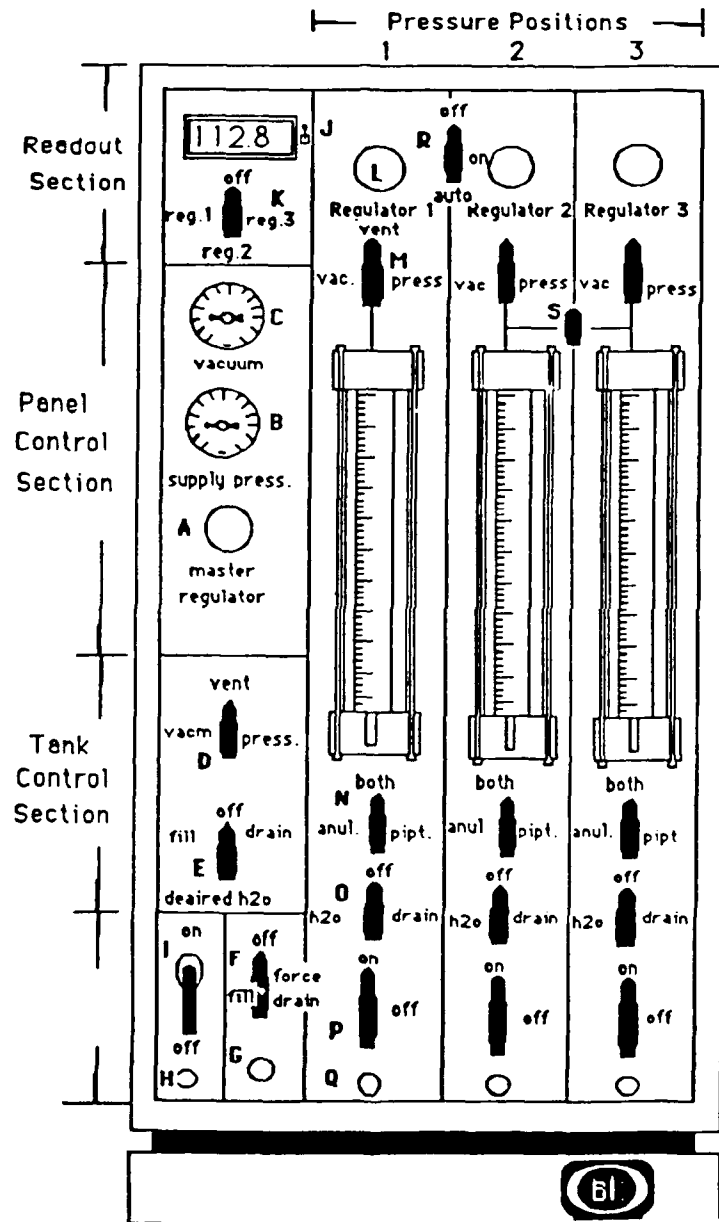


Figure 26. Schematic diagram of Brainard-Kilman panel board

88. Back pressure for each accumulator was independently controlled by a Fairchild bleeding regulator. Maximum allowable back pressure was 200 psi. Back pressure for CIUC test program was provided by an air compressor operating at 120 psi delivery pressure. Back pressure was measured in two ways:

- a. Panel board mounted transducer attached to bleeding regulators.
- b. Pressure transducer mounted on cell pedestal drainage port(s).

89. All fluid used for application of back pressure and permeability testing was de-aired tap water stored under vacuum.

Triaxial cell pressure control

90. For all CIUC and Q tests, cell pressure was applied using a gas pressure over water system. Gas pressure was supplied by high pressure (2,300 psi) nitrogen bottle fitted with a two-stage, non-bleeding union carbide regulator rated at 3,000 psi. The gas-water interface was located in a high pressure stainless steel reservoir, as shown in Figures 27 and 28.

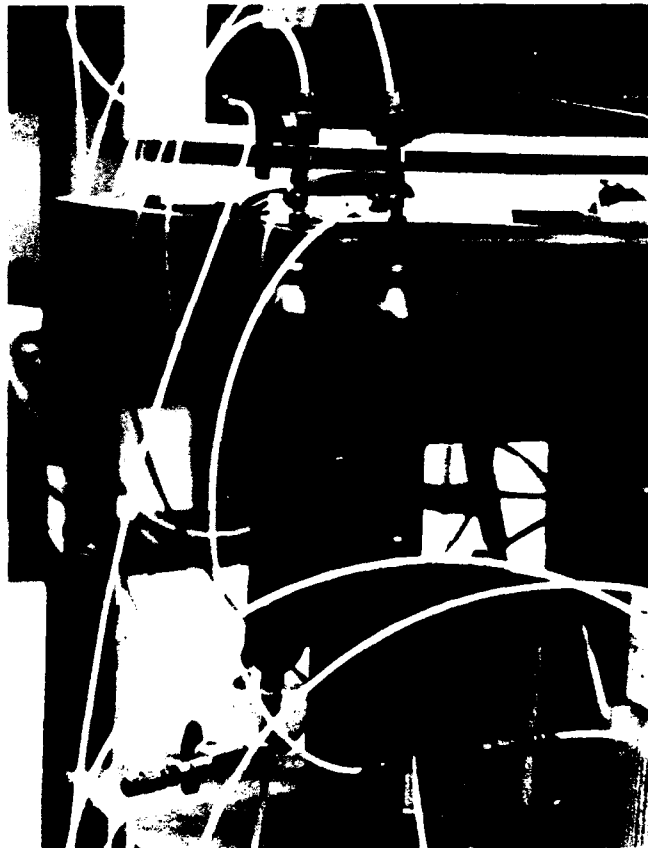


Figure 27. High pressure stainless steel reservoirs containing cell pressure glass-water interface

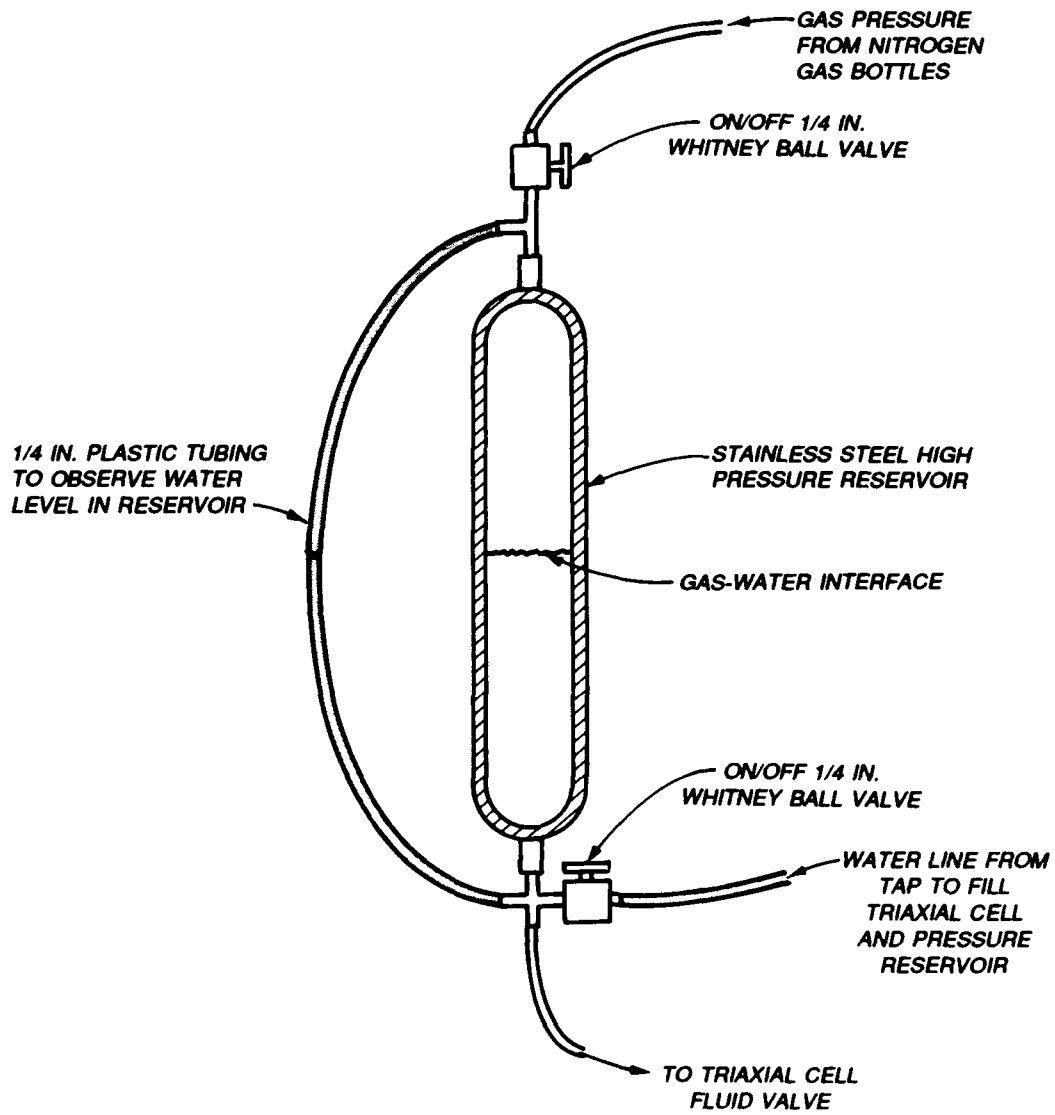


Figure 28. Schematic diagram of stainless steel reservoir containing cell pressure gas-water interface

Cell pressure was measured continually using a pore pressure transducer mounted on the triaxial cell pedestal. The observed drift over 7 days at 400 psi cell pressure was +/- 5 psi.

Q Test Procedure

91. Based on the unconfined strength and modulus data collected in Phase I, it was decided that triaxial tests would be performed on mix designs with a cement factor of 300 lb/cu yd and bentonite contents of 0, 20, and 40 percent. Effective confining pressures of 50, 100, 200, and 300 psi were chosen in order to simulate the range of horizontal confinement an element of concrete would be subjected under various depths of wet concrete after a tremie placement. Because of time limits, the curing ages evaluated were limited to 3, 7, and 14 days. Table 5 shows the bentonite content, age and effective confinement of the Q and CIUC tests conducted.

Table 5
Test Schedule for CIUC and Q Test Groups by Batch Design,
Age and Effective Consolidation Stress

<u>Percent Bentonite</u>	<u>Age Days</u>	<u>Batch ID</u>			
		<u>Effective Consolidation Stress, psi</u>			
		<u>50</u>	<u>100</u>	<u>200</u>	<u>300</u>
0	3	--	080288	091488	*
	7	--	030189	*	*
	14	--	102688	*	*
20	3	082688	080588	091088	--
	7	--	081088	082388	090188
	14	--	--	--	111688
40	3	091588	090988	091888	101488
	7	--	083188	--	092888
	14	--	102888	--	100688
			022289		

Note: All batches have nominal cement factor of 300 lb/cu yd.
 * Tests could not be performed because sample strength was beyond the capacity of the triaxial cell piston (85,000 lb).

92. The Q test procedure described in Paragraphs 93 through 97 was developed according to the procedure outlined in ASTM specification

C 801-81 (CRD-C 93-83), except as noted below. Tests were performed at a strain rate of 0.05 in./min. Deformations were measured using a 0.0001-in. precision dial gage.

Q test sample fabrication and curing

93. All samples were fabricated and cured as described in paragraphs 53 through 58.

Q test sample measurement and preparation

94. All samples were measured as described in Paragraph 60. Q tests are generally performed on uncapped specimens conforming to the planeness requirements outlined in ASTM standard C 801-81 (CRD-C93-83). Many of the Q test sample ends did not conform to ASTM planeness requirements for two reasons:

- a. Tops of samples could not be adequately leveled off during sample formation in sample molds.
- b. Bottoms of some samples were slightly convex due to the deflection of aluminum bottoms of cardboard molds under weight of samples.

95. Lack of planeness can result in "seating deflection" during shear testing. Seating deflections are deflections caused by the localized crushing of high spots on sample ends during the initial stages of compression. Seating deflections therefore result in deflection readings which are erroneously high. This in turn results in strains which are too high and an elastic modulus (i.e., stiffness) which is too low.

96. Two methods were employed in trying to meet planeness requirements. The first method, used on samples 080288-1 through 102888-1, was to shave the sample ends with a large knife. This method worked well only on soft, high bentonite (40 and 60 percent) samples with no protruding coarse aggregate or chipped edges. The second method, used on samples 111688-1 through 030189-1, was to sulfur cap the ends as described in Paragraph 62. Comparison of Q samples of the same batch design, age, and total confining stress indicates that the use of sulphur caps increases initial tangent modulus:

	<u>Uncapped</u>	<u>Capped</u>
Sample	102888-1	022289-1
Cement factor, lb/cu yd	301	308
Percent bentonite	40	40
Total confining stress, psi	100	100
Shear strength, psi	149	160
Initial tangent modulus, ksi	25	43

The problem of seating deflections during Q tests is examined in greater detail in Paragraph 143.

Q shear test procedure

97. The following procedures were used for all Q tests:
- a. A double membrane was placed over the Q test sample. The sample was then positioned on the triaxial cell base, and the membrane ends were sealed to the sides of the pedestal and top capped with O-rings and vacuum grease.
 - b. The cell hood was placed over the sample and attached to the base with a clamping collar. Care was taken not to crimp the top cap water lines. The piston was then seated against the top cap and locked into place.
 - c. The cell was filled with tap water via the stainless steel reservoir bottle and cell pressure hose. The cell hood bleed valve was kept open during filling to purge all air from cell.
 - d. The cell pressure transducer was attached to the cell base and purged of air. The triaxial cell was then positioned under the load head of the Riehle testing machine, and a brass loading block was placed on top of the piston. This loading block prevented the piston from stamping the testing machine load head during loading.
 - e. The cell pressure was applied and the pedestal valve was opened momentarily to check for leaks across the membrane. If no significant leaks (more than a few drops of water) were observed, the load head was brought into contact with the loading block and the piston was unlocked. The deflection dial gage was then adjusted on the piston to provide maximum travel.
 - f. A loading scale was chosen based on prior testing experience. Shear testing was begun and load and deformation readings were taken often enough to develop a complete stress-strain curve. As many post-peak load and deformation readings as possible were taken. The deflection dial gage was reset on the piston as necessary.
 - g. After completion of shear testing, the Q test specimen was removed from the cell and its height and diameter measured and recorded. The specimen was then marked with its batch number and stored in the wet room.

CIUC Test Sample Setup and Consolidation Procedure

98. CIUC tests were performed to simulate the behavior of plastic concrete in a cutoff wall following tremie placement. The CIUC test procedure for soils outlined in Appendix X of EM 1110-2-1906 (Headquarters, Department of the Army 1986) was used as a guideline for developing the procedure described below. In order to form a 6-in.-diam by 12-in.-high test specimen

from wet 8-in. slump concrete, it was necessary to partially consolidate the specimen under a vacuum in a split mold prior to full consolidation in a triaxial chamber. Granular, cohesionless soils are often consolidated in a similar manner. The following procedure was developed by trial and error on preliminary batches made during May, June, and July 1988. Subsequent refinements in procedure made during Phase II testing are also included here. Notations are made, when relevant, explaining why and when each refinement was done.

Setup of CIUC sample formation apparatus

99. All CIUC samples were formed wet directly on the triaxial pedestal inside a double membrane supported by a split mold consolidometer. This section describes the setup of the double membrane and consolidometer.

- a. Prior to the placement of the membrane and consolidometer on the triaxial pedestal, the pedestal and top cap drainage line-porous stone-filter paper systems were presaturated via panel board accumulators to help ensure constant saturation during consolidation. The saturation of the porous stones was maintained by sealing the porous stones to the top cap with plastic wrap and O-rings. An example of this setup is shown in Figure 29.
- b. The double membrane was constructed by placing one membrane inside another and sealing them together with enough vacuum grease such that they behaved like a single membrane. The thickness of the double membrane was then measured and recorded.
- c. The double membrane was attached to the triaxial pedestal with four O-rings and vacuum grease.
- d. The split mold was put together with two strips of duct tape wrapped around three times about 3 in. from the top and bottom of the mold. Strips of duct tape were then placed on each seam to seal the mold for subsequent application of vacuum inside split mold (to hold the double membrane against the inside wall of the split mold consolidometer).
- e. The consolidometer was mounted on the pedestal over the double membrane such that it was supported by the pile of four pedestal O-rings. The top of the membrane was then pulled tightly over the top of the consolidometer and vacuum applied to pull the membrane against the inside wall of the consolidometer. This was done to ensure uniform sample diameter. An example of this setup is shown in Figure 30.

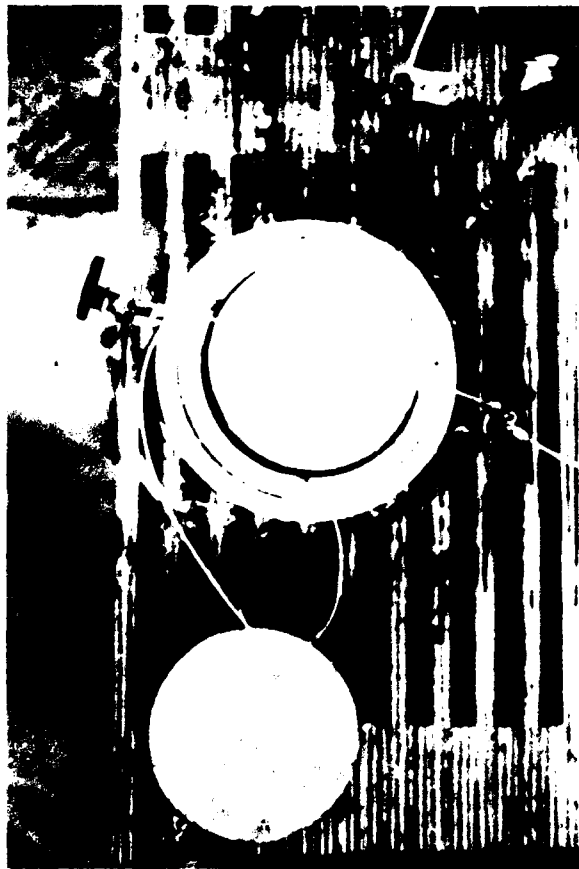


Figure 29. Presaturation of pedestal and top cap porous stones and filter paper

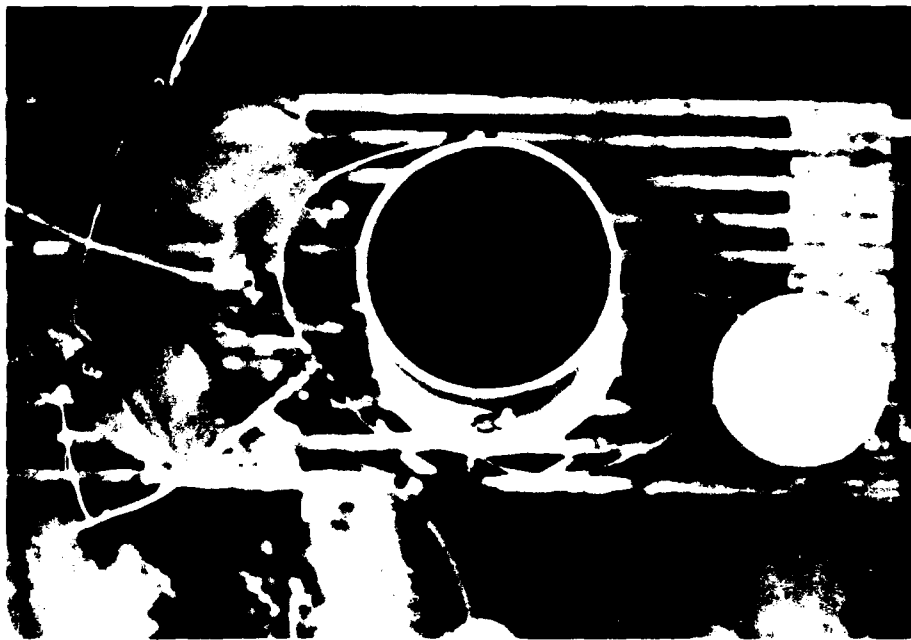
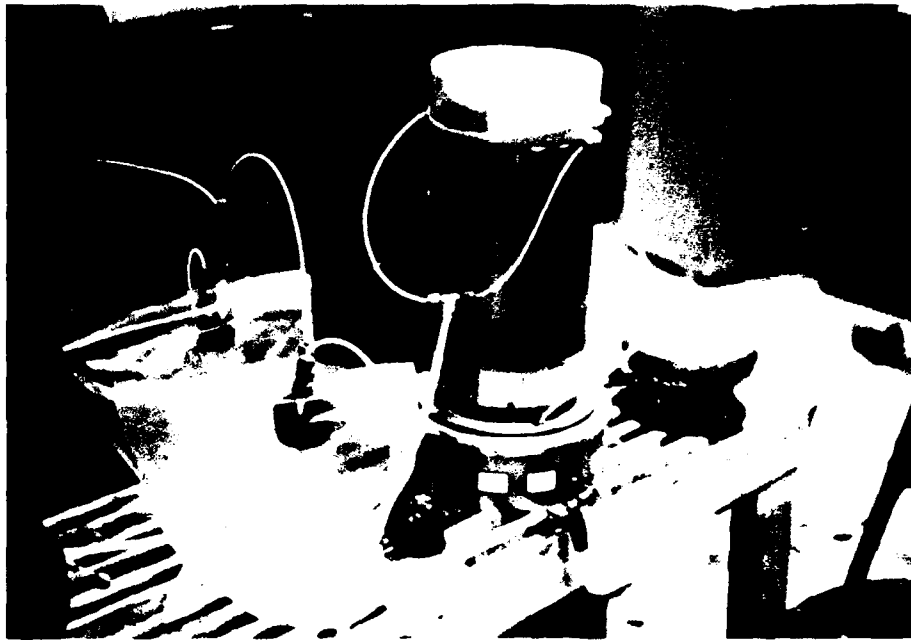


Figure 30. Spilt mold consolidometer with membrane inside just prior to formation of CIUC sample

- f. The inside depth of the membrane/consolidometer was then measured and recorded. The inside diameter of the membrane/consolidometer was then estimated by filling the membrane/consolidometer with a known quantity of water, measuring the depth of the water and using the equation:

$$D = (4V/\pi H)^{1/2}$$

where

D = average diameter

V = volume of water

H = height of water

- g. The water was then removed from the membrane/consolidometer by siphon.

Vacuum and consolidation of CIUC sample

100. The following procedures were used for vacuum and consolidation:
- a. The membrane/consolidometer was filled to approximately 1/2 in. from the top with wet plastic concrete from a container of known weight (Figure 31). The actual depth from the top of the membrane/consolidometer to the top of the wet sample was then measured and recorded.
 - b. The top cap was seated against the top of the sample. The top of the membrane was then peeled up from the top of the consolidometer and sealed against the sides of the top cap with vacuum grease.
 - c. Vacuum was then applied to the sample via the top cap and pedestal. All effluent removed from the sample by vacuum was collected in 1,000 ml. Erlenmeyer flasks were attached in series with the vacuum lines. Vacuuming was continued until approximately 100 ml of effluent was collected from both the top cap and pedestal, or until observation concluded that the sample could stand without the consolidometer. An example of this setup is shown in Figure 32. Vacuumed water is collected in glass flasks in the foreground.
 - d. The consolidometer was stripped from the sample (Figure 33). O-rings were then attached to seal the top end of the membrane against the top cap. The height of the sample was then measured at four points and the diameter measured at top, middle, and bottom.
 - e. The cell hood was placed over the sample and attached to the base with a clamping collar (Figure 34). Care was taken not to crimp the top cap water lines. The piston was then seated against the top cap and locked into place. A dial gage was then attached to the piston and the initial sample height reading was taken (Figure 34).



Figure 31. Wet plastic concrete
in split mold consolidometer



Figure 32. Plastic concrete CIUC
sample being vacuumed



Figure 33. CIUC sample after
vacuuming with consolidometer
removed



Figure 34. Dial gage mounted on triaxial cell piston for deformation measurement

- f. The cell was filled with tap water via the stainless steel reservoir bottle and cell pressure hose. The cell hood bleed valve was kept open during filling to purge all air from cell.
- g. The cell pressure transducer and the pedestal pore/pressure transducer were attached to the cell base and purged off air (Figure 35). The top cap and pedestal were then resaturated via the panel board accumulators in order to eliminate any void space caused by vacuuming.
- h. A B-value check was then performed as described in Appendix X of EM 1110-2-1906 to determine the degree of saturation of the specimen. The B-value check was performed at incremental pressures up to the final back pressure (20 to 100 psi). A 100 percent saturation was essential for accurately measuring sample pore pressures during consolidation, permeability testing, and shear testing.
- i. Consolidation under cell pressure was started as soon as the B-value check reached the final back pressure. Consolidation was generally performed in cell pressure increments of 100 psi until the final effective stress was achieved. This was done to prevent leaks by not "shocking" the sample and to help ensure uniform consolidation across the entire sample. Consolidation effluent was collected and measured in the panel board accumulators, as shown in Table 6. The accumulators

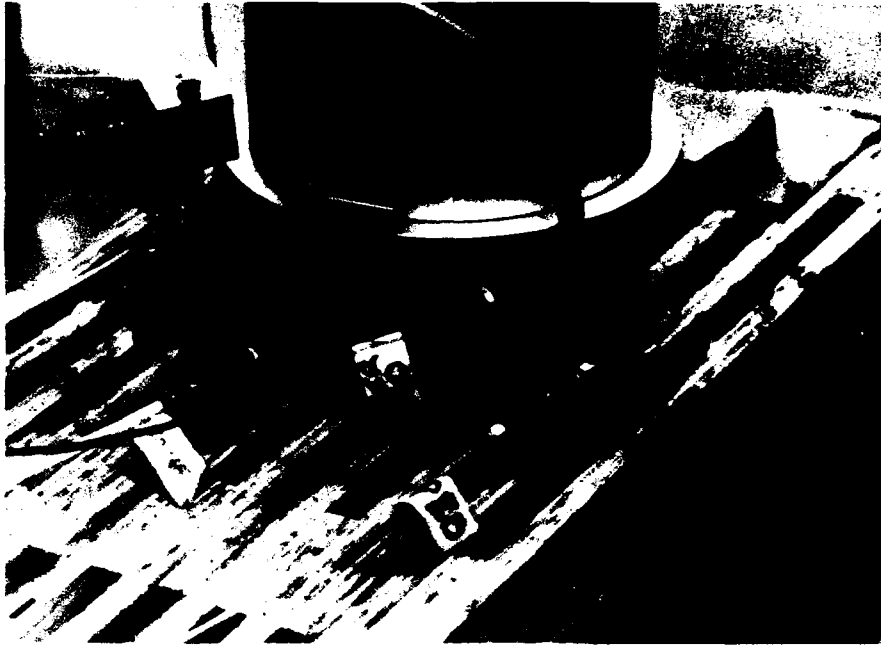


Figure 35. Close-up of pore pressure transducer setup

were drained and resent as necessary. Figure 36 shows a typical consolidation curve, plotted as change in volume versus square root of time.

Permeability Test Procedure

101. Since the primary measure of the effectiveness of a concrete cut-off wall is its ability to impede the flow of water, it was essential that the permeability of plastic concrete be measured. Therefore, constant-head permeability tests were conducted on CIUC samples during triaxial curing. Generally, permeability tests were started approximately 48 hr after the start of consolidation. This was done to ensure that consolidation was finished and that there was no leakage across the membrane. Permeability tests were started earlier on some three-day samples. This is no longer recommended, however, because sample gas generation during early curing causes inaccurate flow readings. Table 7 summarizes the CIUC tests for which permeability tests were performed.

102. The actual procedure used for all tests was developed using "The Permeability Test With Back Pressure" procedure outlined in EM 1110-2-1906 as

Table 6
Summary of Changes in Volume of CIUC Samples
During Vacuum and Consolidation

<u>Batch ID</u>	<u>Ben. %</u>	<u>σ_c psi</u>	<u>Initial Total Volume of Sample cm³</u>	<u>Initial Volume of Water in Sample</u>		<u>Water Removed During Vacuum</u>		<u>Water Removed During Consolidation</u>	
				<u>ml.</u>	<u>% of total</u>	<u>ml.</u>	<u>% of total</u>	<u>ml.</u>	<u>% of total</u>
082088-1	0	100	5478	1488	27.2	279	5.1	163	3.0
091488-1	0	200	5521	1396	25.3	215	3.9	149	2.7
030189-1	0	100	5584	1482	26.5	236	4.2	157	2.8
102688-1	0	100	5564	1492	26.8	225	4.0	159	2.9
082688-1	20	50	5701	1884	33.0	226	4.0	180	3.2
080588-1	20	100	5916	1917	32.4	242	4.1	135	2.3
091088-1	20	200	5394	1900	35.2	121	2.2	359	6.7
081088-1	20	100	5593	1875	33.5	180	3.2	294	5.3
082388-1	20	200	5397	1882	34.9	83	1.5	466	8.6
090188-1	20	300	5518	1943	35.2	77	1.4	428	7.8
111688-1	20	300	5393	1911	35.4	208	3.9	357	6.6
091588-1	40	50	5551	2259	40.7	193	3.5	178	3.2
090988-1	40	100	5449	2151	39.5	128	2.3	546	10.0
091988-1	40	200	5377	2183	40.6	239	4.4	428	8.0
101488-1	40	300	5494	2255	41.0	239	4.4	537	9.8
083188-1	40	100	5790	2247	39.1	136	2.4	232	4.0
092888-1	40	300	5490	2328	42.4	178	3.2	576	10.5
102888-1	40	100	5509	2304	41.8	208	3.8	367	6.7
022289-1	40	100	5714	2291	40.1	64	1.1	406	7.1
100688-1	40	300	5537	2225	40.2	215	3.9	546	9.9

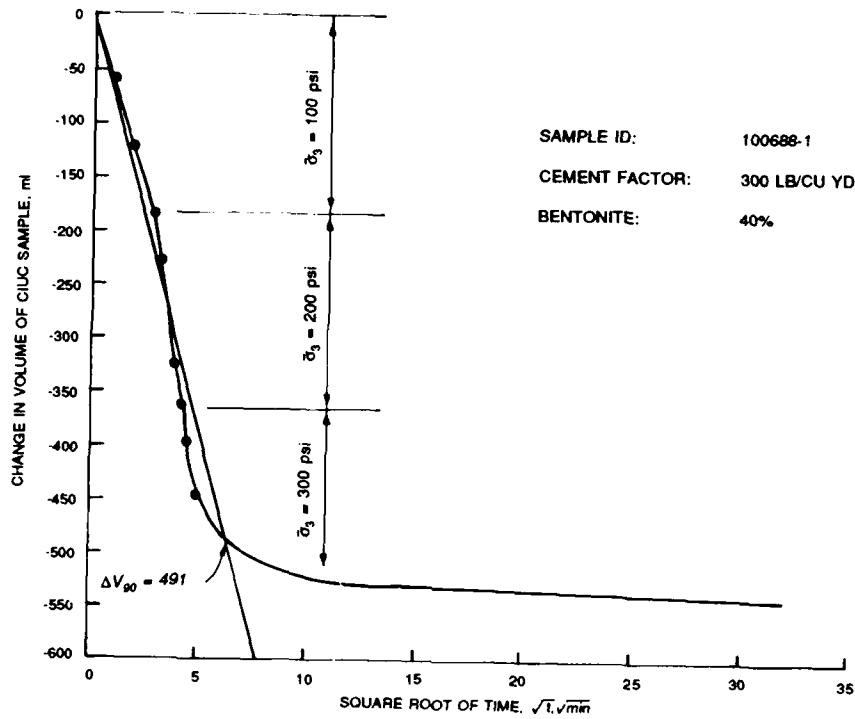


Figure 36. Typical volume change versus square root of time curve for consolidation phase of CIUC test

Table 7

Summary of CIUC Samples for which Permeability Tests were Performed

<u>Batch ID</u>	<u>Percent Bentonite</u>	<u>Age Days</u>	<u>Effective Confining Stress, psi</u>
080288-1	0	3	100
091488-1	0	3	200
030189-1	0	7	100
102688-1	0	14	100
080588-1	20	3	100
091088-1	20	3	200
081088-1	20	8	100
082388-1	20	7	200
090988-1	40	3	100
101488-1	40	3	300
092888-1	40	7	300
102888-1	40	14	100

a guide. Using this procedure, permeability was determined using Darcy's law for flow of through soil:

$$q = kiA \quad (1)$$

where

q = rate of flow of water through soil with cross-section A

k = coefficient of permeability

i = hydraulic gradient

rearranging

$$k = \frac{q}{iA} \quad (2)$$

by definition

$$q = \frac{Q}{t} \quad (3)$$

and

$$i = \frac{h_2 - h_1}{L} \quad (4)$$

where

Q = quantity of water flowing through cross-section A in time t

$h_2 - h_1$ = difference in head across sample

L = length of flow path through sample, i.e., the height of the sample after consolidation

In addition, the following assumptions can be made for a specimen tested in a triaxial cell:

$$h_2 - h_1 = \frac{P_2 - P_1}{\gamma_w} \quad (5)$$

where

$P_2 - P_1$ = the difference in pressure across the sample

γ_w = unit weight of water

Combining equation yields

$$k = \frac{QL\gamma_w}{tA(P_2 - P_1)} \quad (6)$$

103. Since L , A , and γ_w are known constants only time, flow and pressure difference need to be measured during testing. The pressure difference was established by reducing the back pressure on the top cap. Flow through the sample was then measured by periodically reading the water level in the pedestal accumulator and recording the corresponding time. Approximately 12 hr prior to shear testing, the permeability test was stopped, and the top cap back pressure was returned to the original back pressure to allow the pore pressure within the sample time to equalize.

CIUC Shear Test

104. All CIUC shear tests were performed with the Riehle testing machine at a deformation rate of 0.05 in./min. Deformation readings were read from a 0.0001 in. precision dial gage attached to the piston. The actual procedures used for all tests were as follows:

- a. The triaxial cell was positioned under the load head of Riehle testing machine and a brass loading block was placed on top of the piston. This loading block prevented the piston from indenting the test machine load head during loading.
- b. The load head of the testing machine was brought into contact with the loading block and the piston was unlocked. The change in height of the sample due to consolidation was measured by loading the piston until it reestablished contact with the top cap, and then taking a dial reading. The difference between this dial reading and the initial dial reading taken in Paragraph 100 was the change in height due to consolidation. The deflection dial gage was then adjusted on the piston to provide maximum travel.
- c. A loading scale was chosen based on prior testing experience. Shear testing was begun and load and deformation readings were taken often enough to develop a complete stress-strain curve. As many post-peak load and deformation readings as possible were taken. The deflection dial gage was reset on the piston as necessary. In addition, pore pressure readings were taken for samples 080288-1 and 022289-1.
- d. After completion of shear testing, the test specimen was removed from the cell and its height and diameter measured and recorded. The specimen was then marked with its batch number and stored in the wet room.

PART IV: UNCONFINED TEST RESULTS

105. Part IV contains summaries of the results of all unconfined compression tests, splitting tensile tests, flexural beam tests, and erosion tests. The scope of the test programs was as follows:

a. Phase I Unconfined Tests

251 UC tests
cement factors 230 to 450 lb/cu yd.
bentonite contents of 0, 10, 20, 40, and 60 percent.
ages of 3 to 660 days.

b. Phase II (Triaxial Companion) Unconfined Compression Tests

39 UC tests
cement factor 300 lb/cu yd.
bentonite contents of 0, 20, and 40 percent.
ages of 3, 7, and 14, days.

c. Phase I Splitting Tensile Tests

45 splitting tensile (Brazilian) tests
cement factors 240 to 360 lb/cu yd.
bentonite contents of 0, 20, and 60 percent.
ages of 3, 7, 28, and 90 days.

d. Phase II (Triaxial Companion) Splitting Tensile Tests

20 splitting tensile (Brazilian) tests
cement factor 300 lb/cu yd.
bentonite contents of 0, 20, and 40 percent.
ages 3, 7, and 14 days.

e. Other Phase I Tests

6 flexural beam tests
2 erodability tests

106. Summary tables of each test program are presented in Appendix D and discussed in the paragraphs below. The cement factors and water-cement ratios for all of the plastic concrete batches presented in each test series summary table are corrected for actual batch composition as described in Paragraph 62 and in the batch design example, Appendix B, Table B3.

Unconfined Compression Test Data Analysis

107. Load and deflection measurements were taken for all unconfined compression tests and used to construct stress-strain curves. Figure 37 shows the general form of a stress-strain curve and definitions of ultimate

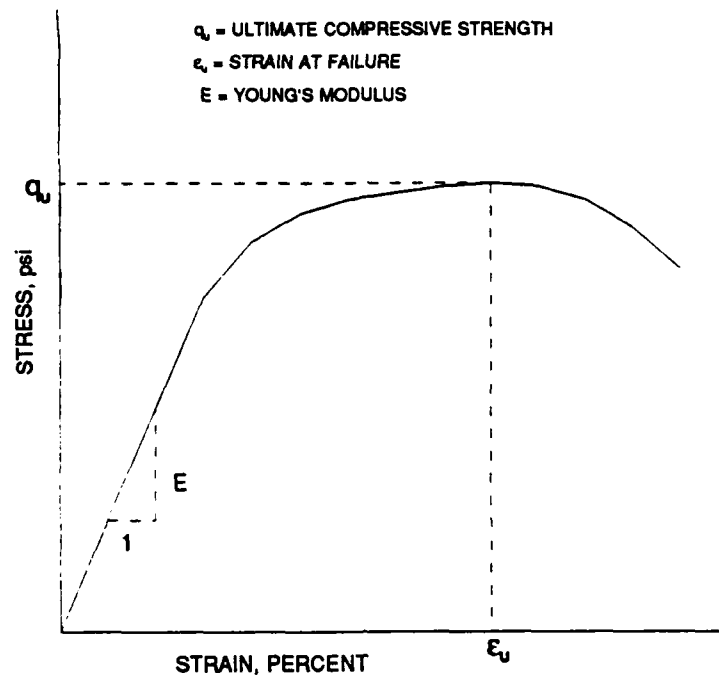


Figure 37. General form of unconfined compression stress-strain curve

compressive strength, strain at failure, and Young's modulus (elastic modulus).

108. All strains were calculated using the general equation for engineering strain:

$$\epsilon = \frac{\Delta l}{l_0} \quad (7)$$

where

ϵ = strain, in./in.

Δl = vertical deformation of specimen, in.

l_0 = initial length of specimen over which deformation is measured, in.

109. For strains measured by gross deflection, Δl is measured directly with a dial gage and l_0 equals initial height of the specimen. For strains measured with a compressometer, Δl equals one-half the dial gage deflection and l_0 equals gage length and distance between top and bottom connection points. The gage length of the compressometer used in this test program was 8 in.

110. Stress was calculated by dividing load by specimen cross-sectional area, corrected for strain:

$$\sigma = \frac{P}{A_o/(1-\epsilon)} \quad (8)$$

where

σ = stress, psi

P = load, lb

A_o = initial cross-sectional area of specimen, sq in.

ϵ = strain at load P, in./in.

and

ultimate compressive strength = $\sigma_{max} = q_u$

111. Young's modulus is defined as the slope of a line tangent to the initial linear segment of the stress-strain curve. Young's modulus for this test program was calculated using:

$$E = \frac{\sigma_b - \sigma_a}{\epsilon_b - \epsilon_a} \quad (9)$$

where

σ_b = maximum stress on the linear portion of the stress-strain curve, psi

σ_a = minimum stress on the linear portion of the stress-strain curve, psi

ϵ_b = maximum strain on the linear portion of the stress-strain curve, psi

ϵ_a = minimum strain on the linear portion of the stress-strain curve, psi

Young's modulus is reported in Table D1 in units of thousands of pounds per square inch.

112. Specimens tested using neoprene end caps are identified in Table D1 under the "strain" heading by the designation "neop". The ultimate compressive strength reported in Table D1 for tests using neoprene caps are uncorrected values. For specimens with ultimate strengths less than 3,000 psi

the use of neoprene end caps results in lower ultimate stresses when compared to specimens tested with sulphur end caps. This lowering of ultimate strengths is the result of the reduction of cross-sectional area caused by spalling of specimen ends. Spalling is caused by shear stresses developed at the neoprene-specimen interface caused by the deformation of the neoprene. The failure mode for all neoprene-capped tests was vertical splitting while diagonal failure occurred with the specimens with sulphur end caps. In order to include ultimate strengths from neoprene-capped specimens in analyses in Part VI, a plot was developed to correct ultimate strength to sulphur-capped values. The plot and its use are described in Paragraph 148.

113. No elastic modulus and ultimate strain values for specimens tested with neoprene end caps are included in Table D1. These values are inaccurate because they include the deformation of the neoprene end caps. A correction procedure for elastic modulus and ultimate strain could not be developed because the deformation of the neoprene end caps could not be measured separately. No ultimate strain and elastic modulus data from neoprene-capped samples were used in any analyses.

Results of Unconfined Compression Test Series

114. The ultimate compressive strength (q_u), ultimate strain (ϵ_u), elastic modulus (E), age, and batch design parameters for each Phase I unconfined compression test specimen are compiled by batch in Table D1. In addition, Table D1 lists the curing location and deflection measurement system used for each specimen. In order to examine the relationship of cement factor, bentonite content, and water-cement ratio to unconfined compressive strength and elastic moduli, Figures 38, 39, and 40 were constructed.

115. Figure 38 shows the relationship between cement factor and water-cement ratio for bentonite contents of 0, 10, 20, 40, and 60 percent and 8 in. wet slump. The straight lines fitted to the data sets for each bentonite content are parallel and show that, for a given bentonite content, a decrease in cement factor requires an increase in water-cement ratio to maintain an 8-in. slump.

116. Figure 39 shows the relationship between unconfined compressive strength and water-cement ratio for all curing ages and bentonite contents.

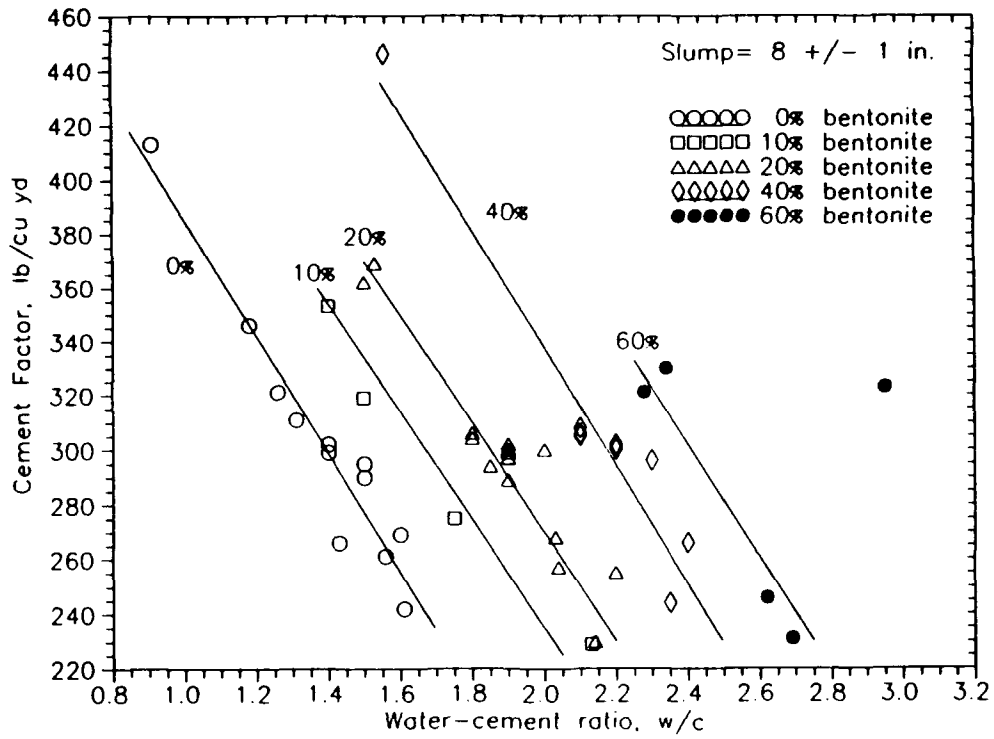


Figure 38. Cement factor versus water-cement ratio and bentonite content

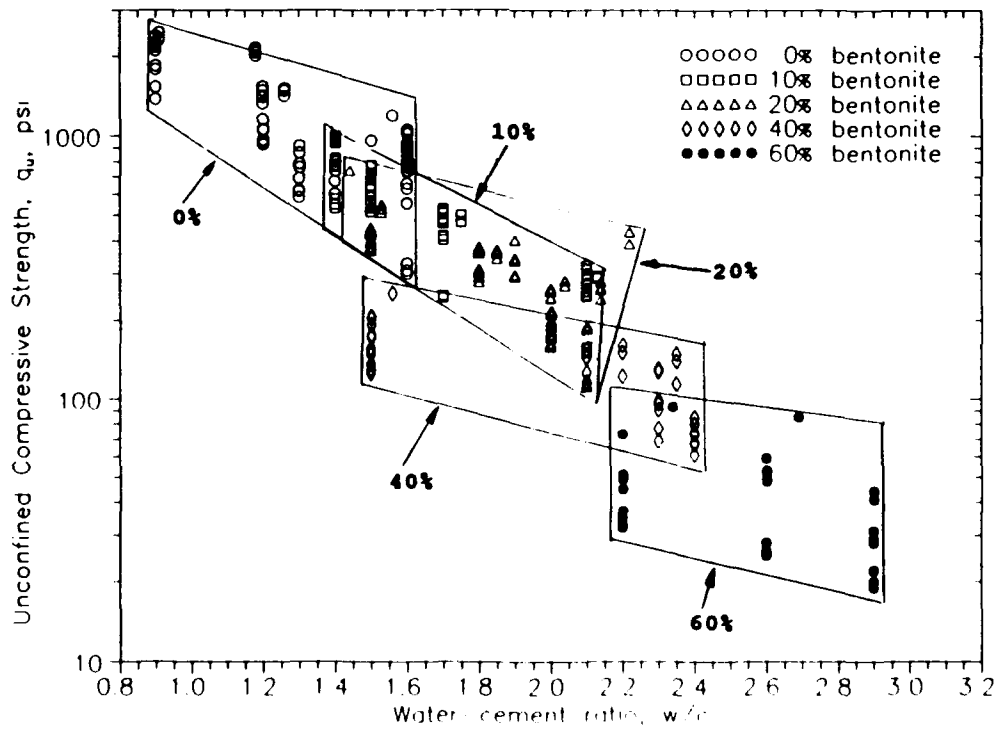


Figure 39. Unconfined compressive strength versus water-cement ratio for all bentonite contents

Each data point corresponds to one test specimen. Boxes are drawn around groups of data points with the same bentonite contents. Figure 39 shows that unconfined compressive strength decreases with the addition of bentonite for the 8-in. slump mixture.

117. Figure 40 shows the relationship between unconfined compressive strength and elastic (Young's) modulus for all ages and bentonite contents. Separate regression lines are drawn through data points with elastic moduli calculated from strain values obtained with both the compressometer and by gross deflection. Figure 40 shows that elastic modulus increases with increasing unconfined compressive strength. The influence of bentonite on elastic modulus is expressed indirectly by the influence of bentonite on unconfined compressive strength. For example, a low unconfined compressive strength corresponding to a high bentonite content obtained from Figure 39 corresponds to a low elastic modulus in Figure 40.

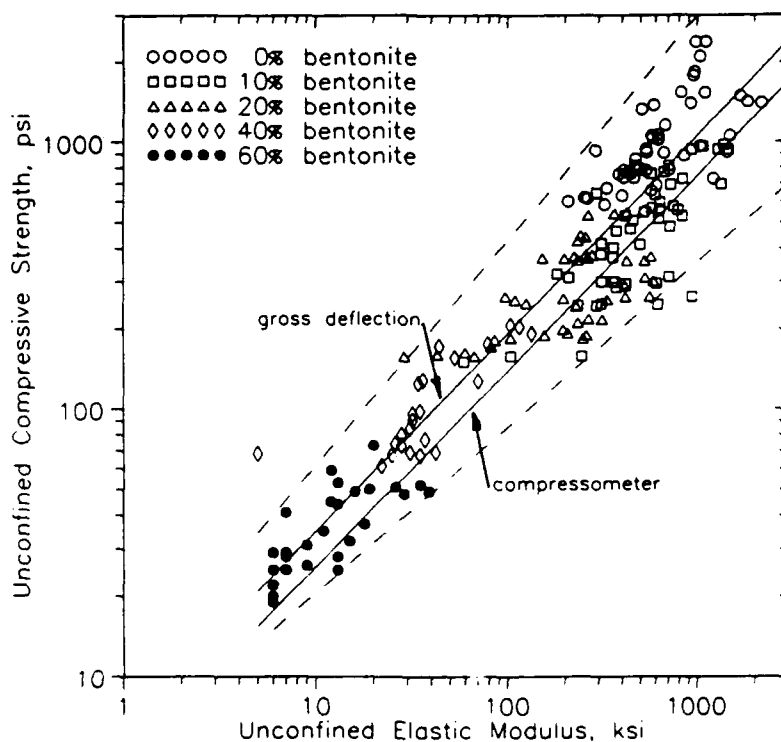


Figure 40. Unconfined compressive strength versus unconfined elastic modulus for all bentonite contents

118. The ultimate compressive strength (q_u), ultimate strain (ϵ_u), elastic modulus (E), age, and batch design parameters for each Phase II unconfined compression test specimen are compiled by batch in Table D2. Two

tests were performed for each Phase II batch. Complete stress-strain curves for each test are shown by batch in Appendix E. The Phase II unconfined compression tests were performed as companion tests to the CIUC and Q tests to ensure repeatability within a batch (i.e. that batch constituents were uniformly mixed). This was important because the estimates of initial proportions of batch constituents in CIUC samples were based on the assumption that constituents were uniformly mixed throughout the batch. In addition, the Phase II unconfined compression tests were performed to ensure that batches with the same cement factor and bentonite content (but which were formed at different times) were the same. Statistical analysis of the unconfined compressive strengths reported in Table D2 shows that the average standard deviation of unconfined compressive strength within batches is 1.7 percent with a maximum standard deviation of 6.1 percent for batch 080288-1. The standard deviations of unconfined compressive strengths between batches of the same bentonite content and age are less than 5 percent, except between batches 080288-1 and 091488-1 which have a standard deviation of 30 percent.

Error Analysis of Unconfined Compression Tests

119. In order to ensure statistical accuracy, most of Phase I batches were proportioned to provide three test cylinders for every test age. Some batches, however, had only one or two cylinders available at a given age, as shown in Table D1. This lack of cylinders was caused by three factors:

- a. Batch yields were smaller than designed, leaving fewer cylinder for high curing age tests.
- b. Tests were performed on a batch at more curing ages than initially planned.
- c. Test cylinders were damaged during capping or curing and subsequently discarded.

120. The actual average standard deviations of unconfined compression tests within test groups (specimens from the same batch tested at the same age) from test group averages are as follows:

- a. Total number of batches, Phase I 22
 - (1) range of bentonite contents 0-60 %
 - (2) range of cement factors 230 to 450 lb/cu yd
 - (3) ages 3 to 660 days
- b. Total number of test specimens 251

(1) strain measured by gross deflection	160
(2) strain measured by compressometer	71
(3) neoprene end caps used	20
c. Total number of test specimen groups (1 to 3 specimens from the same batch tested at same age)	100
d. Number of test specimen groups with only one test specimen	13
e. Average standard deviation of ultimate compressive strength within test specimen groups containing more than one specimen	4 % +/- 3 %
f. Number of test specimen groups with standard deviations from test group average greater than 10%	4
g. Maximum standard deviation within a test specimen group	14 %

The above analysis indicates that the values of unconfined compressive strength obtained in Phase I testing are accurate.

121. The actual degree of accuracy of any given test group is also dependent on the precision to which the stress-strain-strength parameters (q_u , E , and ϵ_u) can be calculated. The precision of each parameter depends on the combined precision of the measured values each parameter is dependent upon (see Paragraphs 107-113). The following is a summary of the precision of q_u , E , and ϵ_u as a function of reading error during testing:

Load Range kips	Corresponding Bentonite percent	Precision, +/-		
		q_u psi	E ksi	ϵ_u percent
3-5	60	0.6	0.8	0.0043
5-10	40	2.0	2.8	0.0043
10-20	20	4.1	10.1	0.0041
20-50	10	9.9	35.5	0.0041
50-75	0	16.4	33.9	0.0041

Conclusions from Unconfined Compression Tests

122. This section summarizes the general effects of bentonite content, cement factor, and age on unconfined plastic concrete behavior and batch characteristics as observed in Tables D1 and D2 and in Figures 38, 39, and 40. The effects of each parameter are listed in order of relative influence.

- a. Ultimate compressive strength (q_u) and elastic modulus (E)
- (1) q_u and E decrease with increasing bentonite content (Figures 39 and 40).
 - (2) q_u and E increase with increasing cement factor (Figures 38, 39, and 40).
 - (3) q_u and E increase with curing age (Tables D1 and D2).
- b. Strain at failure (ϵ_u)
- (1) ϵ_u increases with increasing bentonite content (Tables D1 and D2).
 - (2) ϵ_u decreases with curing age (Tables D1 and D2).
 - (3) ϵ_u decreases slightly with increasing cement factor (Tables D1 and D2).
- c. Water-cement ratio (resulting in 8 in. slump)
- (1) Water cement ratio increases with increasing bentonite content (Figure 38).
 - (2) Water cement decreases with increasing cement factor (Figure 38).
- d. Air content of wet concrete
- Air content decreases with increasing bentonite content (Table D1).

Results of Other Unconfined Tests

123. This section contains summaries of splitting tensile tests (Phases I and II), flexural beam tests, and erosion tests.

Brazilian splitting tensile test series

124. Brazilian splitting tensile tests were performed on 45 specimens from six batches of plastic concrete to evaluate the effect of bentonite content, cement factor, and age on splitting tensile strength. Batches with nominal cement factors of 250 and 350 lb/cu yd and bentonite contents of 0, 20, and 60 percent were chosen in order to bracket the preliminary unconfined compression series data as well as possible with a minimum number of tests.

125. A summary of the batch design and tensile strength of all Phase I test specimens is contained in Table D3. Most specimens were tested at nominal ages of 3, 7, 28, and 90 days. All specimens from the 60 percent bentonite, 250 lb/cu yd batch (062288-1), were too weak to test correctly and

were thrown out. A summary of the batch design and tensile strength of all Phase II test specimens is contained in Table D4.

126. The tensile strength of all splitting tensile tests was calculated according to the procedure outlined in ASTM designation C 496-85 (CRD-C 77-85). The peak load for all tests recorded and splitting tensile strength was calculated as follows:

$$T = \frac{2P}{\pi ld} \quad (10)$$

where

T = Brazilian splitting tensile strength, psi

P = peak load, lb

l = cylinder length, in.

d = cylinder diameter, in.

127. Conclusions on the effect of bentonite content, cement factor, and age on splitting tensile strength observed in Tables D3 and D4 are listed below in order of relative influence:

- a. Splitting tensile strength decreases with increasing bentonite content.
- b. Splitting tensile strength increases with increasing cement factors.
- c. Splitting tensile strength increases with specimen age.

Results of flexural beam series

128. One flexural beam was cast from each Brazilian tensile test batch and tested in single-point simply supported flexure at an age of 28 days. A summary of the batch designs and modulus of rupture of these tests are contained in Table D5. For each test, the peak load was recorded and the modulus of rupture calculated:

$$R = \frac{3Pl}{2bd^2} \quad (11)$$

where

R = modulus of rupture, psi

P = peak load, lb

l = length of beam span, in.

b = width of beam at point of rupture, in.

d = depth of beam at point of rupture, in.

129. Conclusions observed in Table D5 from these tests are similar to those of the unconfined compression and brazilian tensile series:

a. Modulus of rupture decreases with increasing bentonite content.

b. Modulus of rupture increases with increasing cement factor.

Results of erosion test series

130. Two tests were performed to measure the resistance of plastic concrete to erosion by seepage through cracks. Crack conditions were simulated by casting a 3/16-in. hole through each sample and flowing water through it at a velocity of 17 ft/sec. One test had a bentonite content of 0 percent and the other had a bentonite content of 60 percent. Both tests had cement factors of 300 lb/cu yd and were tested continuously between ages 3 and 8 days.

131. For all practical purposes, the tests showed that neither specimen was susceptible to piping. The 0 percent bentonite batch showed no signs of erosion over the 5-day test period. The 60 percent batch lost material at an average approximate rate of 0.05 percent of initial sample weight per day. This number is a rough estimate, however, because the amounts of material eroded on some days were too small (<0.1 grams) to measure precisely on the scale used (precise to 0.1 gram). More erosion tests need to be conducted on plastic concrete before any definitive conclusions can be drawn.

PART V: TRIAXIAL AND PERMEABILITY TEST RESULTS

132. Plastic concrete mixes with cement factors of 300 lb/cu yd and bentonite contents of 20 and 40 percent in addition to a 0 percent bentonite control mix were tested in triaxial compression to evaluate the influence of bentonite content, confinement and age on stress-strain characteristics, undrained shear strength, and permeability. Due to time considerations, it was decided that samples would be tested at 3, 7, and 14 days age. Table 5 shows the 20 different permutations of bentonite content, age, and confinement examined. In addition, one long-term CIUC (batch ID is 031889-1, bentonite content is 20 percent, effective confining stress is 100 psi, and curing age is 58 days) test was performed but finished too late to incorporate into this report. The results of CIUC test 031889-1 are used only in the discussion of pore pressure generated during shear presented in Paragraph 163.

133. For each combination of bentonite content, age, and confinement, five specimens were tested:

- a. 1 CIUC test.
- b. 1 Q test.
- c. 2 UC tests.
- d. 1 T test.

134. In addition continuous constant head permeability tests were conducted on the CIUC samples listed in Table 7 to evaluate the influence of consolidation and bentonite content on permeability.

135. The UC tests were performed as a control to evaluate the material consistency within and between batches with the same bentonite content. A summary of the UC tests is presented in Table D2 and discussed in Paragraph 114. Ideally, CIUC tests of the same bentonite content and age but different confining stresses would have been cast simultaneously from the same batch into three triaxial chambers and tested as a group. This would have eliminated any variables resulting from variations between batches. In practice, however, this procedure was unworkable for two main reasons:

- a. Only two triaxial chambers and control panels were available for use.
- b. Setup of a single CIUC test typically took 8 hr. The formation of multiple CIUC samples simultaneously would have required more personnel than were available.

136. Companion UC tests were also done to determine if correlations could be developed between CIUC, Q, and UC shear strength. In addition, companion Brazilian splitting tensile tests were performed to determine if a correlation could be developed between unconfined compression and splitting tensile strength. A summary of the results of the companion splitting tensile tests is presented in Table D4 and discussed in Paragraph 123.

Results of CIUC Tests

137. A summary of all CIUC stress-strength data is presented in Table 8. Graphical definitions of shear strength, strain at failure, and elastic modulus for CIUC tests are shown in Figure 41. Shear strength (S_u) is defined from a Mohr's circle diagram as one-half of the peak deviator stress (principal axial stress, σ_1 , minus the confining stress, σ_3). Strain at failure (ϵ_u) is defined as the strain corresponding to the peak deviator stress $(\sigma_1 - \sigma_3)_u$. Elastic modulus (E) is defined as the slope of the linear portion of the deviator stress-strain curve. Individual stress-strain curves for each CIUC test are presented by batch in Appendix E. All strain data were corrected for the machine deflection of the triaxial cells. Pore pressure readings were taken for three tests, 080288-1, 022289-1, and 031889-1 and are presented in Paragraph 163 along with corresponding A values. The cement factors and water-cement ratios and unit weights listed in Table 8 were corrected for water removed during consolidation, as summarized in Table 6.

138. Preliminary comparisons of CIUC to companion UC stress-strain-strength parameters summarized in Table D2 indicate that the shear strength, elastic modulus, and strain at failure of plastic concrete all increase with consolidation and confinement. Comparison of CIUC tests in Table 8 of the same age and effective confining stress but different bentonite contents indicates that CIUC strain at failure increases dramatically with the addition of bentonite. Similarly, CIUC elastic modulus decreases with the addition of bentonite. This suggests that the use of plastic concrete would greatly increase the ductility of a diaphragm cutoff wall, particularly at great depths.

Table 8
Summary of CIUC Test Program

Test ID	Cement Factor* lb/cu yd	Ben %	Age days	Water-Cement Ratio	Slump	Unit Weight lb/cu ft	Total		Effective Conf. Press. psi	Shear Strength psi	eu percent	E ksi	Perm cm/sec
							Conf. Stress psi	Back Press. psi					
080288-1	317	0	3	1.1	8	147.7	120	100	695	1.28	919	5.7E-08	
091488-1	328	0	3	1.0	7 1/2	150.0	250	200	1461	1.25	719	3.1E-09	
030189-1	325	0	7	1.1	7	148.0	200	100	1285	0.65	739	4.2E-09	
102698-1	317	0	14	1.1	8	146.1	200	100	1460	0.83	949	1.4E-09	
082688-1	323	20	3	1.4	8 1/2	136.8	70	50	342	1.42	292	--	
080588-1	313	20	3	1.5	8	135.3	120	100	479	1.52	1517	7.0E-09	
091088-1	348	20	3	1.4	8	146.6	250	200	770	2.76	573	5.0E-09	
081088-1	351	20	8	1.3	8 1/2	147.3	120	100	606	0.90	661	3.7E-09	
082388-1	340	20	7	1.4	8 1/4	148.7	250	200	826	1.92	361	2.5E-09	
090188-1	346	20	7	1.4	8 1/2	146.7	350	300	1010	1.73	611	--	
111688-1	340	20	14	1.3	8	143.0	400	300	1194	1.80	563	--	
091588-1	337	40	3	1.8	8 1/4	135.5	70	50	190	4.50	232	--	
090988-1	365	40	3	1.4	8	143.1	120	100	351	3.37	215	1.2E-08	
091988-1	368	40	3	1.5	8 1/2	143.7	250	200	499	5.92	468	--	
101488-1	370	40	3	1.4	8 1/4	145.1	350	300	710	8.77	244	1.2E-08	
083188-1	346	40	7	1.8	8 1/4	139.8	120	100	292	4.89	228	--	
092888-1	364	40	7	1.5	8	144.7	350	300	697	7.64	301	9.5E-10	
102888-1	357	40	14	1.6	8 1/2	142.9	200	100	417	6.44	221	9.3E-09	
022289-1	356	40	14	1.7	7 1/2	141.0	200	100	364	9.81	251	--	
100688-1	368	40	14	1.4	8	144.6	350	300	680	3.53	320	--	

* Cement factor = pounds of cement + bentonite per cubic yard of concrete;

Ben = percent of cement factor, by weight, which is bentonite;

Age = curing age, days;

Slump = wet slump, in.;

Unit weight = theoretical unit weight, lb/cu ft;

Su = shear strength = 1/2 maximum deviator stress, psi;

eu = strain at Su, percent

E = Young's modulus, kips (1,000 lb) per square in. (ksi);

Perm = lowest 24 hr average permeability, cm/sec.

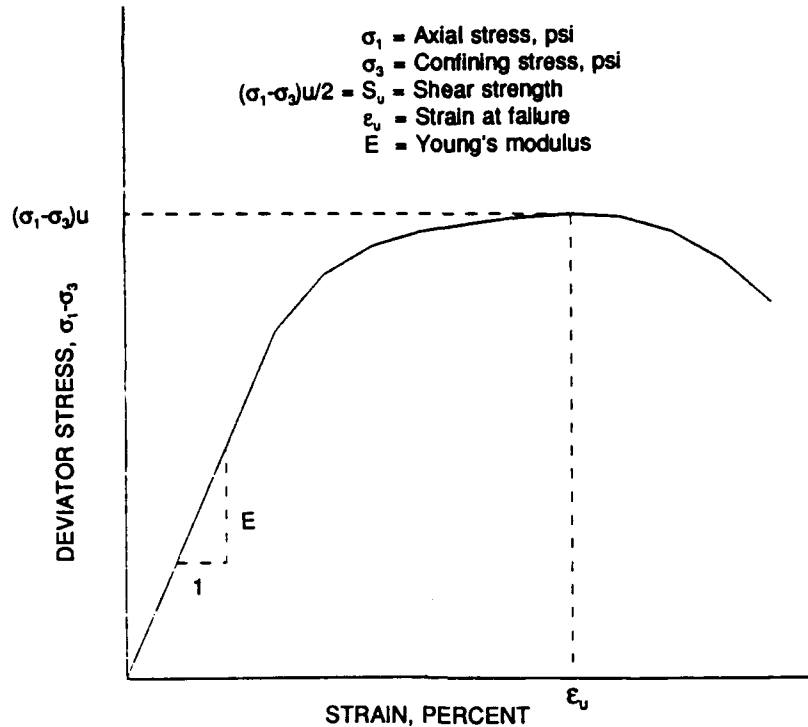


Figure 41. General form of triaxial stress-strain curve

Results of Unconsolidated Undrained Compression Tests

139. A summary of all Q stress-strain-strength data is presented in Table 9. Shear strength, elastic modulus, and strain at failure are defined as described in Paragraph 137. Individual stress-strain curves for each Q test are presented by batch in Appendix E. All strain data were corrected for the machine deflection of the triaxial cells. There is no Q test for batch 101488-1 because the sample was accidentally broken during setup. In addition, the strain at failure of the Q test specimen of batch 083188-1 could not be measured because the dial gage jammed during shear testing.

140. Comparison of Q tests in Table 9 of the same age and effective confining stress but different bentonite contents indicates that Q strain at failure increases dramatically with the addition of bentonite. Preliminary comparisons of Q to companion UC stress-strain-strength parameters summarized in Table D2 indicate that the shear strength and strain at failure of plastic concrete increase with confinement.

Table 9

Summary of Q-Test Program

Test ID	Cement Factor* lb/cu yd	%Ben	Age days	Weight per Cement Factor	Slump in.	Unit Weight lb/cu ft	Conf. Stress psi	Shear Strength psi	eu		E ksi
									percent	percent	
080288-1	290	0	3	1.5	8	144.6	100	450	2.65		81
091488-1	302	0	3	1.4	7 1/2	146.5	200	767	3.63		164
030189-1	299	0	7	1.4	7	145.2	100	511	3.68		307
102688-1	295	0	14	1.5	8	143.9	100	549	1.39		173
082688-1	304	20	3	1.8	8 1/2	133.4	49	192	3.91		40
080588-1	297	20	3	1.9	8	128.8	99	254	4.87		54
091088-1	302	20	3	1.9	8	139.7	200	345	11.32		37
081088-1	306	20	8	1.8	8 1/2	139.2	99	271	4.73		58
082388-1	298	20	7	1.9	8 1/4	138.8	199	311	3.88		94
090188-1	299	20	7	1.9	8 1/2	138.1	300	277	2.71		35
111688-1	300	20	14	1.9	8	138.8	300	561	7.97		96
091588-1	305	40	3	2.1	8 1/4	133.2	50	105	7.46		14
090988-1	306	40	3	2.1	8	133.3	100	146	13.85		14
091988-1	305	40	3	2.1	8 1/2	132.9	200	143	11.68		23
101488-1**	302	40	3	2.2	8 1/4	134.3	--	--	--		--
083188-1†	305	40	7	2.1	8 1/4	129.5	99	140	NA		19
092888-1	296	40	7	2.3	8	133.6	300	154	11.35		36
102888-1	301	40	14	2.2	8 1/2	135.0	100	149	12.03		25
022289-1	308	40	14	2.1	7 1/2	132.9	103	160	11.95		43
100688-1	300	40	14	2.2	8	129.7	300	196	10.98		33

* Cement factor = pounds of cement + bentonite per cubic yard of concrete;

%Ben = percent of cement factor, by weight, which is bentonite;

Age = curing age, days;

Slump = wet slump, in.;

Unit weight = theoretical unit weight, lb/cu ft;

Su = shear strength = 1/2 maximum deviator stress, psi;

eu = strain at Su, percent;

E = Young's modulus, kips (1,000 lb) per square in. (ksi).

** No Q-test.

† Dial gage jammed; unable to read peak strain.

141. However, all Q elastic modulus values listed in Table 9 are less than corresponding UC elastic modulus values listed in Table D2. This suggests that elastic modulus, and hence, material stiffness decrease with confinement, a conclusion not consistent with the results of the CIUC test series. Concrete subjected to confining stress should become stiffer. The most likely cause of this anomaly is lack of planeness of Q test specimen ends. Seating deflections probably occurred in the early stages of compression due to crushing of high points on specimen ends. These seating deflections resulted in higher than actual strains, and thus lower than actual elastic moduli. The Q test strain and failure values were probably influenced very little by any seating deflection. Most of the strain at failure occurs during plastic deformation, at almost constant load, long after sample seating during elastic deformation. These broad zones of plastic deformation are shown in the Q test stress-strain curves in Appendix E.

142. An attempt was made to eliminate seating deflections by sulfur capping Q test specimen ends, as described in Paragraph 94. Q test specimens 111688-1, 022289-1, and 030189-1 were sulfur capped. Comparison of the stress-strain curves of Q specimens 022289-1 and 102888-1 (same batch design, confining stress, and age of 022289-1 capped; 102888-1 uncapped) shows that sulfur capping increased elastic modulus from 25 to 43 ksi or by 72 percent. However, the Q elastic modulus of 022289-1 is still significantly less than its companion UC elastic modulus (43 ksi compared to 207 ksi or 79 percent less). This suggests that seating deflection problems still existed between the sulfur caps and the pedestal and top cap of the triaxial chamber. Thus, the Q elastic moduli values listed in Table 9 are probably incorrect and should not be used for design. The Q strain at failure values listed in Table 9 are probably nearly correct; however, they should not be used for anything except rough approximation until the Q tests are reproduced and the seating deflection problems solved.

Results of Permeability Tests

143. A summary of the CIUC batches on which permeability tests were performed is presented in Table 7. A complete compilation of all permeability tests is located in Appendix F. Table 8 lists the lowest 24 hr average permeability for each CIUC test on which a permeability test was performed.

Permeability values were calculated using the following equation, which is derived from Darcy's law for flow through soil:

$$K = \frac{QL\gamma_w}{tA(P_2 - P_1)} \quad (12)$$

where

k = coefficient of permeability

Q = quantity of water flowing through cross-section A in time t

L = length of flow path through sample

γ_w = unit weight of water

$P_2 - P_1$ = the difference in pressure across the sample

144. Permeability tests were attempted on all but the following samples:

- a. 111688-1
- b. 091588-1
- c. 091988-1
- d. 083188-1
- e. 100688-1
- f. 022288-1

145. In addition, permeability tests on samples 082688-1 and 090188-1 failed because of gas generation and/or leaks. Gas was generated within all samples during curing, a by-product of the reaction of cement. Gas pushed out of specimens formed bubbles in outflow lines and accumulators. Flow readings from outflow accumulators were therefore inaccurate and could not be used to check flow readings from inflow accumulators. All of the permeability values contained in Appendix F and Table 8 were calculated from flows read from inflow accumulators. Preliminary comparison of the 24 hr minimum permeabilities listed in Table 8 indicates that permeability decreases with increasing confining pressure and age. No definite trend can be observed as to the influence of bentonite content on permeability.

PART VI: ANALYSIS AND DISCUSSION

146. Part VI analyzes factors influencing the stress-strain-strength behavior and permeability of plastic concrete. The graphs and equations presented herein were developed to be used in a design procedure for plastic concrete cutoff walls. Particular emphasis is placed on quantifying the relationship between mix composition and stress-strain-strength behavior in order to minimize or eliminate the trial and error approach to mix design commonly used today.

147. The guiding philosophy behind the analyses was to correlate complex and time-consuming (expensive) triaxial tests to simple and quick (less expensive) unconfined tests. This allows designers to estimate triaxial stress-strain-strength parameters from unconfined stress-strain-strength data. In addition, unconfined behavior is examined at ages up to 660 days, a much longer time frame than typical project test programs allow.

Relationship of Unconfined Compressive Strength and Splitting Tensile Strength to Cement Factor and Water-Cement Ratio

148. Figures 42, 43, and 44 are companion plots for selecting a plastic concrete batch design (cement factor, water-cement ratio, and percent bentonite) which will produce a certain unconfined compressive strength and splitting tensile strength at a particular age. For a given cement factor and bentonite content, there is a unique water-cement ratio which will produce an 8 in. slump plastic concrete. Figure 42 shows cement factor as a function of water-cement ratio and bentonite content. Figure 42 was initially developed from the Phase I unconfined compression test series data (Figure 38) and was subsequently used to specify batch designs for the preliminary splitting tensile test series and the triaxial test series. In addition, Figure 43 can be used in conjunction with Figure 40 to specify unconfined elastic modulus.

149. Figure 43 shows unconfined compressive strength as a function of water-cement ratio, bentonite content, and age. Figure 43 was developed from Figure 39 by visual-fitting of data of equal curing age for each bentonite content. Because Figure 43 is difficult to read, blow-ups of each bentonite content are presented in Figures 44 to 48. These figures allow more precise

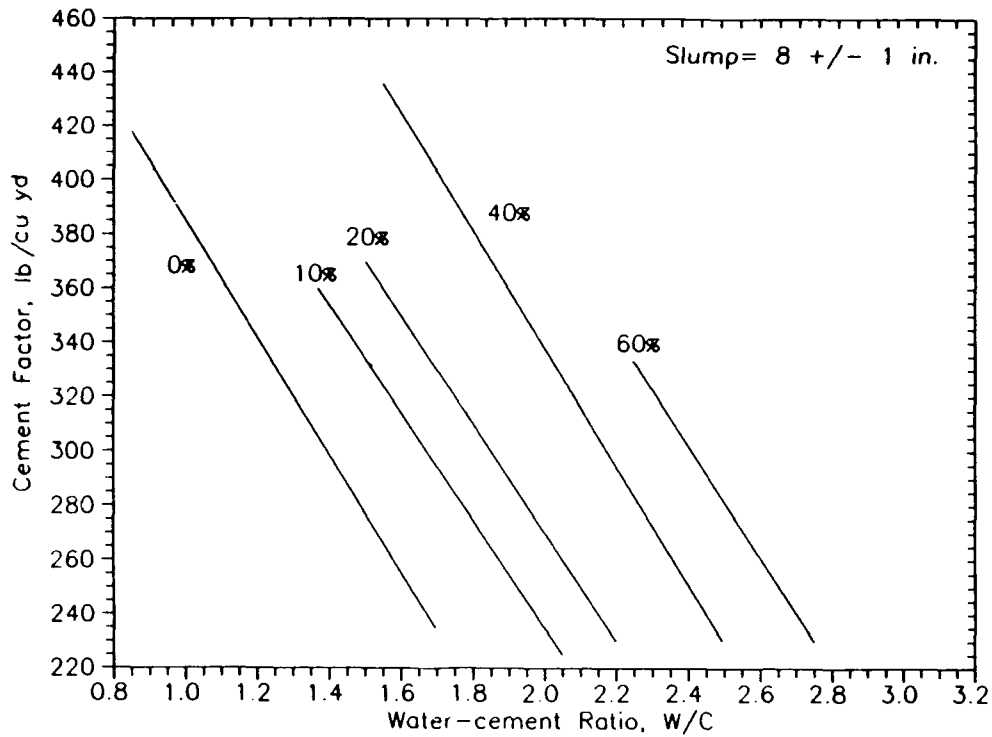


Figure 42. Cement factor versus water-cement ratio and bentonite content

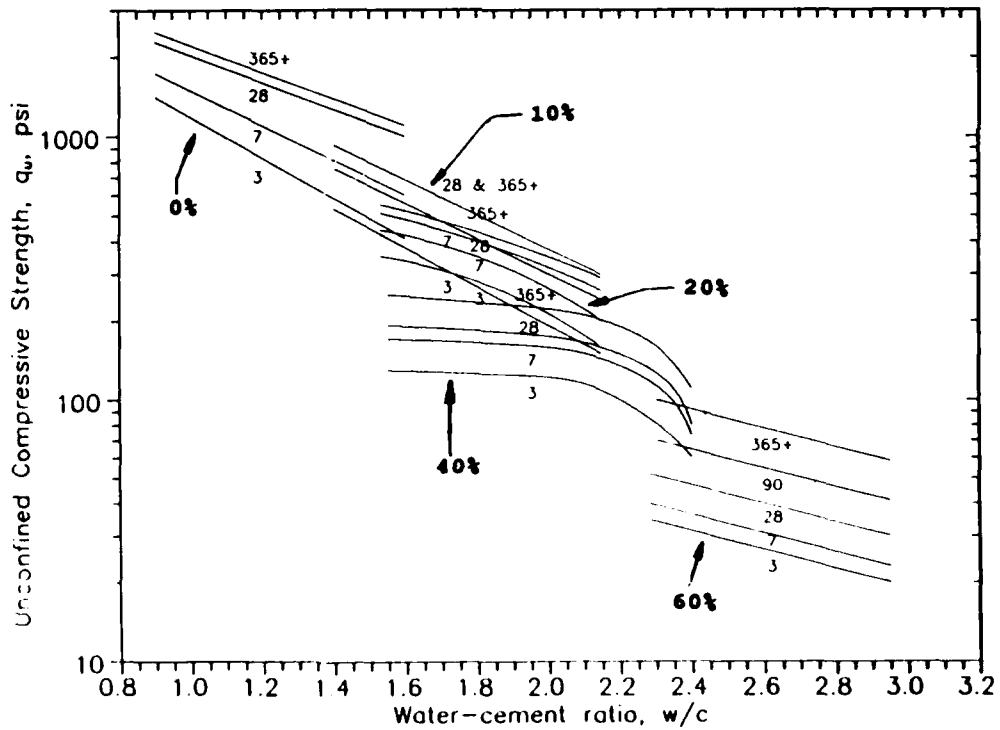


Figure 43. Unconfined compressive strength versus water-cement ratio for all bentonite contents with lines being isobars of curing age

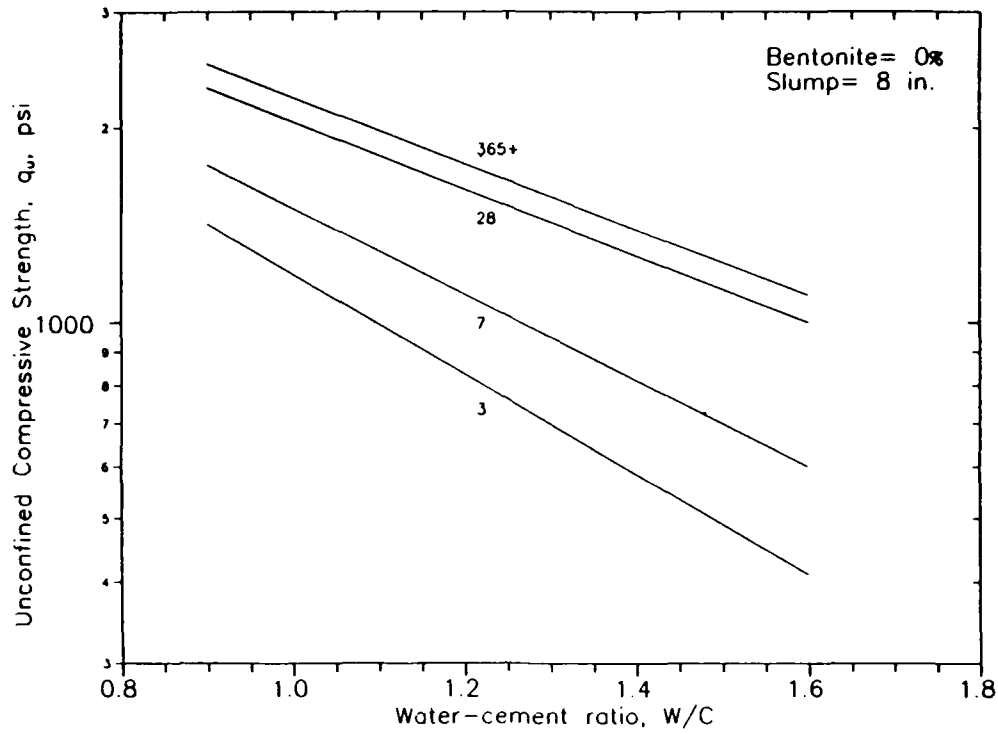


Figure 44. Unconfined compressive strength versus water-cement ratio for 0 percent bentonite content with lines being isobars of curing age

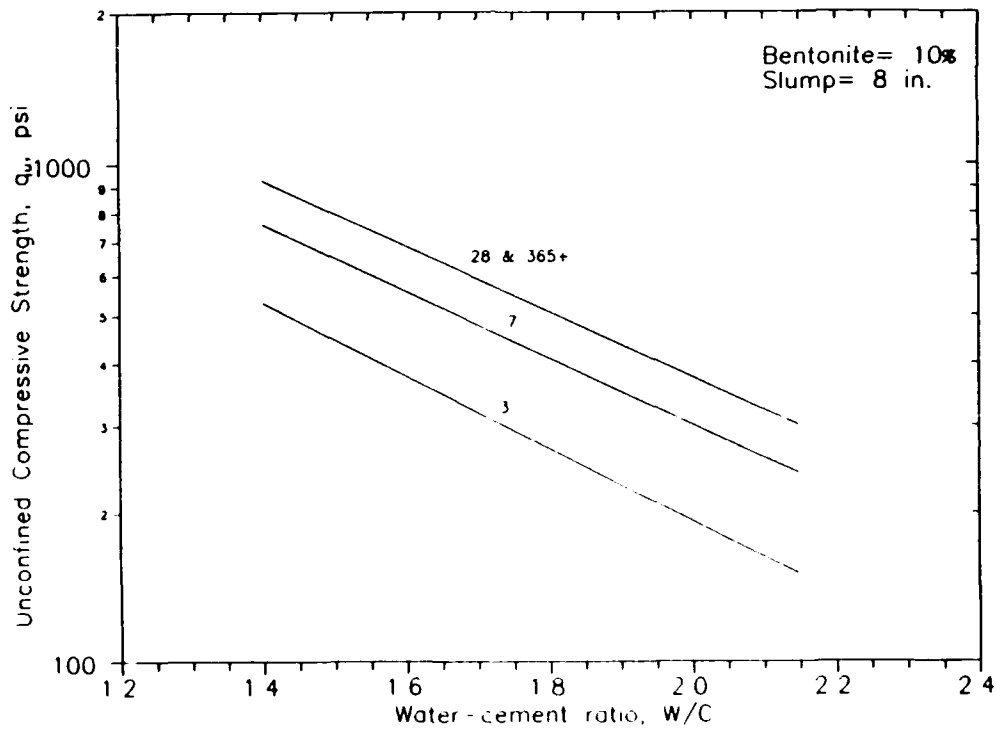


Figure 45. Unconfined compressive strength versus water-cement ratio for 10 percent bentonite content with lines being isobars of curing age

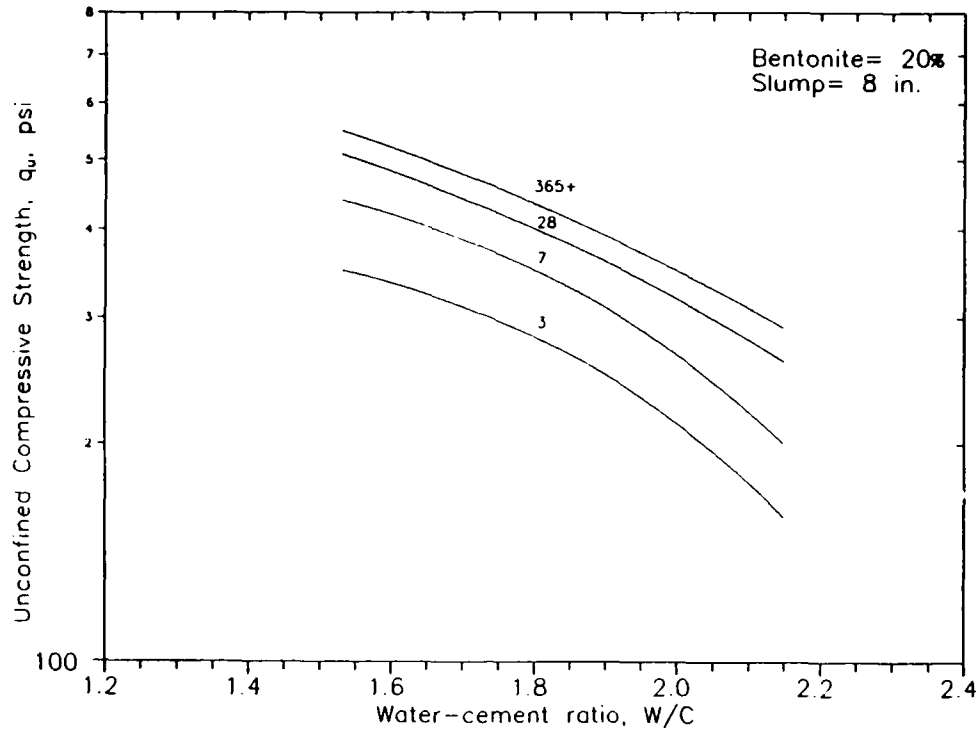


Figure 46. Unconfined compressive strength versus water-cement ratio for 20 percent bentonite content with lines being isobars of curing age

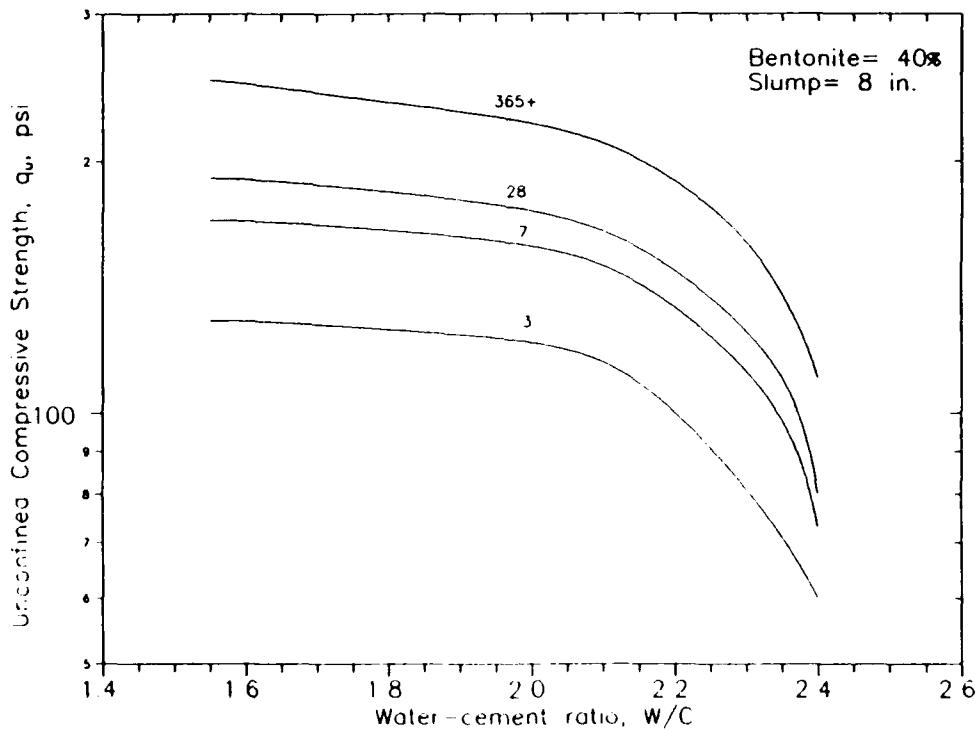


Figure 47. Unconfined compressive strength versus water-cement ratio for 40 percent bentonite content with lines being isobars of curing age

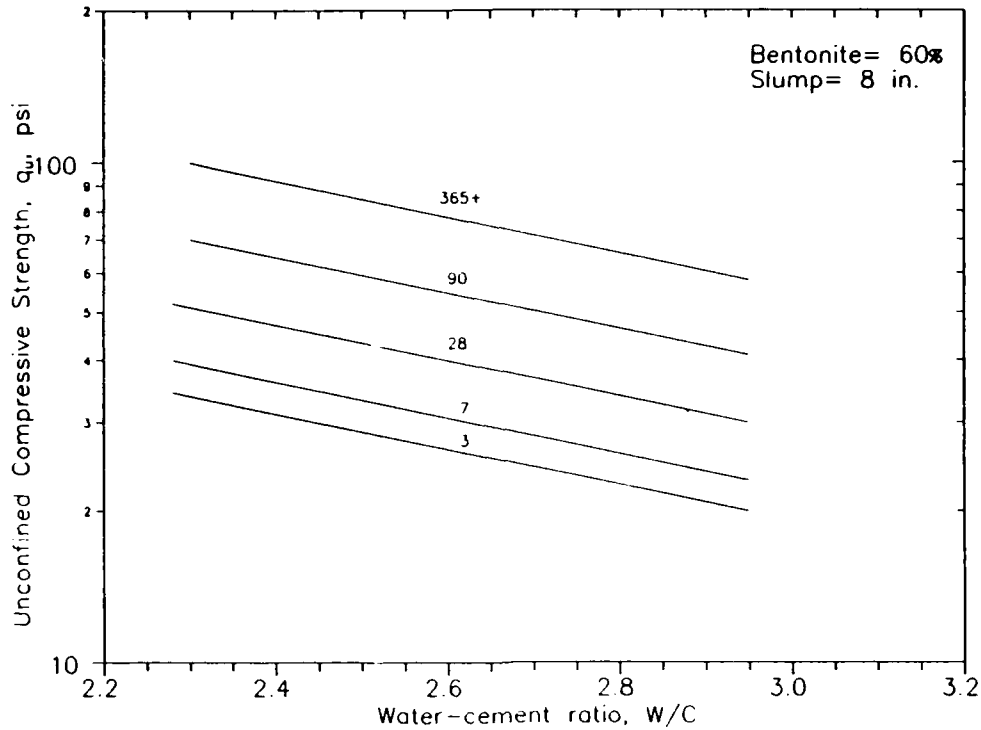


Figure 48. Unconfined compressive strength versus water-cement ratio for 60 percent bentonite content with lines being isobars of curing age

values of unconfined compressive strength and water-cement ratio to be obtained. Figure 49 similarly presents splitting tensile strength as a function of water-cement ratio, bentonite content, and age. Figure 49 is incomplete, however, because of the limited number of tensile batch designs and curing ages.

150. A designer who needs plastic concrete of a certain unconfined compressive strength and/or modulus at a certain age can enter Figures 43 to 49 and Figure 40 to obtain a corresponding water-cement ratio and bentonite content, and then enter Figure 42 to obtain the corresponding cement factor. For example, a designer has measured the unconfined elastic modulus of a proposed compacted embankment soil as 200 ksi (using a compressometer to measure deflection) and wants to specify a plastic concrete cutoff wall of matching long-term stiffness. Figure 40 yields a corresponding unconfined compressive strength of 210 psi. Figure 43 then shows a choice exists at 210 psi between 10 and 20 percent bentonite mixes at curing ages of 3 days, and a 40 percent bentonite mix at a curing age of 365+ days. Since the criterion is long-term stiffness, the designer chooses the 40 percent bentonite mix. The designer

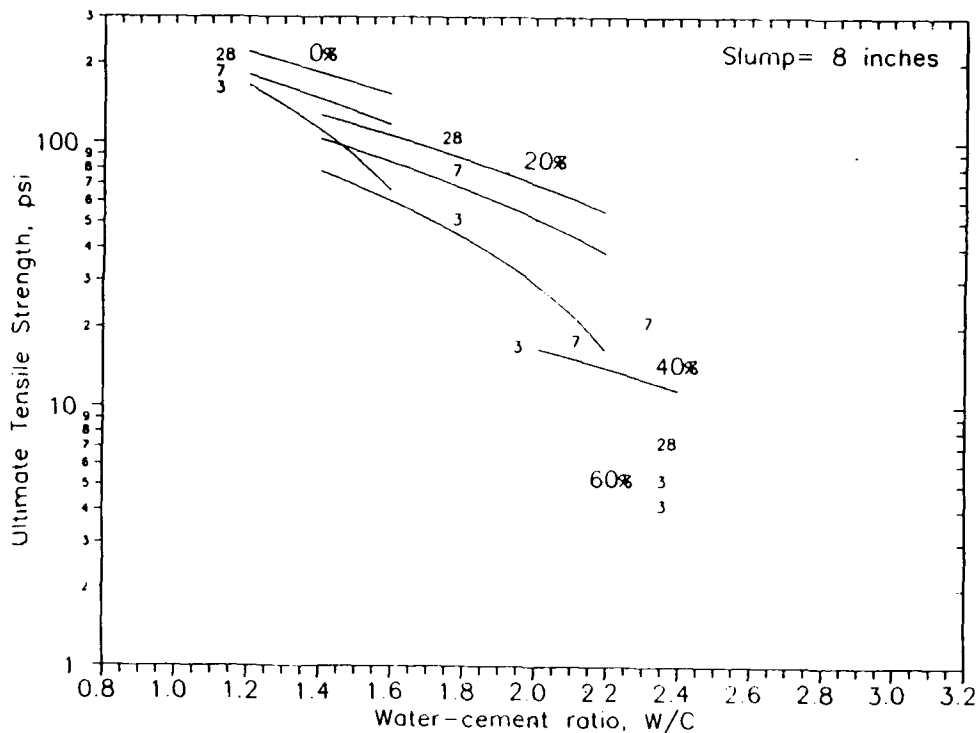


Figure 49. Ultimate tensile strength versus water-cement ratio and bentonite content with lines being isobars of curing age

then moves to Figure 47 (a blow-up of the 40 percent bentonite age lines) to estimate more precisely the corresponding water-cement ratio at 2.05. The designer then moves up to Figure 42 and reads a cement factor of 325 lb/cu yd corresponding to 40 bentonite content and 2.05 water-cement ratio. The designer thus has all the mix design parameters necessary to proportion a batch (see batch design example, Table B3). An identical procedure can be used to specify a batch design based on splitting tensile strength using Figure 49.

151. A comparison between actual unconfined compressive strengths of specimens from the (triaxial companion) unconfined compression test series and unconfined compressive strengths predicted using Figure 43 showed that the actual strengths are, on average, 7 percent greater than the predicted strengths. This indicates that Figure 43 produces slightly conservative but essentially accurate strength estimates.

152. Unconfined compressive strengths of specimens tested with neoprene end caps were included in Figure 43 after being corrected using Figure 50. Figure 50 shows that as concrete unconfined compressive strengths go below 3,000 psi, neoprene caps yield progressively lower unconfined compressive

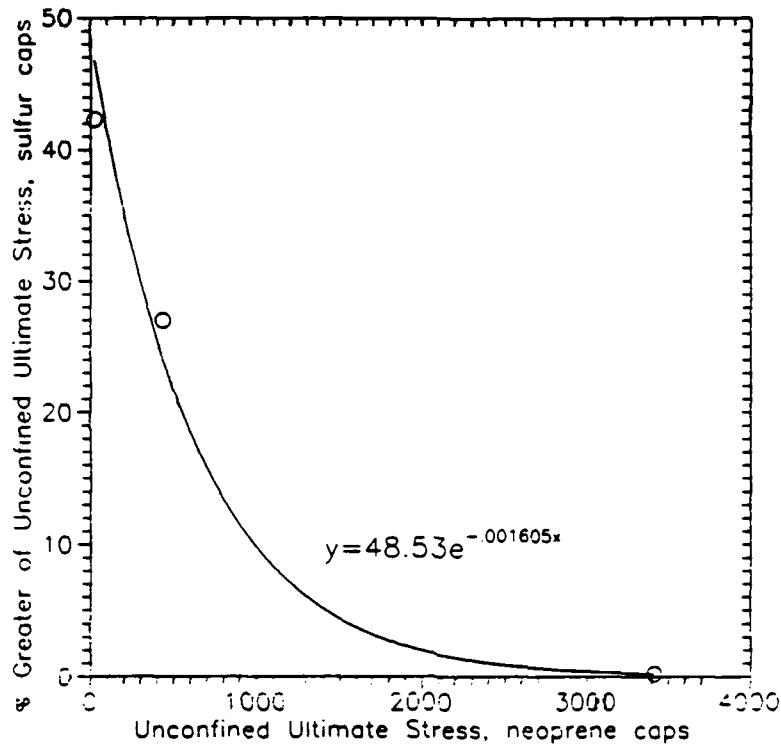


Figure 50. Unconfined compressive strength correction curve for neoprene end caps

strengths than sulphur caps for the same specimen. An example of how Figure 50 was used is as follows:

$$q_u \text{ with neoprene caps} = 1,000 \text{ psi}$$

entering Figure 50 yields percent greater of unconfined compressive strength with sulphur caps of 10 percent.

$$q_{u, \text{ sulphur caps}} = 1.10q_{u, \text{ neoprene caps}}$$

Relationship of Elastic Modulus and Strain at Failure to Unconfined Compressive Strength

153. A comprehensive design procedure requires that estimates of unconfined elastic modulus and strain at failure be calculated. In addition to Figure 40, regression analysis was performed on the normalized parameter E/q_u versus bentonite content and time to characterize the relationship between elastic modulus and unconfined compressive strength. No correlation was

observed between E/q_u and bentonite content. This suggests that the addition of bentonite has an equal effect on both unconfined elastic modulus and unconfined compressive strength. However, E/q_u as a function of age yielded the following relationship:

$$\frac{E_{comp}}{q_u} = 400 \log t_A + 1,000 \quad (13)$$

where

E_{comp} = elastic modulus, psi, calculated from strains measured with a compressometer at age t_A

t_A = concrete age, days

q_u = unconfined compressive strength, psi at age t_A

154. Equation 13 can be used in conjunction with Figure 49 instead of, or as a check on, Figure 40 to estimate the elastic modulus corresponding to a specified unconfined compressive strength or to obtain an estimate of unconfined confined compressive strength corresponding to a specified elastic modulus.

155. The relationship of unconfined compressive strength to strain at failure was examined using values of ultimate secant modulus, q_u/ϵ_u , where ϵ_u was measured with a compressometer. Figure 51 shows ultimate secant modulus as a function of sample age and bentonite content with regression lines drawn for each bentonite content. Figure 51 indicates that strain at failure decreases more slowly with age for increasing bentonite contents. Figure 51 can be used in conjunction with Figure 49 to obtain an estimate of strain at failure for a specified unconfined compressive strength. Estimates obtained using Figure 43, however, must be viewed with caution because of the high degree of scatter of q_u/ϵ_u data, as shown in Figure 51, particularly for 0 and 10 percent bentonite contents.

Relationship between Unconfined Compressive Strength and Splitting Tensile Strength

156. Splitting tensile tests were included as part of the triaxial companion unconfined tests in an effort to develop a simpler relationship between unconfined compressive strength and splitting tensile strength than

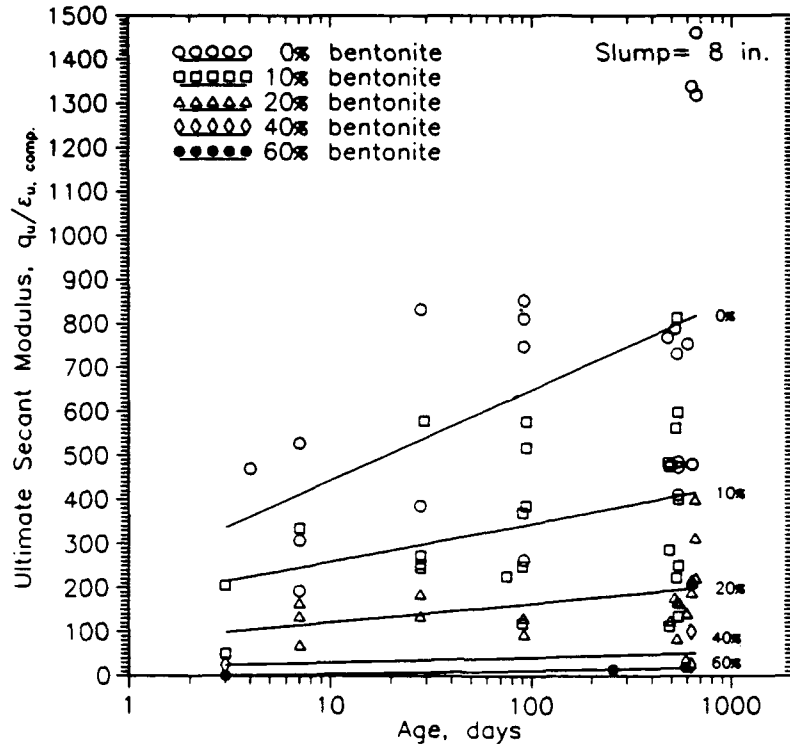


Figure 51. Ultimate secant modulus, q_u/ϵ_u , versus curing age and bentonite content with all strains (ϵ_u) measured with compressometer

offered by Figures 43 and 49. Figure 52 shows normalized values of splitting tensile strength (T) divided by unconfined shear strength (S_u or US, = $q_u/2$) for each Phase II test plotted against unconfined shear strength.

157. From Figure 52 it appears that T/US is about constant at 0.26 and is independent of bentonite content and age. This allows a designer to eliminate the use of Figure 49 to obtain an estimate of tensile strength corresponding to a given unconfined shear strength. The use of T/US is limited, however, because it was developed only from data with cement factor equaling 300 lb/cu yd and ages 3 to 14 days. Further study must be conducted before this equation can hold for the full range of cement factors and ages contained in Figure 43.

Effect of Curing Age and Bentonite Content on Unconfined Compressive Strength

158. Figure 53 shows a plot of unconfined compressive strength as a function of curing age and bentonite content. Regression lines are drawn for

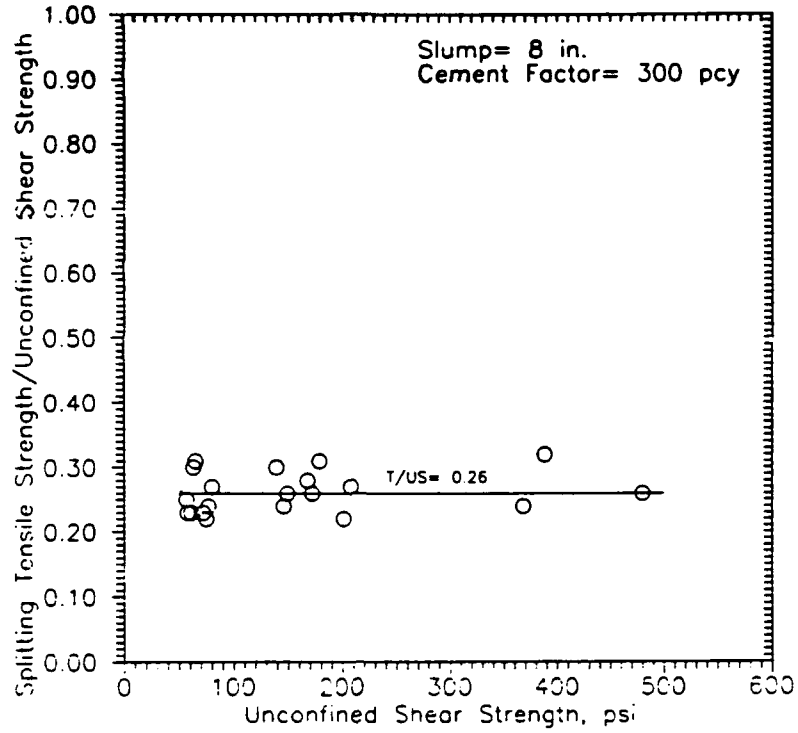


Figure 52. Splitting tensile strength/unconfined shear strength versus unconfined shear strength

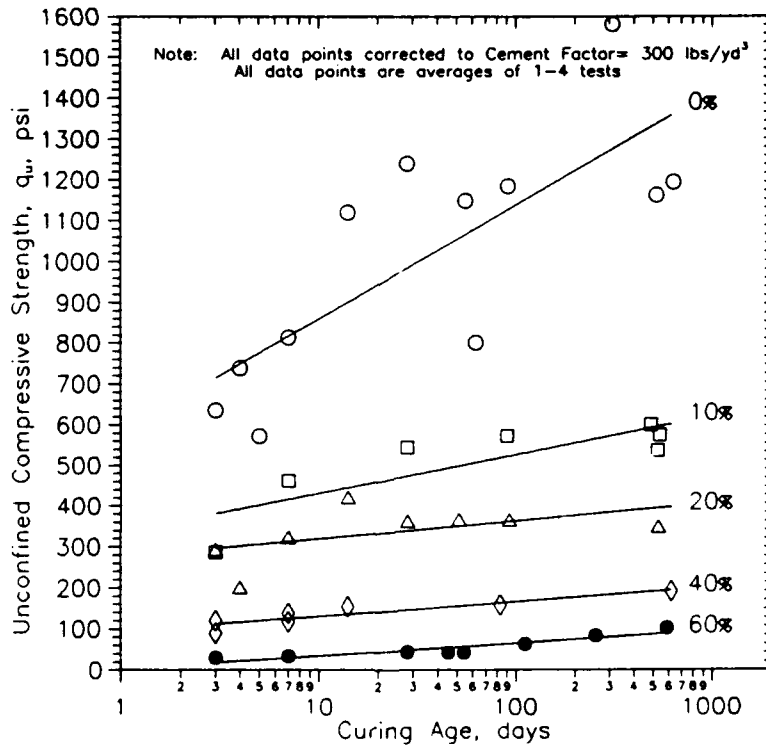


Figure 53. Unconfined compressive strength, q_u , versus curing age and bentonite content

each bentonite content. All the data points shown are averages of 1 to 4 tests and were corrected to a cement factor of 300 lb/cu yd using Figure 43. The equations for the regression lines are as follows:

$$\begin{aligned}
 q_{u, 0\%} &= 278 \cdot \log(\text{age}) + 580 \\
 q_{u, 10\%} &= 95.6 \cdot \log(\text{age}) + 340 \\
 q_{u, 20\%} &= 45.6 \cdot \log(\text{age}) + 280 \\
 q_{u, 40\%} &= 40.0 \cdot \log(\text{age}) + 100 \\
 q_{u, 60\%} &= 26.1 \cdot \log(\text{age}) + 0
 \end{aligned}
 \tag{14}$$

where q_u is in units of pounds per square inch and age is in units of days. The percent increase in unconfined compressive strength between ages of 3 and 600 days for each bentonite content are:

<u>Bentonite Content</u>	<u>Percent Increase in q_u, 3-600 days</u>
0%	90%
10%	58%
20%	36%
40%	85%
60%	300%

159. Figure 53 shows that the addition of bentonite to concrete decreases the rate of increase in unconfined compressive strength with curing age. No clear trend, however, is evident in the percent increase in unconfined compressive strength between ages of 3 and 600 days. Figure 53 does indicate that mix designs with 60 percent bentonite develop long-term unconfined compressive strength much more slowly than mix designs with bentonite contents of 0 to 40 percent.

Effect of Consolidation on Cement Factor and Water-Cement Ratio

160. For all CIUC tests the amount of water removed during consolidation was carefully measured in order to better understand the influence of consolidation on the stress-strain-strength behavior of plastic concrete. Table 6 summarizes the amount of water removed during consolidation for each CIUC test. The cement factor and water-cement ratio of a CIUC sample are defined as:

$$CF = \text{weight of cement+bentonite in sample} * \frac{1 \text{ cu yd}}{\text{volume of sample}}$$

$$W/C = \frac{\text{weight of water in sample}}{\text{weight of cement+bentonite in sample}}$$

161. During consolidation, water is removed and the total volume of a CIUC sample is reduced, but the amount of cement is assumed to remain constant. Thus, the cement factor of the sample is increased and the water-cement ratio of the sample is decreased.

162. Figures 54 and 55 are companion plots which show cement factor and water-cement ratio as a function of consolidation stress and bentonite content when initial (prior to consolidation) cement factor equals 300 lb/cu yd. Figure 54 shows that, for all bentonite contents, the rate of increase of cement factor decreases as consolidation stress increases. This is due to the reduction of the compressibility of the sample as the particles in the concrete matrix are squeezed closer together by the consolidation stress. Figures 54 and 55 can be used to predict the change in cement factor and water-cement ratio which will occur during consolidation under a given confining stress.

Effect of Bentonite Content on Pore Pressure Generation and Stress Path

163. Pore pressure readings were taken for the CIUC tests of batches 080288-1 (bentonite content at 0 percent), 031889-1 (bentonite content at 20 percent) and 022289-1 (bentonite content at 40 percent). Plots of deviator stress ($\sigma_1 - \sigma_3$), change in pore pressure (Δu), and pore pressure coefficient A ($\Delta u / \Delta \sigma_1$) versus axial strain (ϵ) are shown in Figures 56, 57, and 58. The effective and total stress paths for each test are shown in Figures 59, 60, and 61. Figures 56 through 61 show that greater pore pressures are developed for higher bentonite contents. All of the tests have values of A_{\max} less than 0.1, indicating that pore water carries relatively little of the load applied during shear. Figure 59 shows that the total and effective stress paths for 0 percent bentonite content samples are essentially identical. However, Figures 60 and 61 show the excess pore pressures generated during

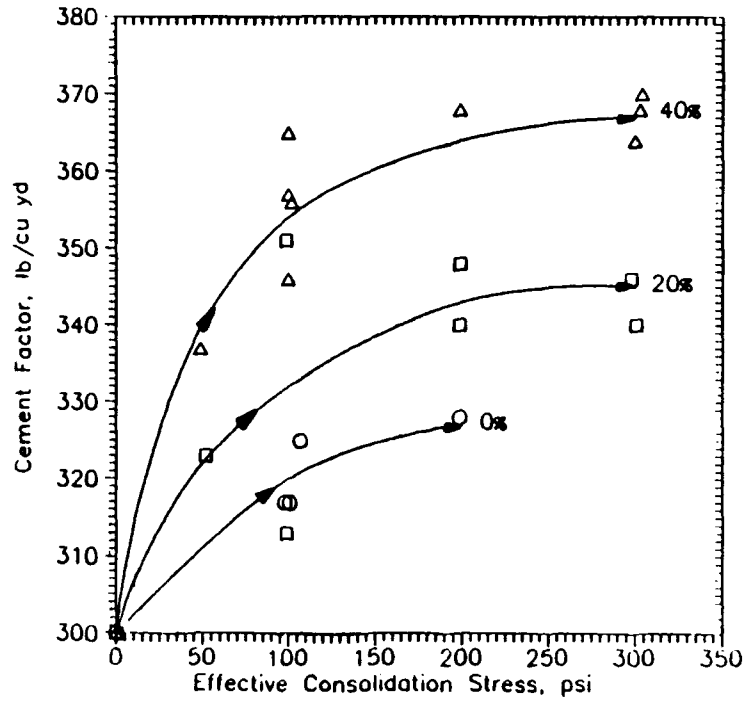


Figure 54. Cement factor versus effective consolidation stress

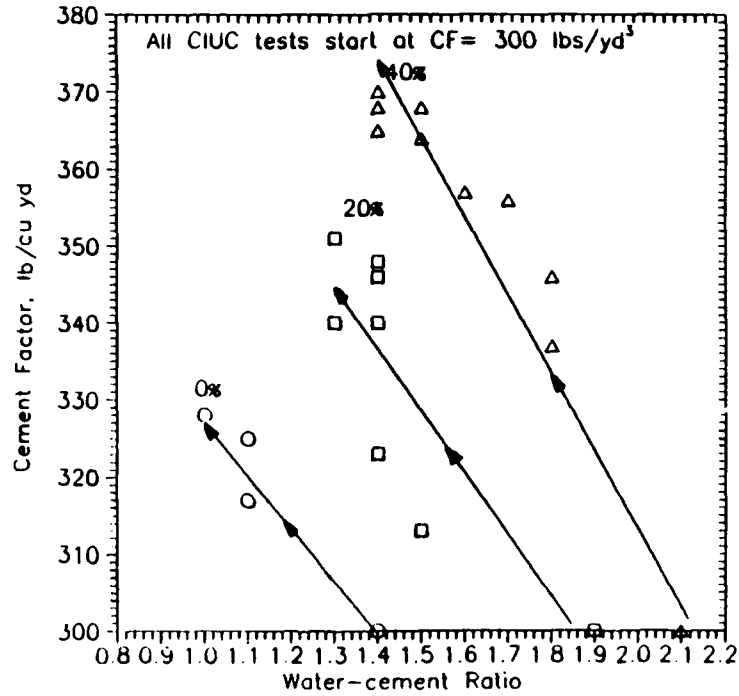


Figure 55. Cement factor versus water-cement ratio during consolidation

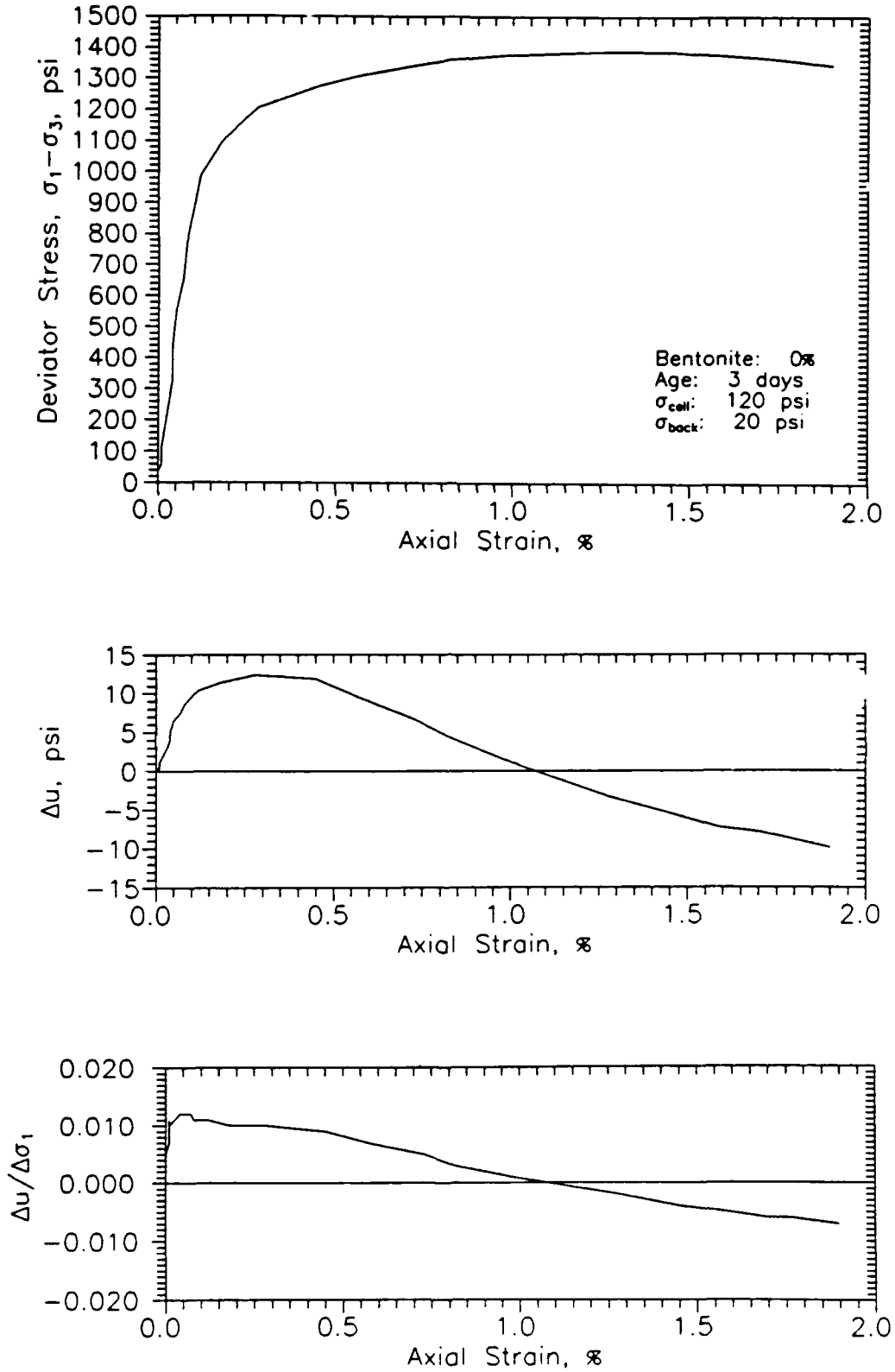


Figure 56. Deviator stress, change in excess pore pressure and pore pressure parameter A versus axial strain for CIUC test 080288-1

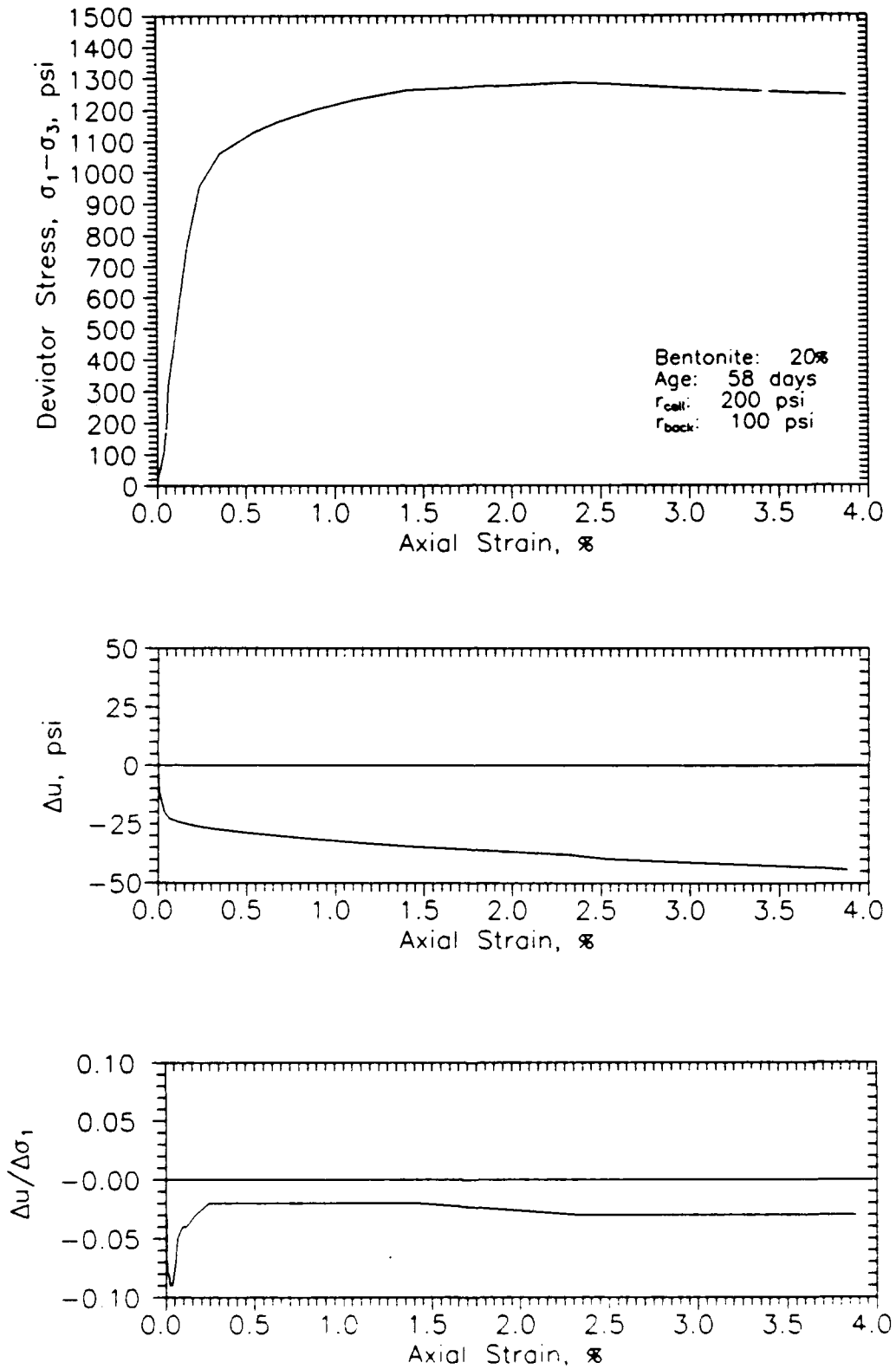


Figure 57. Deviator stress, change in excess pore pressure and pore pressure parameter A versus axial strain for CIUC test 031889-1

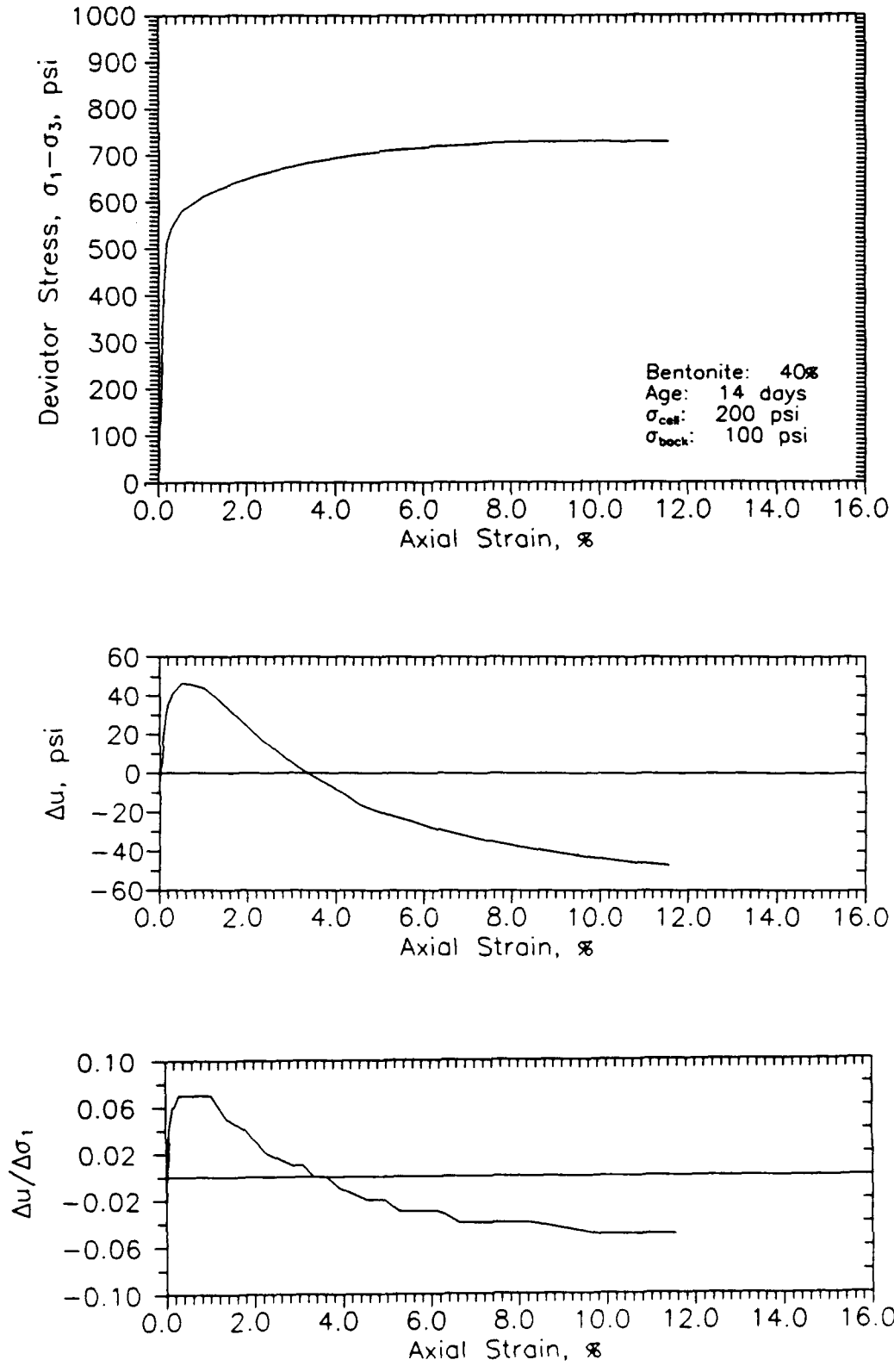


Figure 58. Deviator stress, change in excess pore pressure and pore pressure parameter A versus axial strain for CIUC test 022289-1

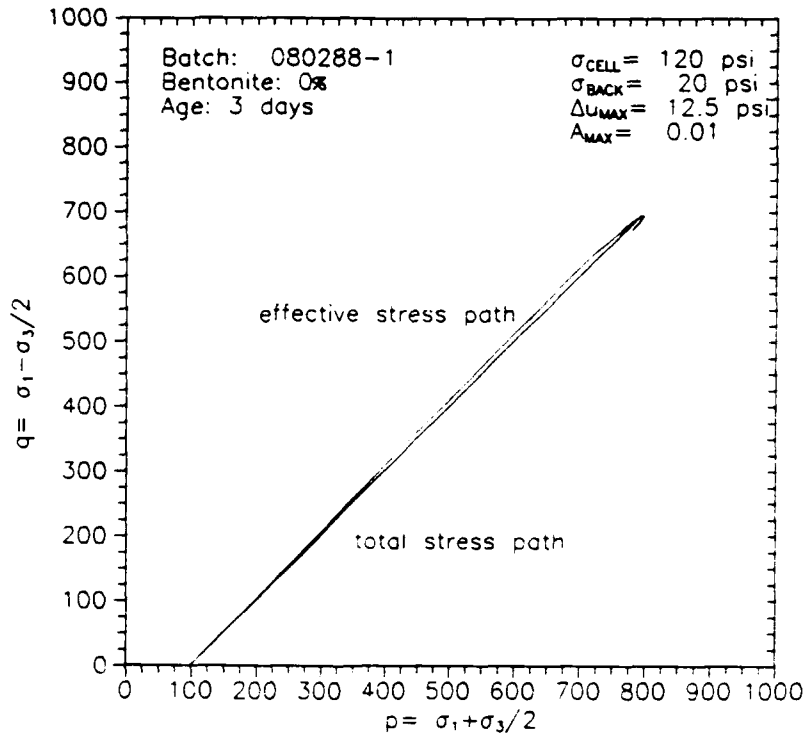


Figure 59. Total and effective stress paths for CIUC test 080288-1

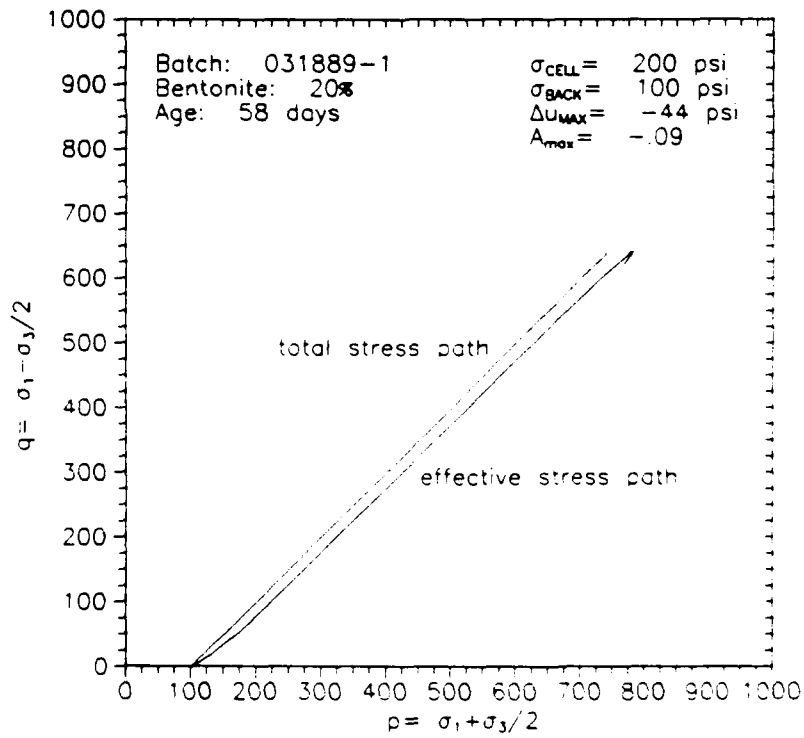


Figure 60. Total and effective stress paths for CIUC test 031889-1

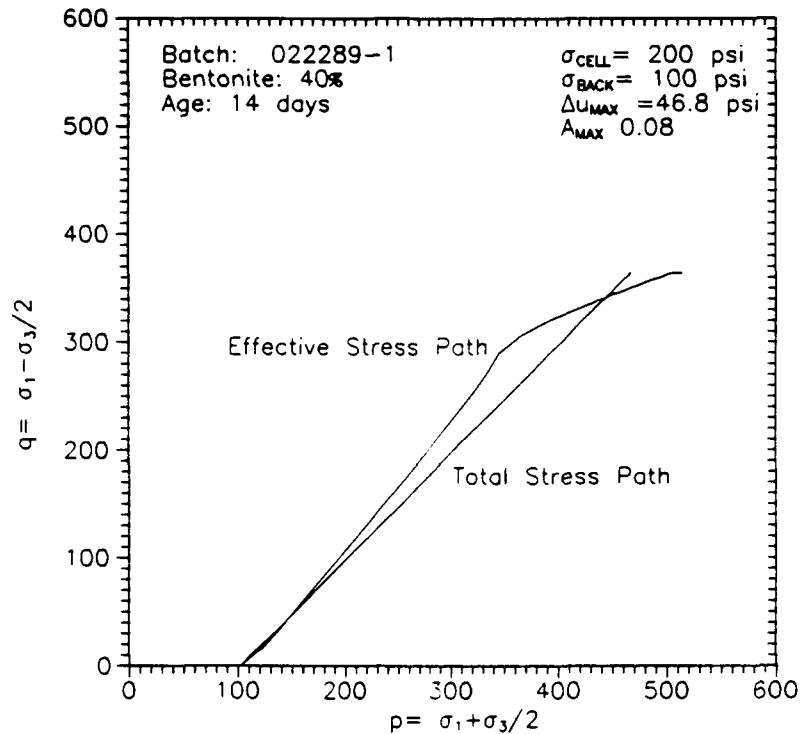


Figure 61. Total and effective stress paths for CIUC test 022289-1

shear for the 20 and 40 percent bentonite content samples are great enough to cause significant differences between total and effective stress paths.

164. Figure 62 shows 14-day age failure envelopes for each bentonite content. Each failure envelope was constructed from two points, a CIUC test and its corresponding UC test. For the 0 percent failure envelope, the CIUC data point is the effective failure point of test 102688-1. For the 20 and 40 percent failure envelopes, the CIUC data points are the effective failure points of tests 031889-1 and 022289-1 (Figures 60 and 61). The values of effective friction angle, ϕ , from Figure 62 for bentonite contents of 0, 20, and 40 percent are 65, 50, and 42°, respectively. Because these friction angles were developed from so few points they are only rough estimates. They are presented only for use in obtaining preliminary approximations of CIUC shear strength. More CIUC tests with pore pressure measurements are required to better define plastic concrete friction angles.

165. Additional testing was planned to study the effect of strain rate on pore pressure generation but was unable to be performed because the testing

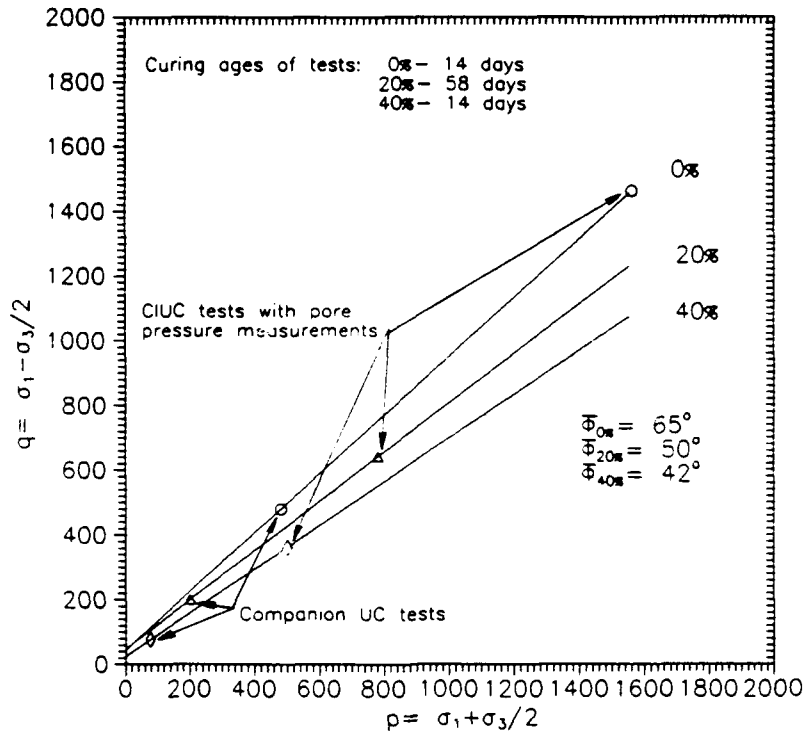


Figure 62. Effective failure envelopes and friction angles for 0, 20, and 40 percent bentonite

machine could not deflect at a rate significantly slower than the 0.05 in./min deflection rate used for the tests described above.

Relationship Between Triaxial Stress-Strain-Strength Behavior and Unconfined Stress-Strain-Strength Behavior

166. Large-scale triaxial tests on plastic concrete are complex and time-consuming and therefore expensive. They may also be beyond the capability of many soils laboratories to perform because of the specialized equipment and high capacity testing machine required. Most laboratories, however, are capable of performing standard unconfined compression tests. The above idea was one of the reasons that the unconfined companion tests were performed as part of the triaxial test program.

167. Figure 63 shows a plot of CIUC shear strength (Table 8) normalized with corresponding companion UC shear strength (Table D2, $S_u = q_u/2$) as a function of effective confining stress. Figure 63 is intended to be used as a design aid to enable a designer to obtain an estimate of CIUC shear strength from corresponding UC shear strength. The UC shear strength can come either

from the design charts presented in Figures 42 and 43 or from an actual UC tests. For example, a designer needs an estimate of the 7-day CIUC shear strength of a sample with a 20 percent bentonite content at a confining stress of 200 psi. First, an estimate of the UC, 7-day, 20 percent bentonite shear strength is obtained from Figure 43. Then the normalized shear strength value corresponding to 200 psi confinement and 20 percent bentonite content is obtained from Figure 63. Finally, the unconfined shear strength is multiplied by the normalized shear strength value to obtain the CIUC shear strength.

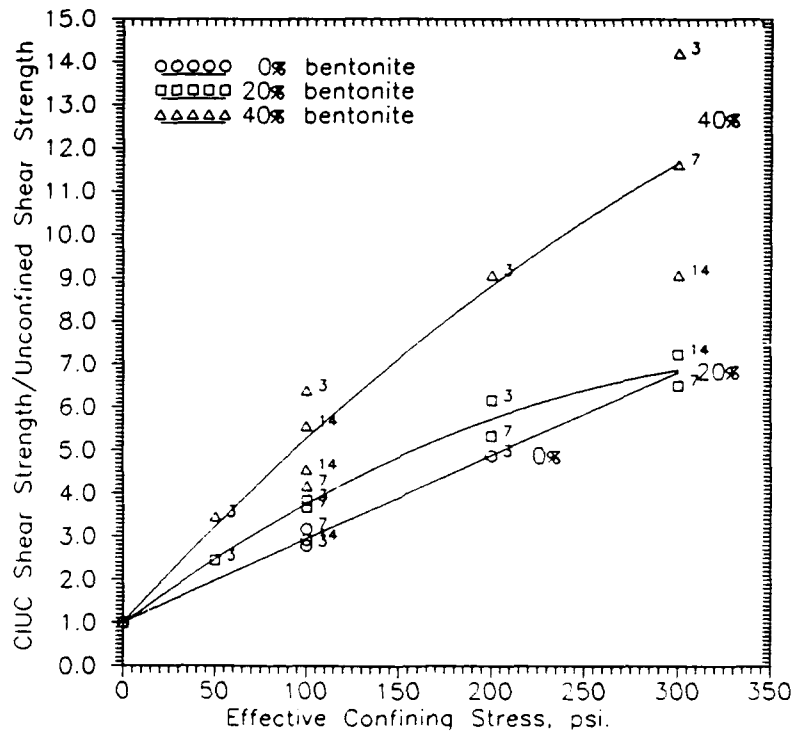


Figure 63. Normalized CIUC shear strength versus effective confining stress

168. Similarly, Figures 64 and 65 show plots of CIUC elastic modulus and strain at failure normalized by corresponding companion UC values versus effective confining stress. Because CIUC elastic moduli were calculated from strains measured by gross deflection and corresponding UC moduli were calculated from strains measured with a compressometer, it was necessary to correct the UC elastic moduli to gross deflection. Correlations were done by dividing UC elastic moduli by a factor of 2, as shown in Figure 66. Figure 66 shows a plot of UC elastic moduli of samples from the same batch designs tested at the same age with deflection measurements taken with both the compressometer and by gross deflection (see Paragraph 68).

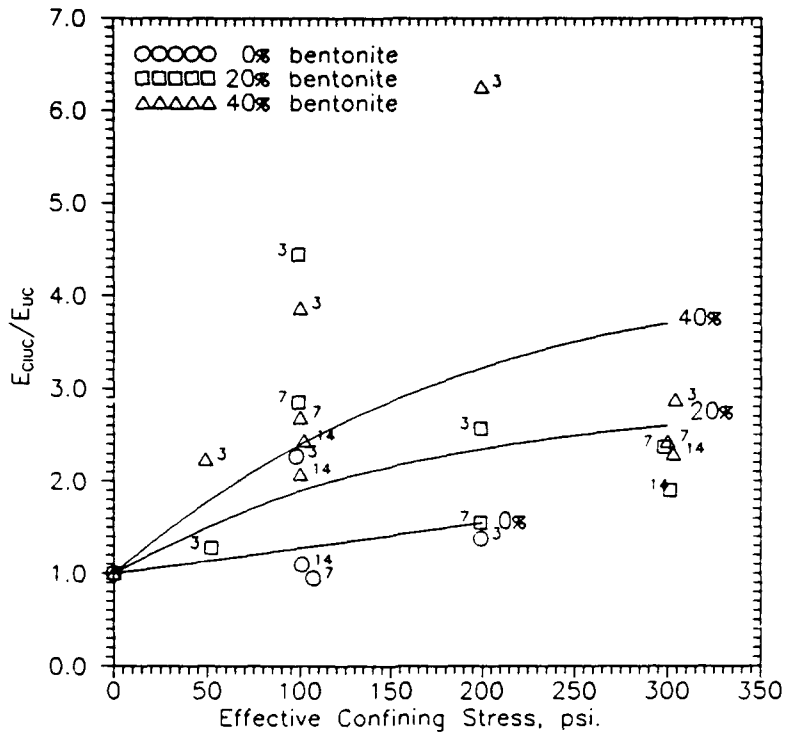


Figure 64. Normalized CIUC elastic modulus versus effective confining stress

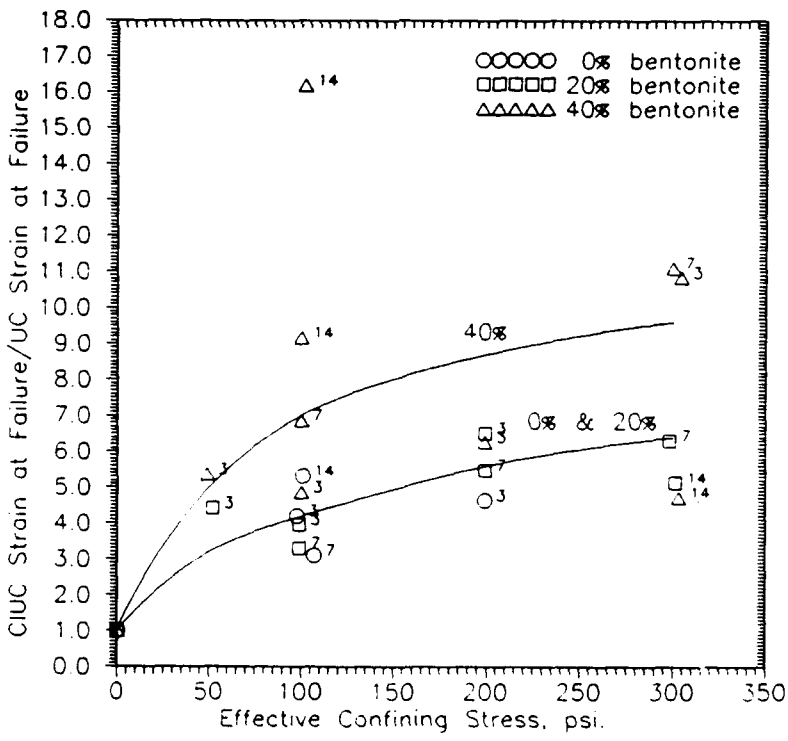


Figure 65. Normalized CIUC strain at failure versus effective confining stress

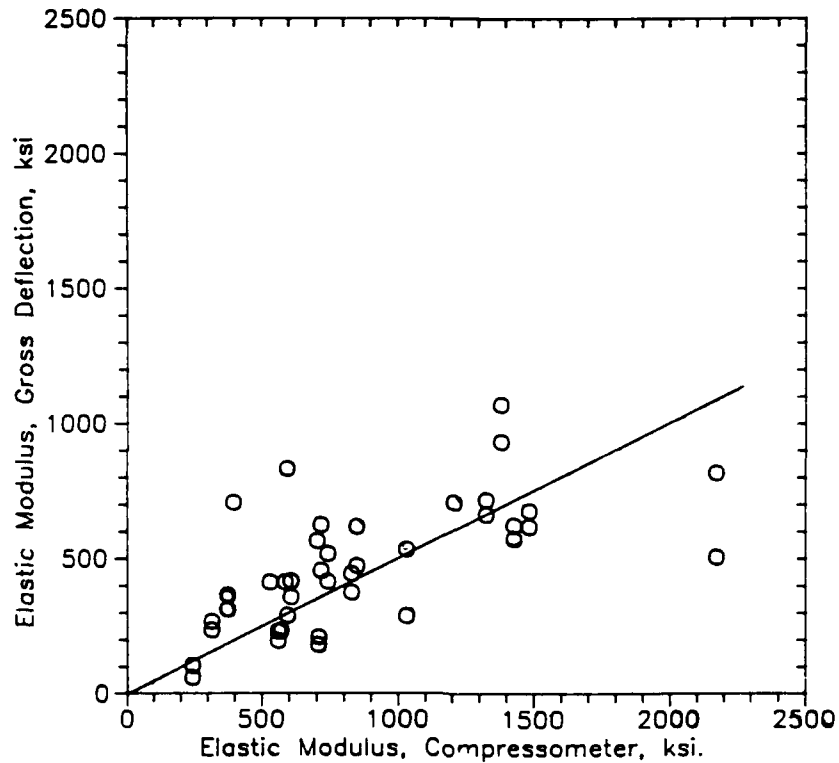


Figure 66. Unconfined elastic modulus measured by gross deflection versus unconfined elastic modulus measured by compressometer

169. In addition, Figure 67 shows a plot of Q test shear strength normalized by corresponding UC shear strength as a function of confining stress. No normalized plots of Q test elastic moduli and Q strain at failure were constructed because of the possible incorrectness of Q elastic moduli and Q strain at failure, as described in Paragraph 139.

170. Figures 63 through 65 and 67 allow a designer to estimate the stress-strain-strength behavior of plastic concrete over a wide range of drainage and confinement conditions. It must be emphasized, however, that the estimates obtained using Figures 63 through 65 and 66, particularly of elastic modulus and strain at failure, are approximate due to the large degree of scatter in the data. Actual stress-strain-strength values may vary markedly from the predicted values and any design must take the variability of the plots into account.

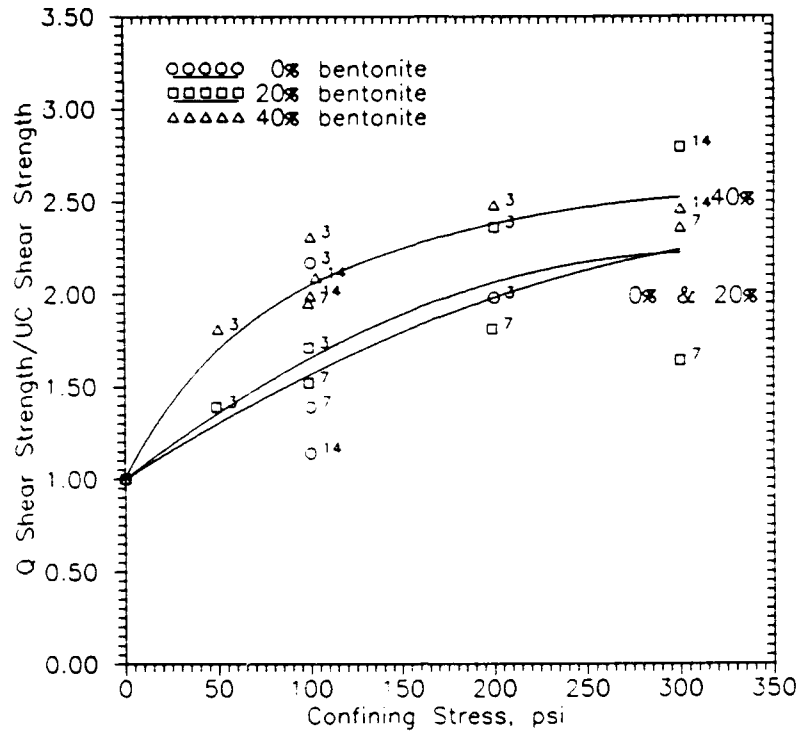


Figure 67. Normalized Q shear strength versus confining stress

Comparison of a CIUC Test and a Q Test Having the Same Cement Factor, Bentonite Content, and Water-Cement Ratio Tested at the Same Age

171. Q test were included in the triaxial test program so that the effect of consolidation on the stress-strain-strength behavior of plastic concrete could be evaluated. As discussed in Paragraph 158, consolidation increases a specimens cement factor and decreases its water-cement ratio. Some researchers have suggested (US Army Engineer Division, North Pacific 1987) that the effects of consolidation can be simulated by forming a Q test specimen at the cement factor and water-cement ratio and what a CIUC test would have at the end of consolidation. Implicit within this statement is the idea that the mechanical effect of consolidation, i.e., the squeezing together of particles within the soil matrix, has no effect on stress-strain-strength behavior.

172. To evaluate the validity of this claim, two Q specimens were formed at the cement factor and water cement ratio of CIUC test 091488-1 and tested in shear at the same age and confining pressure as 091488-1. The tests compared as follows:

a. CIUC Test 091488-1, at Time of Shear Test

Bentonite content	0 percent
Cement factor	328 lb/cu yd
Water-cement ratio	1.0
Confining stress	250 psi
Back pressure	50 psi
Test age	3 days
Slump at mixing	8 in.
Void ratio, after consol	0.217

b. Comparison Q Tests, at Time of Shear Tests

Bentonite content	0 percent
Cement factor	326 lb/cu yd
Water-cement ratio	1.0
Confining stress	200 psi
Test age	3 days
Slump at mixing	8 in.
Void ratio	0.252

173. A comparison of the stress-strain curves of each test is presented in Figure 68. Figure 68 shows clearly that the behavior of the Q tests is significantly different from the behavior of the CIUC test:

<u>Test</u>	<u>S_u, psi</u>	<u>E ksi</u>	<u>ε_f %</u>
CIUC	1,463	719	1.4
Q	963	225	5.5
% difference	-34%	-69%	293%

174. Much of the difference in elastic moduli and strain at failure can probably be attributed to the seating deformation problems with Q tests described in Paragraph 139. The difference in shear strength, however, is due entirely to differences in internal structure of the specimen. Because they were not consolidated, the void ratios of the Q tests were higher than that of the CIUC test. A higher void ratio implies greater spacing of particles within the concrete matrix. This greater spacing allows more interparticle movement in the Q tests which in turn results in lower shear strengths and elastic moduli and higher strains at failure.

Influence of Bentonite Content, Confining Stress,
Consolidation, and Age on Triaxial Stress-Strain-
Strength Behavior of Plastic Concrete

175. This section attempts to summarize and quantify the effects of bentonite content, confining stress, consolidation, and age on triaxial

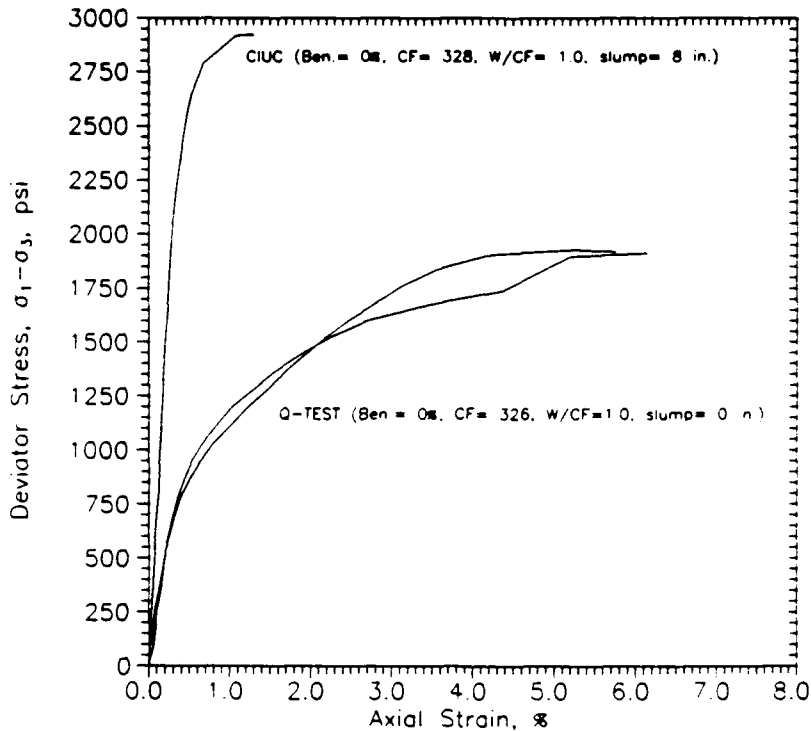


Figure 68. Deviator stress versus strain, comparison of CIUC, and Q tests with batch design at same age with effective confining stress equaling 100 psi

stress-strain-strength behavior discussed in preceding parts of this report. The effects of bentonite, confining stress, and age are each addressed below. The effect of consolidation is addressed by comparing CIUC and Q tests within each section. All of the comparisons discussed are based on stress-strain curves for each triaxial batch contained in Appendix E and test summaries in Tables 8 and 9.

The influence of
bentonite content on triaxial
stress-strain-strength behavior

176. Bentonite content has the most dramatic effect on the triaxial stress-strain-strength of plastic concrete. Comparison of batches at 100 psi effective consolidation/confinement stress, 3 days age and 0, 20, and 40 percent bentonite shows that shear strength and elastic modulus decline quickly with the addition of bentonite:

<u>Bentonite percent</u>	<u>S_u, psi</u>	
	<u>CIUC</u>	<u>Q</u>
0	695	450
20	479	254
40	351	146

From 0 to 20 percent bentonite, CIUC shear strength is reduced by 31 percent, and from 20 to 40 percent bentonite, CIUC shear strength is reduced by 27 percent. The effect of bentonite on the Q shear strength is more dramatic. From 0 to 20 percent bentonite, Q shear strength is reduced by 44 percent, and from 20 to 40 percent bentonite, Q shear strength is reduced by 43 percent. This suggests that consolidation reduces the rate of loss of shear strength. The cause of this phenomena is most likely the increase in cement factor and reduction of water-cement ratio that accompanies consolidation.

177. The effect of bentonite content on triaxial elastic modulus and strain of failure are much more difficult to quantify because of the high variability of these parameters. Elastic modulus generally decreases with the addition of bentonite in columns as written:

<u>Bentonite percent</u>	<u>E, ksi</u>		<u>ε_u, percent</u>	
	<u>CIUC</u>	<u>Q</u>	<u>CIUC</u>	<u>Q</u>
0	919	81	1.28	2.65
20	1,517	54	1.52	4.47
40	215	14	3.37	13.85

The percent drop in elastic modulus between 0 and 40 percent bentonite content is 77 percent for CIUC tests and 83 percent for Q tests. These decreases are more dramatic than those of shear strength and indicate that the addition of bentonite reduces stiffness more than it reduces shear strength. Strain at failure generally increases with the addition of bentonite. This increase, however, is much greater between 20 and 40 percent bentonite than between 0 and 20 percent bentonite. This indicates that a threshold exists somewhere between 20 and 40 percent bentonite where the space between aggregate particles in the concrete matrix becomes great enough to allow particle movement. In addition, the increase in strain at failure is greater for Q tests than for CIUC tests, most probably because the Q tests have higher water-cement ratios and lower cement factors. However, comparisons of Q elastic modulus and strain at failure may be incorrect due to the seating deflection problems discussed in Paragraph 139.

The influence of confining stress on triaxial stress-strain-strength behavior

178. In general, shear strength, elastic modulus, and strain at failure all increase with confinement. These increases with confinement are greater with increasing bentonite content. A comparison between any batches at the same age and confining stress shows that the ratios of CIUC shear strength and Q shear strength to companion unconfined shear strength increase with increasing bentonite content, as shown in Figures 63 and 67, respectively. This is also true of the ratios CIUC elastic modulus and strain at failure to companion unconfined elastic modulus and strain at failure as shown in Figures 64 and 65, respectively. These trends suggest that confinement has a greater effect on the looser matrices of higher bentonite mixes. The rate of increase of shear strength, elastic modulus, and strain at failure decreases above 100 psi effective confining stress, particularly for Q tests. For CIUC tests, this phenomena is the result of the reduced effects of consolidation on cement factor, water-cement ratio, and void ratio as consolidation/confining stress is increased (Paragraph 160). As consolidation stress is increased, incremental gains in shear strength, elastic modulus, and strain at failure are more a function of confinement than of changes in cement factor and water-cement ratio. At a certain consolidation pressure, no additional consolidation can occur because the particles in the concrete matrix cannot be pushed any closer together. Gains in shear strength, elastic modulus, and strain at failure at confining pressures above this point are only a function of confinement.

The influence of age on triaxial stress-strain-strength behavior

179. In general, shear strength and elastic modulus increase with age. The magnitudes of these changes are larger between 3- and 7-days age than between 7- and 14-days age. In addition, the magnitudes of the changes decrease with increasing bentonite content. Strain at failure decrease with age at 0 and 20 percent bentonite and increases with age at 40 percent bentonite.

180. For CIUC tests at 100 psi effective confining stress:

Bentonite percent	S_u , psi			E, ksi			ϵ_u , percent		
	age, days			age, days			age, days		
	3	7	14	3	7	14	3	7	14
0	695	1,285	1,460	919	739	949	1.28	0.65	0.83
20	479	606*	--	1,517	661*	--	1.52	0.90*	--
40	351	292	391**	215	228	236**	3.37	4.89	8.13**

* Age = 8 days.

** Average of two tests.

0 percent bentonite concrete experiences an 85 percent increase in shear strength between 3- and 7-days age. In contrast, at the same effective confining stress, 20 percent bentonite concrete experiences a 27 percent increase in shear strength, and 40 percent bentonite concrete experiences a 17 percent loss in shear strength between 3- and 7-days age. Strain at failure exhibits similar behavior with age, except in reverse. For tests at 100 psi confining stress between 3- and 7-days age, 0 percent bentonite concrete experiences a 49 percent reduction in strain at failure, and 20 percent bentonite concrete experiences a 41 percent reduction in strain at failure. For 40 percent bentonite concrete, strain at failure actually increases between 3- and 7-days age and between 7- and 14-days age.

181. For the Q test, the patterns of behavior are the same as described above; however, the magnitudes of the changes are much less. For Q tests at 100 psi effective confining stress:

Bentonite percent	S_u , psi			E, ksi			ϵ_u , percent		
	age, days			age, days			age, days		
	3	7	14	3	7	14	3	7	14
0	450	511	549	81	307	173	2.65	3.68	1.39
20	254	271*	--	54	58*	--	4.87	4.73*	--
40	146	140	155**	14	19	34**	13.85	--	11.99**

* Age = 8 days.

** Average of two tests.

The increases in shear strength between 3- and 7-days age are 12 and 6 percent for 0 and 20 percent bentonite concrete, respectively. The values of strain at failure and elastic modulus of the Q tests are too variable to draw any specific conclusions.

Permeability of Plastic Concrete

182. For plastic concrete to be an effective cutoff wall material, it not only needs stress-strain-strength properties similar to the in situ soil, but must also be at least as impervious as normal concrete. The permeability of plastic concrete is the function of four criteria (Fenoux 1985):

- a. Bentonite content. At a constant water-cement ratio, the addition of bentonite to concrete can cause a decrease in permeability by up to a factor of 10 by increasing the percentage of platey fines in the particle matrix.
- b. Water-cement ratio. Permeability increases as water-cement ratio increases. This occurs because an increase in water-cement ratio increases the space between particles in the concrete matrix.
- c. Consolidation stress. Permeability decreases with increasing consolidation stress. Increases in consolidation stress decrease the space between particles in the concrete matrix.
- d. Age. Permeability decreases with increasing age. This is probably the result of tighter binding which occurs between particles in the concrete matrix as cement cures with time.

183. Figure 69 shows a summary graph of all the permeability tests contained in Appendix F as a function of age, confining stress, and bentonite content. Figure 69 shows that permeability clearly decreases with age and consolidation stress for all bentonite contents. Permeability decreases by a factor of 10 for an increase in consolidation stress of 100 psi. Permeability also decreases by a factor of 10 between 2- and 11-days age.

184. Bentonite content, however, does not appear to have much influence on permeability. This is due to the opposing effects on bentonite content and water-cement ratio. In order to maintain an 8 in. slump when bentonite is added to concrete, it is necessary to increase water-cement ratio (see Paragraph 148). It appears that any decrease in permeability due to the addition of bentonite is negated by the corresponding increase in interparticle spacing due to increased water-cement ratio. Of prime importance is that the addition of bentonite to concrete does not increase permeability. A designer can therefore assume that a plastic concrete cutoff is just as effective against seepage as a normal concrete cutoff.

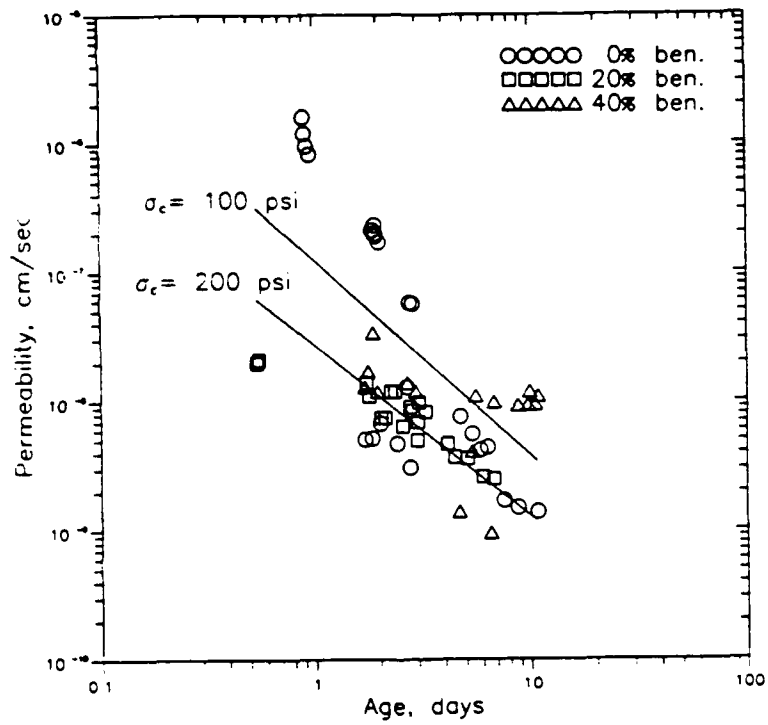


Figure 69. Permeability versus curing age as a function of bentonite content and confining stress

PART VII: SUMMARY AND RECOMMENDATIONS

185. Part VII summarizes the important findings of the research program. In addition, recommendations for further study are discussed.

Summary

186. This research program has shown that the addition of bentonite clay to conventional concrete significantly increases the ductility and plastic deformation of the concrete while simultaneously reducing its shear strength. This research has also shown that it is necessary to perform consolidated and unconsolidated triaxial tests in order to thoroughly understand the stress-strain-strength and permeability behavior of plastic concrete under confinement in a diaphragm cutoff wall. Particular attention should be paid to simulating potential drainage conditions in the cutoff wall because of the significantly greater shear strength and stiffness plastic concrete develops when allowed to freely consolidate. The sections below list the specific influences of bentonite content, age, confinement, and consolidation on the stress-strain-strength behavior of plastic concrete.

Stress-strain-strength behavior of plastic concrete

187. A summary of the stress-strain-strength behavior of plastic concrete is listed below:

- a. Shear strength and elastic modulus decrease with increasing bentonite content (Figures 39 and 40).
- b. Strain at failure increases with increasing bentonite content (Tables 8, 9, D1, and D2).
- c. Shear strength and elastic modulus increase with age (Paragraph 151 and Figure 53).
- d. Strain at failure decreases with age (Tables D1 and D2 and Figure 61).
- e. Shear strength, elastic modulus, and strain at failure increase with confinement (Tables 8 and 9 and Figures 63, 64, 65, and 67).
- f. Shear strength and elastic modulus increase with consolidation (Tables 8 and 9, Figures 63, 64, 65, and 67).
- g. Strain at failure decreases with consolidation (Appendix E).

Permeability and erodibility of plastic concrete

188. Permeability and erodibility of plastic concrete are as following:

- a. The permeability of plastic concrete at an age of 10 days is between 10^{-8} and 10^{-9} (Figure 69).
- b. Permeability decreases with age (Figure 69).
- c. Permeability decreases with consolidation (Figure 69).
- d. Permeability does not decrease with increasing bentonite content because of corresponding increases in water-cement ratio (Table 8 and Paragraph 180).
- e. The permeability of plastic concrete is the same or less than the permeability of normal concrete (Table 8).
- f. Unconfined plastic concrete specimens with bentonite contents of 0 and 60 percent do not experience erosion failure at a seepage velocity of 17 ft/sec applied for 5 days (Paragraph 128).

Scope of plastic concrete design data

189. The following is a list of the scope of plastic concrete design data:

- a. Estimates of unconfined compressive strength, elastic modulus, and strain at failure and corresponding mix design can be obtained for 8 in. slump plastic concrete within these scopes:
 - (1) Cement factor 230 to 450 lb/cu yd
 - (2) Bentonite content 0 to 60 percent of cement factor
 - (3) Concrete age 3 to 660 days
- b. Estimates of consolidated shear strength, elastic modulus strain at failure and friction angle, and unconsolidated shear strength can be obtained for 8 in. slump plastic concrete within these scopes:
 - (1) Cement factor 300 lb/cu yd
 - (2) Bentonite content 0 to 40 percent cement factor
 - (3) Effective consolidation/
confining stress 0 to 300 psi
 - (4) Concrete age 0 to 660 days

Recommendations

190. Additional CIUC tests need to be performed in order to better evaluate the effect of excess pore pressure generation on triaxial shear strength and stress paths and to better define plastic concrete friction

angles. Additional CIUC tests should also be performed over a greater range of cement factors to expand the scope of the design data. In addition, all of the Q tests in this test program should be repeated to better evaluate Q elastic modulus and strain at failure. Specific additional triaxial testing should include the following:

- a. Mix designs of 250 and 400 lb/cu yd.
- b. More CIUC shear tests with pore pressure readings to evaluate CIUC stress paths and friction angles.
- c. Triaxial shear tests at strain rates of 0.005 in./min or less to confirm independence of pore pressure generation from strain rate.
- d. Long-term triaxial testing, i.e. 28 and 90 days, to confirm age independence of normalized CIUC and Q stress-strain-strength parameters.
- e. Long-term permeability testing, i.e. 1 year or more, to obtain design permeability values.

191. In addition, a Phase III test program should be conducted to evaluate the behavior of plastic concrete under different loading and environmental conditions. This program should include the following:

- a. Creep testing to evaluate the long-term strain behavior of plastic concrete under constant load.
- b. Cyclic triaxial testing to simulate the changes in stress an earth dam cutoff wall might experience due to fluctuations in reservoir level.
- c. Permeability tests with typical ground water pollutants to evaluate plastic concrete performance in an aggressive subsurface environment.
- d. Additional erosion tests should be conducted to quantify the erodibility of plastic concrete.

REFERENCES

- Alvarez, L., and Mahave, G. 1982. "Convento Viejo's Plastic Concrete Cutoff," Proceedings, Fourteenth International Conference on Large Dams, pp 339-353.
- Amsler, D. E., and Grygiel, J. S. 1977. "Capping Concrete Cylinders with Neoprene Pads," Research Report No. 46, New York State Department of Transportation, New York.
- Binnie and Partners, Consulting Engineers. 1968. "Balderhead Dam," in house publication.
- Evans, J. C., Stahl, E. D., and Drooff, E. 1987. "Plastic Concrete Cutoff Walls," Proceedings, Specialty Conference, Geotechnical Practice for Waste Disposal, Geotechnical Division, American Society of Civil Engineers, Special Publication 13, pp 462-472.
- Fenoux, G. Y. 1985. "Filling Materials for Watertight Cutoff Walls," Fifteenth International Conference on Large Dams, Bulletin 51.
- Habib, P. 1977. "Grout Mixes and Plastic Concretes for Impervious Cutoffs," Proceedings of the Ninth Conference of International Conference on Soil Mechanics and Foundation Engineering, pp 89-91.
- Hankour, R. (Translator). 1979. "Interface Between a Dam and It's Abutments and Foundations-Continuity of Sealing Works," Proceedings of Thirteenth International Conference on Large Dams, p 4.
- Headquarters, Department of the Army. 1986. "Laboratory Soils Testing," Engineer Manual EM 1110-2-1906, Washington, DC,
- _____ 1986. "Seepage Analysis and Control for Dams," Engineer Manual EM 1110-2-1901, Washington, DC.
- Noguera, G. 1985. "Performance of Colbun Main Dam During Construction," Proceedings of Fifteenth International Conference on Large Dams, pp 1049-1059.
- Pablo, L. M., and Cruz, A. 1985. "Performance of Colbun Main Dam During Construction," Proceedings of Fifteenth International Conference on Large Dams, pp 1135-1151.
- Peck, R. 1986. "Report on Seepage Control Measures," Mud Mountain Dam for Seattle District, Corps of Engineers, pp 1-21.
- Sliwinski, Z., and Fleming, W. G. K. 1975. "Practical Considerations Affecting the Construction of Diaphragm Walls," Proceedings of the Conference on Diaphragm Walls and Anchorages, Institution of Civil Engineers, London, pp 1-10.
- Tamaro, G. 1988. "Plastic Concrete Cutoff Walls," Proceedings of REMR Workshop on New Remedial Seepage Control Methods for Embankment-Dams and Soil Foundations, US Army Engineer Waterways Experiment Station, Vicksburg, MS.
- Tardieu, B., and Costaz, J. 1987. "Plastic Concrete Cutoff Wall," Technical Lecture on Plastic Concrete for Slurry Walls, US Bureau of Reclamation.

US Army Engineer Division, North Pacific. 1987. "Report of Tests on Plastic Concrete," North Pacific Division, Corps of Engineers Memorandum W.O No. 87-C-329.

Woodward-Clyde Consultants. 1981. "Data from Laboratory Testing Program, Colbun Main Dam," Clifton, NJ.

APPENDIX A: DETAILED TEST DATA FROM COLBUN MAIN DAM LABORATORY
PROGRAM AND MUD MOUNTAIN DAM LABORATORY PROGRAM

Table A1
Summary of Batch Designs for Colbun Main Dam Research
Program (Woodward-Clyde Consultants 1981)

First Phase Testing Program

The batches prepared, and their components and quantities used are as follows:

<u>Components</u>	<u>Proposed Mix</u>	<u>Alternate Mix A</u>	<u>Alternate Mix B</u>
Water	500 ml	400 ml	500 ml
Bentonite*	20 gm	16 gm	20 gm
Cement	100 gm	100 gm	150 gm
Silty Clay**	600 gm	600 gm	600 gm
Concrete Sand*	<u>600 gm</u>	<u>1,000 gm</u>	<u>800 gm</u>
	1,820	2,116	2,070

Second Phase Testing Program

This phase also consisted of preparing three different batches of plastic concrete specimens. The batches were identified as Proposed Mix-AD, Mix No. 1 and Mix No. 2. On each batch a permeability test and unconfined-compression test (UC) were performed. In addition, on one batch (Mix No. 2), two consolidated-isotropic-undrained compression (CIUC) tests were performed.

The batches prepared, and their components and quantities used are as follows:

<u>Components</u>	<u>Proposed Mix - AD</u>	<u>Mix No. 1</u>	<u>Mix No. 2</u>
Water	500 ml	500 ml	600 ml (500)
Bentonite*	20 gm	30 gm	48 gm (40)
Cement	100 gm	50 gm	90 gm (75)
Silty clay**	600 gm	600 gm	720 gm (600)
Concrete sand†	600 gm	600 gm	720 gm (600)

* Bentonite sample No. 1 used.

** Silty clay Sample No. 1 used after oven-drying.

† Concrete sand sample No. 1 used after oven-drying.

Table A2
Summary of Colbun Main Dam Research Phases I and II CIUC Tests
(Woodward-Clyde Consultants 1981)

Batch Identification	Test Phase No.	$\frac{\sigma_c + \sigma_{vc}}{2}$ kg/cm ²	t_c days	$\frac{e_a}{hr}$	$\frac{e_{ac}}{vc}$	$\frac{e_a}{a}$	At Peak Deviator Stress/Peak Oblivity					Initial E_{s2} kg/cm ²	Remarks
							$\frac{\sigma_1 \cdot \sigma_3}{a}$ kg/cm ²	$\frac{\sigma_1 + \sigma_2}{a}$ kg/cm ²	$\frac{\sigma_1 + \sigma_2}{a}$ kg/cm ²	$\frac{\sigma_1 + \sigma_2}{a}$ kg/cm ²	A-factor		
Proposed mix	1	3.007	1	1.8	0.21 2.37	4.48 0.65	5.474 4.301	7.361 4.710	8.490 7.316	6.805 22.031	0.103 0.302	4,798	
Alternate mix A	1	3.011	2	1.7	0.07 2.75	5.68 0.47	11.311 8.864	15.725 9.512	14.330 11.881	6.125 28.322	0.062 0.134	8,690	
Alternate mix B	1	3.007	1	1.8	0.17 2.63	1.87 0.51	14.533 13.118	17.658 13.478	17.548 16.133	10.299 73.970	0.004 0.101	12,668	
Mix No. ?	2	1.010	1	1.7	0.16 1.08	1.41 0.81	3.222 3.157	3.557 3.244	4.238 4.173	20.231 73.611	0.106 0.147	2,704	For conditions of peak obliquity
	2	4.976	1	1.7	0.45 2.49	1.35 1.21	4.055 4.021	4.509 4.454	9.044 9.010	18.884 19.574	0.557 0.565	3,796	c = 2.45 kg/cm ² φ = 10.3° c = 1.20 kg/cm ² φ = 45.6°

Table A3

Summary of Colbun Main Dam Research Phase III CIUC Tests
(Woodward-Clyde Consultants 1981)

Batch Identification	Test Phase No.	$\frac{\sigma_c}{\sigma_{vc} + \sigma_{hc}}$ kg/cm ²	t _c days	e _a 1/hk	$\frac{e_{ac}}{vc}$	At Peak Deviator Stress/Peak Oblivity				Initial $\frac{F_s}{E}$ kg/cm ²	Remarks	
						e _a kg/cm ²	$\frac{\sigma_1 - \sigma_3}{\sigma_1 + \sigma_3}$ kg/cm ²	$\frac{\sigma_1}{\sigma_3}$	A- factor			
Mix No. 2	3	1.008	1	0.58	0.095 0.074	4.43 0.38	5.420 2.977	7.568 3.015	6.046 157.82	0.105 0.969	5,650	For conditions of peak obliquity φ = 37.8° ψ = 8.5° c = 1.43 kg/cm ² C = 2.41 kg/cm ²
	3	5.012	2	0.58	0.24 0.71	10.0 0.61	6.760 3.676	9.893 4.156	5.314 16.320	0.139 0.616	8,670	
Mix No. 1	3	1.008	1	0.59	0.125 0.25	6.51 0.44	4.096 2.155	5.983 2.253	5.341 45.224	0.107 0.211	4,060	For conditions of peak obliquity φ = 47.4° ψ = 13.0° c = 0.73 kg/cm ² c = 1.48 kg/cm ²
	3	5.004	1	0.59	0.30 0.92	7.87 0.75	5.058 3.317	7.413 3.831	5.296 13.895	0.262 0.677	7,790	
Mix No. 3	3	1.014	2	0.59	0.11	6.19	2.509	3.614	5.540	0.018	3,870	Problem with consolidation stresses
	3	4.983	2	0.60	0.83 2.39	7.08 1.31	3.393 2.556	4.982 3.315	20.895 7.730	0.384 0.825	10,100	For conditions of peak obliquity φ = 43.1° ψ = 15.0° c = 0.40 kg/cm ² c = 0.62 kg/cm ²

Table A4
Summary of Colbun Main Dam Research Phase I Permeability Tests
(Woodward-Clyde Consultants 1981)

<u>Batch Identification</u>	$\bar{\sigma}_c$ <u>kg/cm²</u>	<u>Stage No.</u>	<u>Hyd. System</u>	<u>i_o</u>	<u>ke 20°C cm/sec × 10⁻⁸</u>
Proposed Mix	2.980	1	Closed	42	43.1
	2.980	2-1	Open	45	42.9
	2.980	2-2	Open	45	43.2
	2.980	2-3	Open	45	40.7
	2.980	2-4	Open	45	41.0
	2.973	3-1	Open	84	41.4
	2.973	3-2	Open	84	41.7
	2.973	3-3	Open	84	42.3
	2.973	3-4	Open	84	41.8
	2.973	3-5	Open	84	37.4
	Alternate Mix A	2.994	1	Closed	36
2.987		2-1	Open	45	4.1
2.987		2-2	Open	45	3.8
2.987		3-1	Open	84	3.6
2.987		3-2	Open	82	3.6
Alternate Mix B	2.973	1	Closed	35	3.5
	2.973	2-1	Open	45	4.0
	2.973	2-2	Open	45	3.2
	2.966	3-1	Open	84	3.0
	2.966	3-2	Open	82	3.2

Table A5

Summary of Colbun Main Dam Research Phase II Permeability Tests
(Woodward-Clyde Consultants 1981)

<u>Batch Identification</u>	$\bar{\sigma}_c$ kg/cm ²	<u>Stage No.</u>	<u>Hyd. System</u>	i_o	k_e 20°C cm/sec $\times 10^{-8}$
Proposed Mix - AD	3.001	1	Closed	20	17.2
	3.001	2-1	Open	100	17.8
	3.001	2-2	Open	100	17.5
	3.001	2-3	Open	100	17.8
	2.994	3-1	Open	200	18.2
	2.994	3-2	Open	200	18.1
	2.994	3-3	Open	200	17.8
	2.994	3-4	Open	200	18.2
Mix No. 1	2.994	1	Closed	24	17.4
	2.987	2-1	Open	100	17.0
	2.987	2-2	Open	100	17.3
	2.987	2-3	Open	100	17.3
	2.994	3-1	Open	200	17.4
	2.994	3-2	Open	200	17.4
	2.994	3-3	Open	200	17.2
	2.994	3-4	Open	200	17.2
Mix No. 2	3.001	1	Closed	19	9.6
	3.001	2-1	Open	100	9.4
	3.001	2-2	Open	100	9.7
	3.001	2-3	Open	100	9.9
	3.001	3-1	Open	200	9.5
	3.001	3-2	Open	200	9.8
	3.001	3-3	Open	200	9.7
	3.001	3-4	Open	200	9.6

Table A6

Summary of Colbun Main Dam Research Phase III Permeability Tests(Woodward-Clyde Consultants 1981)

<u>Batch Identification</u>	$\bar{\sigma}_c$ <u>kg/cm²</u>	<u>Stage No.</u>	<u>Hyd. System</u>	<u>i_o</u>	<u>ke 20°C</u> <u>cm/sec</u> <u>× 10⁻⁸</u>	<u>Remarks</u>	
Mix No. 2	2.99	1-1	Closed	20	7.3		
	2.99	2-1	Closed	40	7.2		
	2.99	3-1	Open	100	7.0	Initial	
W/C = 5.56	2.99	3-2	Open	100	6.9	After overnight	
	2.99	3-3	Open	100	7.1	After overnight	
	2.99	4-1	Open	200	7.2	After overnight	
	2.99	5-1	Open	282	7.9	At maximum i _o	
	2.99	5-2	Open	281	7.5	At maximum i _o	
	2.99	5-3	Open	282	7.4	At maximum i _o	
Mix No. 1	3.00	1-1	Closed	20	11.9		
	3.00	2-1	Closed	40	11.8		
	3.00	3-1	Open	100	12.1	Initial	
W/C = 5.97	3.00	3-2	Open	100	11.7	After overnight	
	3.00	4-1	Open	200	12.5		
	3.00	5-1	Open	282	13.5	At maximum i _o	
	Took specimen down and installed No. 4 screens						
	3.07	1A-1	Closed	20	11.8		
	3.00	2A-1	Open	100	11.8		
	3.00	3A-1	Open	200	12.2		
	3.00	4A-1	Open	282	13.6	Initial at maximum i _o	
	3.00	4A-2	Open	282	10.0	After 24 hr	
	Mix No. 3	3.00	1-1	Closed	20	12.9	
			2-1	Closed	40	12.9	
3-1			Open	100	15.5	Initial	
W/C = 6.4		3-2	Open	100	13.7		
		3-3	Open	100	13.5		
		3-4	Open	100	13.5	After overnight	
		4-1	Open	200	14.1		
		5-1	Open	280	9.9	Initial	
		5-2	Open	280	15.1	After overnight	
		5-3	Open	280	16.0		

Table A7

Summary of Plastic Concrete Mix Designs and Tests

NPDL No.	Mix No			
	A	B	C	D
	3097 (Control)	3098	3099	3100
1. <u>Mix Characteristics</u>				
Cement + Bentonite (C + B),* lb/cu yd	300 + 0	180 + 120	120 + 180	60 + 240
Unit water, lb/cu yd	354.2	535.1	682.6	1050.0
W/(C + B) ratio, by weight	1.18	1.78	2.28	3.50
Sand content, percent	50.0	48.0	48.0	48.0
Slump, in. (measured)	7 1/2	8	8	8 1/4
Air, percent (measured)	1.2	0.5	0.5	0.6
2. <u>Stress - Strain Tests</u>				
<u>Compressive Strength,** psi</u>				
3-day	220	60	25 (15)†	5
7-day	370	80	35 (15)	5
28-day	790	120	70 (25)	10
90-day	1,270	230	130 (60)	15
365-day				
<u>Tangent Modulus (Initial), $E_t \times 10^3$ psi</u>				
3-day	251.5	48.8	27.1 (15.1)	1.6
7-day	569.5	51.2	38.5 (10.3)	2.5
28-day	854.5	126.5	44.6 (25.4)	3.8
90-day	1,235.0	275.6	115.9 (43.4)	5.4
365-day				
<u>Secant Modulus, $E_s \times 10^3$ psi (at ultimate load)</u>				
3-day	124.0	9.8	3.3 (1.9)	0.4
7-day	226.1	15.4	5.6 (1.6)	0.6
28-day	446.1	34.7	12.4 (3.9)	1.2
90-day	702.7	84.5	31.6 (10.1)	2.2
365-day				
<u>Percent Strain at Ultimate Load</u>				
3-day	0.18	0.58	0.72 (0.83)	1.48
7-day	0.16	0.47	0.58 (0.86)	0.90
28-day	0.18	0.35	0.54 (0.68)	0.83
90-day	0.18	0.27	0.39 (0.59)	0.58
365-day				

(Continued)

* Mixes were batched with laboratory processed dry-screened 3/4-in. MSA aggregates from Corliss Ready-Mix Co. Pit, Enumclaw, Washington, Ash Grove Types I and II cement, and National Brand Western Bentonite.

** On nominal 6 by 12-in. cylinders.

† Values in parentheses are results for cylinders moist cured at 50°F.

Table A7 (Concluded)

NPDL No.	Mix No			
	A 3097 (Control)	B 3098	C 3099	D 3100
3. <u>Flexural Tests</u> ††, ‡				
Flexural strength, psi	265	70	25	10
Young's modulus, E × 10 ³ psi	295.7	102.6	41.2	20.7
4. <u>Triaxial Tests, Maximum Deviator Stress, $\sigma_1 - \sigma_3$ psi**</u> , ‡				
Confining pressure, σ_3 psi				
50	--	233.0	67.7	9.6
100	--	301.5	74.0	20.3
200	--	298.0	69.8	19.8
5. <u>Pressure Test</u> **, ‡				
Consolidation; percent	--	12.5	17.5	20.8
in.	--	1.5	2.1	2.5
Weight loss, percent	--	7.9	11.0	16.2
Compressive strength, psi	--	620	300	15
Tangent modulus, E _t × 10 ³ psi	--	582.8	161.9	7.6
Secant modulus, E _s × 10 ³ psi	--	319.7	125.2	1.8
Percent strain at ultimate load	--	0.20	0.24	0.74
6. <u>Erodibility, percent loss by weight**</u> , ‡				
Time, min				
24	--	0.2	0.0	2.6
48	--	--	--	3.8

†† On nominal 3 by 3-in. beams, third point loading with 9-in. span.

‡ At age 28 days.

APPENDIX B: CHEMICAL ANALYSIS OF CEMENT AND BENTONITE FINE AND
COARSE AGGREGATE GRAIN SIZE DISTRIBUTION
AND BATCH DESIGN EXAMPLE

Table B1
Comparison of Grain Size Distribution of Tufts University
Aggregate to Grain Size Distribution of MUD Mountain
Dam Research Aggregate (NPSEN)

<u>Sieve Size</u>	<u>Percent Coarser By Weight</u>					
	<u>Mud Mountain</u>		<u>Tufts Phase I</u>		<u>Tufts Phase II</u>	
	<u>Sand</u>	<u>Gravel</u>	<u>Sand</u>	<u>Gravel</u>	<u>Sand</u>	<u>Gravel</u>
3/4 in.	--	4	--	6	8	7
1/2 in.	--	34	--	34	14	29
3/8 in.	--	60	--	60	--	68
4	5	97	3	93	3	94
8	16	99	11	98	14	97
16	28	100	26	100	37	100
30	52	--	56	--	65	--
50	79	--	86	--	85	--
100	91	--	96	--	95	--
PAN	100	--	100	--	100	--

Table B2
Chemical Analysis of Cement Used in Research

New Portland Type I Cement Sample 1		
<u>Analysis</u>	<u>Result</u>	<u>Specification Requirements</u>
SiO ₂	18.6	--
Al ₂ O ₃	5.9	--
Fe ₂ O ₃	1.8	--
CaO	62.2	--
MgO	2.5	6.0
SO ₃	4.4	3.5
Moisture Loss	0.3	--
Loss on Ignition	1.3	3.0
Na ₂ O	0.26	--
K ₂ O	1.09	--
Total as Na ₂ O	0.98	--
TiO ₂	0.26	--
P ₂ O ₅	0.26	--
Insoluble Residue	0.25	0.75
Free CaO	0.34	--
Fineness (Air permeability)	375 m ² /kg	160
Density	3.12 Mg/m ³	--
 <u>Calculated Compounds</u>		
C ₃ A	15	--
C ₃ S	52	--
C ₂ S	14	--
C ₄ AF	6	--

(Continued)

Table B2 (Concluded)

New Portland Type I Cement Sample 2		
<u>Analysis</u>	<u>Result</u>	<u>Specification Requirements</u>
SiO ₂	18.9	--
Al ₂ O ₃	6.1	--
Fe ₂ O ₃	1.9	--
CaO	63.2	--
MgO	2.6	6.0
SO ₃	3.8	3.5
Moisture Loss	0.7	--
Loss on Ignition	2.1	3.0
Na ₂ O	0.30	--
K ₂ O	1.19	--
Total as Na ₂ O	1.08	--
TiO ₂	0.28	--
P ₂ O ₅	0.25	--
Insoluble Residue	0.27	0.75
Free CaO	0.31	--
Fineness (Air permeability)	399 m ² /kg	160
Density	3.08 Mg/m ³	--
<u>Calculated Compounds</u>		
C ₃ A	15	--
C ₃ S	55	--
C ₂ S	13	--
C ₄ AF	6	--

Table B3
Chemical Analysis of Bentonite Used in Research

90 Barrel Bentonite Sample 4	
<u>Analysis</u>	<u>Result</u>
SiO ₂	55.8
Al ₂ O ₃	16.2
Fe ₂ O ₃	3.5
CaO	2.9
MgO	3.0
SO ₃	0.1
Moisture Loss	9.8
Loss on Ignition	3.2
Na ₂ O	2.02
K ₂ O	0.61
Sulfide Sulfur as SO ₃	0.5
Free CaO	0.00

X-ray Diffraction Analysis:

Present as clays: smectite, kaolinite, and clay-mica (illite, muscovite, biotite)

Nonclays: quartz, calcite, and plagioclase-feldspar

Table B4
Batch Design Example

Batches were proportioned according to the following procedure:

- a. Cement factor, percent bentonite, and water cement ratio were chosen.
- b. Dry weights of cement, bentonite, and sand and gravel were calculated using the absolute volume method for 1 cu yd of concrete.
- c. Dry weights were corrected for hygroscopic moisture content using water content data from previous batches.
- d. Corrected material weights were scaled for desired batch size.
- e. After batches were made, material weights were corrected for any difference in water added and for actual hygroscopic moisture of constituents.
- f. Actual cement factor, bentonite content, and water-cement ratio were back figured from final corrected weights.

The following is an illustrative example:

- a. Selected and assumed batch parameters:
 - Cement factor: 300 lb/cu yd
 - Percent bentonite: 20 %
 - Water-cement ratio: 1.9 (from previous experience)
 - Batch yield: 1.4 cu ft
- b. Gravity of solids values:
 - G_s cement = 3.5
 - G_s bentonite = 2.75
 - G_s sand & gravel = 3.65
 - Unit weight water = 62.4
- c. Water contents, from previous batches:
 - Cement = 0.05 %
 - Bentonite = 10.0%
 - Sand = 3.0 %
 - Gravel = 1.5 %
- d. Dry unit weights are calculated:
 - (1) Weight of cement, bentonite, and water are calculated from definitions of batch parameters:

(Continued)

(Sheet 1 of 6)

Table B4 (Continued)

Cement factor = (cement+bentonite) per cubic yard of concrete

Cement factor = 300 of which 20 percent is bentonite

therefore: cement = 240 lb

bentonite = 60 lb

$$\text{Water-cement ratio} = \frac{\text{weight of water}}{\text{weight of cement+bentonite}} = 1.9$$

therefore: weight of water = 1.9 (300)

= 570 lb

- (2) The volumes of cement, bentonite, and water are calculated using the following equation:

$$V_s = \frac{W_s}{G_s \gamma_w} \quad (B1)$$

where

W_s = dry weight of material

G_s = gravity of solids of material

γ_w = unit weight of water

therefore

$$\text{Volume cement} = \frac{240}{3.15 (62.4)} = 1.22 \text{ cu ft}$$

$$\text{Volume bentonite} = \frac{60}{2.75 (62.4)} = 0.35 \text{ cu ft}$$

$$\text{Volume water} = \frac{570}{62.4} = 9.14 \text{ cu ft}$$

$$\text{Total} = 10.71 \text{ cu ft}$$

- (3) The remaining volume of the cubic yard is made up to equal volumes of sand and gravel:

$$1 \text{ cu yd} = 27 \text{ cu ft}$$

$$27 - 10.71 = 16.29 \text{ cu ft}$$

$$\frac{16.29}{2} = 8.15 \text{ cu ft}$$

(Continued)

(Sheet 2 of 6)

Table B4 (Continued)

- (4) The dry weight of sand and gravel is then calculated using equation B1 to solve for W_s :

$$W_s = N_s \gamma_w$$

therefore

$$\text{Weight sand} = (8.15)(2.65)(62.4) = 1,348 \text{ lb}$$

$$\text{Weight gravel} = (8.15)(2.65)(62.4) = 1,348 \text{ lb}$$

Summary of dry weights (W_s):

$$\text{Cement} = 240$$

$$\text{Bentonite} = 60$$

$$\text{Sand} = 1,348$$

$$\text{Gravel} = 1,348$$

$$\text{Water} = 570$$

- e. The dry weights are then corrected for hygroscopic moisture content:

$$\text{Total weight} = \text{dry weight} + \text{weight of water}$$

or

$$W_T = W_s + W_w \tag{B2}$$

by definition

$$\text{Water content, } W_c = \frac{W_w}{W_s}$$

therefore

$$W_w = W_c W_s \tag{B3}$$

Substituting equation B3 into equation B2

(Continued)

(Sheet 3 of 6)

Table B4 (Continued)

$$W_T = W_s + W_c W_s$$

or

$$W_T = W(1+W_c)$$

Corrected weights:

$$\text{Cement} = 240 (1.005) = 241.2 \text{ lb}$$

$$\text{Bentonite} = 60 (1.10) = 66.0 \text{ lb}$$

$$\text{Sand} = 1,348 (1.03) = 1,388.0 \text{ lb}$$

$$\text{Gravel} = 1,348 (1.015) = 1,368.0 \text{ lb}$$

The total hygroscopic moisture on all the constituents is then calculated and subtracted from the initial weight of water:

$$\text{Weight of water in: Cement} = 241.2 - 240 = 1.2 \text{ lb}$$

$$\text{Bentonite} = 66.0 - 60.0 = 6.0 \text{ lb}$$

$$\text{Sand} = 1,388 - 1,348 = 40 \text{ lb}$$

$$\text{Gravel} = 1,368 - 1,348 = \underline{20 \text{ lb}}$$

$$\text{Total} = 67.2 \text{ lb}$$

$$\text{Corrected weight of water} = 570 - 67.2 = 502.8 \text{ lb}$$

Summary of corrected weights:

$$\text{Cement} = 241.2 \text{ lb}$$

$$\text{Bentonite} = 66.0 \text{ lb}$$

$$\text{Sand} = 1,388.0 \text{ lb}$$

$$\text{Gravel} = 1,368.0 \text{ lb}$$

$$\text{Water} = 502.8 \text{ lb}$$

f. Corrected weights are then scaled to batch size:

$$\text{Batch size} = 1.4 \text{ cu ft}$$

$$\text{Reduction factor} = \frac{1.4 \text{ cu ft}}{1 \text{ cu yd}} = \frac{1.4 \text{ cu ft}}{27 \text{ cu ft}} = 0.052 \text{ cu ft}$$

Summary of scaled weights:

$$\text{Cement} = 241.2 (0.052) = 12.51 \text{ lb}$$

$$\text{Bentonite} = 66.0 (0.052) = 3.42 \text{ lb}$$

$$\text{Sand} = 1,388.0 (0.052) = 72.0 \text{ lb}$$

$$\text{Gravel} = 1,368.0 (0.052) = 70.9 \text{ lb}$$

$$\text{Water} = 502.8 (0.052) = 26.1 \text{ lb}$$

(Continued)

(Sheet 4 of 6)

Table B4 (Continued)

These are the weights of materials that were actually added to the mixer.

- g. After batch was made weights were corrected for any difference in water added and for actual hygroscopic moisture content:

Suppose an additional 0.9 lb of water were needed to achieve an 8-in. slump and that the following actual hygroscopic moisture contents were calculated for the materials:

Actual Water Content, W_c

Cement -	0.3 %
Bentonite -	10.3 %
Sand -	1.9 %
Gravel -	0.8 %

Summary of Actual Weights Added

<u>Components</u>	<u>Total Weight</u>	<u>Weight of Solids, W_s</u>	<u>Weight of Water, W_w</u>
Cement	12.51	12.46	0.05
Bentonite	3.42	3.05	0.37
Sand	72.0	70.63	1.37
Gravel	70.9	70.33	0.57
Water	27.0	--	<u>27.0</u>
			29.36 lb

- h. The values of the dry weights are then calculated and actual cement factor, bentonite content, and water-cement ratio back calculated.

Volumes were again calculated using equation B1.

<u>Components</u>	<u>Weight lb</u>	<u>Volume cu ft</u>
Cement	12.46	0.063
Bentonite	3.05	0.018
Sand	70.63	0.427
Gravel	70.33	0.425
Water	<u>29.36</u>	<u>0.471</u>
Total	185.83	1.403

(Continued)

(Sheet 5 of 6)

Table B4 (Concluded)

$$\text{Theoretical unit weight} = \frac{185.83 \text{ lb}}{1.403 \text{ cu ft}} = 132.5 \text{ lb/cu ft}$$

$$\text{Cement factor} = (12.46 + 3.05) \left(\frac{27}{1.403} \right) = 298 \text{ lb/cu yd}$$

$$\text{Bentonite content} = \frac{3.05}{(12.46 + 3.05)} = 0.197 = 20 \%$$

$$\text{Water-cement ratio} = \frac{29.36}{(12.46 + 3.05)} = 1.893 = 1.89$$

— SP SAND USED IN PHASE II



ASTM C33-86 FINE AGGREGATE RANGE

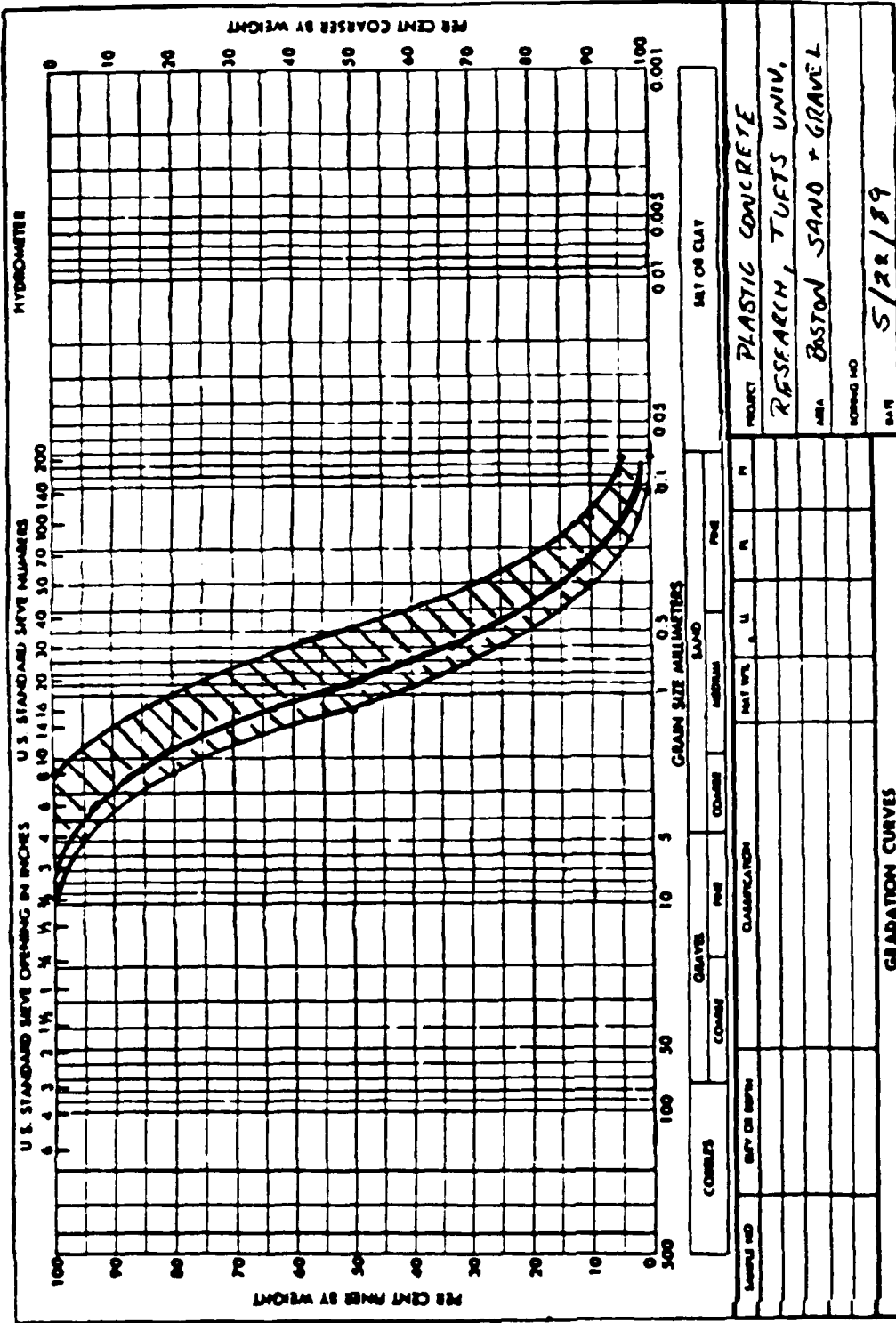


Figure B3. Grain size curve of fine aggregate used to make Phase II samples

APPENDIX C: CALIBRATIONS OF RIEHLE TESTING MACHINE
AND 1,000 LB BEAM BALANCE SCALE

TESTING MACHINE CALIBRATION REPORT AND DATA

AMERICAN CALIBRATION & TESTING CO.

176 Walnut Street
Lawrence, MA 01841

OWNER				Machine Reading lb	Proving Reading lb	Machine Error		P. R. Code	
						lb	%		
Name Tufts University				1	1	0	0	3	
Location Anderson Hall				Loading Range	2	2	0	0	3
Civil Engineering Div.					4	4	0	0	3
Medford, Ma. 02155					6	6	0	0	3
MACHINE					8	8	0	0	3
Manufacturer Fairbanks				10	10	0	0	5	
Type Platform Balance				10	10	0	0	3 & 5	
Capacity 0 - 1,000 lbs.				Loading Range	20	20	0	0	5 & 5
Serial No. Tufts No. 22378					40	40	0	0	5 & 5
CALIBRATION APPARATUS DATA					60	60	0	0	5 & 5
Type of Apparatus Used Dead Wts. Baldwin Calibration Unit					80	80	0	0	5 & 5
Manufacturer Toledo scale ELH Electronics, Inc.				100	100	0	0	5 & 5	
Apparatus Verified & Directly Traceable to the N.B.S., Washington, D.C.				100	100	0	0	5 & 5	
Apparatus Verified in Accordance With ASTM Specification E74				Loading Range	199.5	200	-0.5	0.25	1 & 2
PROVING RINGS					398.7	400	-1.3	0.33	1 & 2
P. R. Code	Serial No.	Loading Range	Verif. Date Lab. No.		598.2	600	-1.8	0.3	1 & 2
1	1046	Cal. Ind.	6-1-88 SJT.01/103817		796.6	800	-3.4	0.43	1 & 2
2	18248	0-2,400 lb	6-1-88 SJT.01/103817	996.2	1,000	-4.9	0.49	1 & 2	
3	123	0-25 lb	6-1-88 Waltham, City						
4			Bureau of Wts. & Measures	Loading Range					
5	A1-1-7	0-150 lb	Bureau of Wts. & Measures						
6									
Computed Loads Corrected For Temp. of 70 F									
Service Engineer G. W. Mooney									
Date Aug. 29, 1988									

ASTM Spec. E1 Calibration frequency : 1 year

Figure C1. Calibration of 1,000-lb beam
balance scale

Certificate of Verification

American Calibration & Testing Co.

178 Walnut Street Lawrence, MA 01841

This is to Certify That the following described testing machine has been calibrated by us and the loading range shown below found to be within a tolerance of 1.0 %

Machine Riehle, Universal Testing Machine, s/n 77779
(Make, type and serial number)

Location Tufts University, Anderson Hall
Civil Engineering Division, Medford, MA 02155

Date of Verification May 21, 1987

<i>Machine Range</i>	<i>Loading Range</i>	<i>Machine Range</i>	<i>Loading Range</i>
0 - 3,000 lb	300 - 3,000 lb	0 - 300,000 lb	30,000 - 300,000 lb
0 - 15,000 lb	1,500 - 15,000 lb	_____	_____
0 - 30,000 lb	3,000 - 30,000 lb	_____	_____
0 - 60,000 lb	6,000 - 60,000 lb	_____	_____
0 - 150,000 lb	15,000 - 150,000 lb	_____	_____

Method of verification and pertinent data is in accordance with A.S.T.M. Spec. E4-79. The testing device(s) used for this calibration have been certified by National Standards Testing Laboratory and are traceable to the National Bureau of Standards, A.S.T.M. Spec. E74. Lab. No. STT-01/108200; Trans. Letter 5-27-86

Serial No. (s) of testing device(s) used for calibration:

Cal. Ind.	1046	18249	10234	40795
_____	5-27-86	5-27-86	5-27-86	5-27-86

Date(s) of certification

Attest

Name _____

Title _____

Company _____

Company Representative

American Calibration & Testing Co.

By G. W. Mooney
Senior Engineer
G. W. Mooney

Figure C2. Calibration of Riehle testing machine, 1987 (Sheet 1 of 3)

Americar Calibration & Testing Co.
178 Walnut St.
Lawrence, MA 01841

OWNER				Machine Reading lb.	Proving Reading lb.	Machine Error		P. R. Code
						lb	%	
Name Tufts University				299.0	300	-1.0	0.33	1 & 2
Location Anderson hall				600.7	600	0.7	0.11	1 & 2
Civil Engineering Div.				1,201.6	1,200	1.6	0.13	1 & 2
Medford, Ma. 02155				1,802.8	1,800	2.8	0.16	1 & 2
MACHINE								
Manufacturer Riehle				2,404.1	2,400	4.1	0.17	1 & 2
Type Universal Testing Machine				2,989.0	3,000	-11.0	0.37	1 & 3
Capacity 0 - 300,000 lbs. (6 ranges)				1,490.0	1,500	-10.0	0.67	1 & 1
Serial No. R-77779				2,987	3,000	-13	0.43	1 & 3
CALIBRATION APPARATUS DATA								
Type of Apparatus Used Baldwin Calibration Unit				5,963	6,000	-37	0.61	1 & 3
Manufacturer BLH Electronics, Inc.				8,934	9,000	-66	0.73	1 & 3
Apparatus Verified & Directly Traceable to the N.B.S., Washington, D.C.				11,906	12,000	-94	0.78	1 & 3
Apparatus Verified in Accordance with ASTM Specification E74				14,631	15,000	-149	0.99	1 & 3
PROVING RINGS								
P. R. Code	Serial No.	Loading Range	Verif. Date Lab. No.	11,944	12,000	-56	0.47	1 & 3
1	1046	Cal. Ind.	5-27-86 SJT.01 /103221	17,901	18,000	-99	0.55	1 & 3
2	18248	0-2,400 lb	5-27-86 SJT.01 /103221	23,853	24,000	-147	0.61	1 & 3
3	10234	0-24,000 lb	5-27-86 SJT.01 /103221	29,979	30,000	-21	0.07	1 & 4
4	40796	0-240,000 lb	5-27-86 SJT.01 /103221	5,994	6,000	-6	0.1	1 & 3
5				9,979	10,000	-21	0.21	1 & 3
6				19,907	20,000	-93	0.47	1 & 3
Computed Loads Corrected For Temp. of 70 F.				29,966	30,000	-34	0.11	1 & 5
Service Engineer G. W. Mooney				39,954	40,000	-46	0.11	1 & 5
Date May 21, 1987				49,942	50,000	-58	0.11	1 & 5
				59,952	60,000	-68	0.03	1 & 5

ASTM Spec. E1 Calibration frequency = 1 year

G. W. Mooney

Figure C2. (Sheet 2 of 3)

American Calibration & Testing Co.
178 Walnut St.
Lawrence, MA 01841

OWNER		Machine Reading lb	Proving Reading lb	Machine Error		P. R. Code
				lb	%	
Name Tufts University		15,005	15,000	5	0.03	1 & 3
Location Anderson hall		30,016	30,000	16	0.05	1 & 4
Civil Engineering Div.		60,052	60,000	52	0.09	1 & 4
Medford, Ma. 02155		90,077	90,000	77	0.09	1 & 4
MACHINE						
Manufacturer Riehle		120,088	120,000	88	0.07	1 & 4
Type Universal Testing Machine		150,087	150,000	87	0.06	1 & 4
Capacity 0 - 300,000 lb (6 ranges)		30,016	30,000	16	0.05	1 & 4
Serial No. R-77779		40,029	40,000	29	0.07	1 & 4
CALIBRATION APPARATUS DATA						
Type of Apparatus Used Baldwin Calibration Unit		80,195	80,000	195	0.24	1 & 4
Manufacturer BLH Electronics, Inc.		120,338	120,000	338	0.28	1 & 4
Apparatus Verified & Directly Traceable to the N.B.S., Washington, D.C.		160,333	160,000	333	0.21	1 & 4
Apparatus Verified in Accordance With ASTM Specification E74		200,554	200,000	554	0.26	1 & 4
PROVING RINGS						
P. R. Code	Serial No.	Loading Range	Verif. Date Lab. No.			
1	1046	Cal. Ind.	5-27-86 SJT.01 /103221			
2	18248	0-2,400 lb	5-27-86 SJT.01 /103221			
3	10234	0-24,000 lb	5-27-86 SJT.01 /103221			
4	40796	0-240,000 lb	5-27-86 SJT.01 /103221			
5						
6						
Computed Loads Corrected For Temp. of 70 F						
Service Engineer G. W. Mooney		Date May 21, 1967				

G. W. Mooney

ASTM Spec. E1 Calibration frequency = 1 year

Figure C2. (Sheet 3 of 3)

Certificate of Verification

American Calibration & Testing Co.

176 Walnut Street

Lawrence, MA 01841

This is to Certify That the following described testing machine has been calibrated by us and the loading range shown below found to be within a tolerance of 1.0 %

Machine Riehle, Universal Testing Machine, s/n R-77779
(Make, type and serial number)

Location Tufts University

Anderson Hall, Civil Engineering Div., Medford, Ma. 02155

Date of Verification Aug. 29, 1988

Machine Range	Loading Range	Machine Range	Loading Range
0 - 3,000 lb	300 - 3,000 lb	0 - 300,000 lb	30,000 - 200,000 lb
0 - 15,000 lb	1,500 - 15,000 lb	_____	_____
0 - 30,000 lb	3,000 - 30,000 lb	_____	_____
0 - 60,000 lb	6,000 - 60,000 lb	_____	_____
0 - 150,000 lb	15,000 - 150,000 lb	_____	_____

Method of verification and pertinent data is in accordance with ASTM Spec. E4-83. The testing device(s) used for this calibration have been certified by National Standards Testing Laboratory and are traceable to the National Bureau of Standards, ASTM Spec. E74-83. Lab No. SJT.01/103817
 Trans. letter 6-1-88

Serial No. (s) of testing device(s) used for calibration:

Cal. Ind.	1046	18248	10234	40796
_____	6-1-88	6-1-88	6-1-88	6-1-88

Date(s) of certification

Attest

Name _____

Title _____

Company _____

Company representative

American Calibration & Testing Co.

By *G. W. Mooney*
Senior Engineer
G. W. Mooney

Figure C3. Calibration of Riehle testing machine, 1988 (Sheet 1 of 3)

TESTING MACHINE CALIBRATION REPORT AND DATA

AMERICAN CALIBRATION & TESTING CO.
176 Walnut Street
Lawrence, MA 01841

OWNER				Machine Reading lb	Proving Reading lb	Machine Error		P. R Code
						lb	%	
Name	Tufts University			298.3	300	-1.7	0.57	1 & 2
Location	Anderson hall			596.7	600	-3.3	0.55	1 & 2
	Civil Engineering Div.			1,196.4	1,200	-3.6	0.3	1 & 2
	Medford, Ma. 02155			1,793.8	1,800	-6.2	0.34	1 & 2
MACHINE				2,389.1	2,400	-10.9	0.45	1 & 2
Manufacturer	Riehle			2,985.0	3,000	-15	0.5	1 & 3
Type	Universal Testing Machine			1,490	1,500	-10	0.67	1 & 2
Capacity	0 - 300,000 lb (6 ranges)			2,982	3,000	-18	0.6	1 & 3
Serial No.	R-77779			5,974	6,000	-26	0.43	1 & 3
CALIBRATION APPARATUS DATA				8,960	9,000	-40	0.44	1 & 3
Type of Apparatus Used	Baldwin Calibration Unit			11,942	12,000	-58	0.48	1 & 3
Manufacturer	BLH Electronics, Inc.			14,920	15,000	-80	0.53	1 & 3
Apparatus Verified & Directly Traceable to the N.B.S., Washington, D.C.				2,995	3,000	-5	0.17	1 & 3
Apparatus Verified in Accordance With ASTM Specification E74				5,986	6,000	-14	0.23	1 & 3
PROVING RINGS				11,966	12,000	-34	0.28	1 & 3
P. R Code	Serial No.	Loading Range	Verif. Date Lab. No.	17,953	18,000	-47	0.26	1 & 3
1	1046	Cal. Ind.	6-1-88 SJT.01/103817	23,931	24,000	-69	0.29	1 & 3
2	18248	0-2,400 lb	6-1-88 SJT.01/103817	29,973	30,000	-27	0.09	1 & 4
3	10234	0-24,000 lb	6-1-88 SJT.01/103817	5,986	6,000	-14	0.23	1 & 3
4	40796	0-240,000 lb	6-1-88 SJT.01/103817	9,967	10,000	-33	0.33	1 & 3
5				19,956	20,000	-44	0.22	1 & 3
6				29,963	30,000	-37	0.12	1 & 4
Computed Loads Corrected For Temp. of 70°F				39,956	40,000	-44	0.11	1 & 4
Service Engineer				49,945	50,000	-55	0.11	1 & 4
G. W. Mooney				59,948	60,000	-52	0.11	1 & 4
Date								
Aug. 29, 1988								

G. W. Mooney

ASTM Spec. E1 Calibration frequency - 1 year

Figure C3. (Sheet 2 of 3)

TESTING MACHINE CALIBRATION REPORT AND DATA

AMERICAN CALIBRATION & TESTING CO.
176 Walnut Street
Lawrence, MA 01841

OWNER				Machine Reading lb	Proving Reading lb	Machine Error		P. R Code	
						lb	%		
Name Tufts University				15,005	15,000	5	0.03	1 & 3	
Location Anderson Hall				Loading Range	30,027	30,000	27	0.09	1 & 4
Civil Engineering Div.					60,062	60,000	62	0.1	1 & 4
Medford, Ma. 02155					90,090	90,000	90	0.1	1 & 4
MACHINE					120,114	120,000	114	0.1	1 & 4
Manufacturer Riehle				150,190	150,000	190	0.13	1 & 4	
Type Universal Testing Machine				30,027	30,000	27	0.09	1 & 4	
Capacity 0-300,000 lb (6 ranges)				Loading Range	40,031	40,000	31	0.08	1 & 4
Serial No. R-77779					79,985	80,000	-15	0.02	1 & 4
CALIBRATION APPARATUS DATA					119,864	120,000	-136	0.11	1 & 4
Type of Apparatus Used Baldwin Calibration Unit					159,673	160,000	-327	0.2	1 & 4
Manufacturer BLH Electronics, inc.					199,721	200,000	-279	0.14	1 & 4
Apparatus Verified & Directly Traceable to the N.B.S., Washington, D.C. Apparatus Verified in Accordance With ASTM Specification E74									
PROVING RINGS				Loading Range					
P. R Code	Serial No.	Loading Range	Verif. Date Lab. No.						
1	1046	Cal. Ind.	6-1-88 SJT.01/103817						
2	18248	0-2,400 lb	6-1-88 SJT.01/103817						
3	10234	0-24,000 lb	6-1-88 SJT.01/103817						
4	40796	0-240,000 lb	6-1-88 SJT.01/103817						
5									
6									
Computed Loads Corrected For Temp. of 70 F									
Service Engineer G. W. Mooney									
Date Aug. 29, 1988									

ASTM Spec. E1 Calibration frequency = 1 year

Figure C3. (Sheet 3 of 3)

APPENDIX D: SUMMARY TABLES OF UNCONFINED COMPRESSION TESTS (PHASES I
AND II), BRAZILIAN TENSILE TESTS (PHASES I AND II), AND
FLEXURAL BEAM TESTS

Table D1
Summary of Phase I Unconfined Compression Test Program

EXPLANATION OF TABLE HEADINGS

CF	cement factor, pounds of cement+bentonite per cubic yard of concrete
ben	percent of cement factor, by weight, which is bentonite
w/c	ratio of water to cement+bentonite, by weight
SL	slump, inches
G	wet unit weight, pounds per cubic foot (theoretical)
%air	air content of wet concrete, %
age	curing age in days
storage	storage location (wet room or cure box)
strain	type of strain measuring system (gross deflection, compressometer, neoprene end caps)
water	post-test oven dry water content, %
qu	ultimate unconfined compressive strength, psi (samples tested with neoprene end caps not corrected)
E	Young's modulus, kips (1000 pounds) per square inch
eu	strain at qu, inch per inch
AVG	average qu of test groups of more than one cylinder of same age and batch design
STD	standard deviation of test groups of more than one cylinder of same age and batch design
%STD	STD/AVG, %

Batch ID	CF	ben	w/c	SL	G	%air	cylinder ID	age	storage	strain	water	qu	E	eu	AVG	STD	%STD
060387-1	266	0	1.43	7.25	142	0.5	060387-1-DS	5	cure box	gross	-	603	206	0.0035	603		
							060387-1-A	7	cure box	gross	-	674	329	0.0025	674		
							060387-1-B	62	cure box	gross	-	774	432	0.0022	774		
							060387-1-C	131	wet room	gross	9.4	797	492	0.0025	797		
Batch ID	CF	ben	w/c	SL	G	%air	cylinder ID	age	storage	strain	water	qu	E	eu	AVG	STD	%STD
060387-2	311	0	1.31	8.75	146	0	060387-2-J	5	wet room	gross	-	760	382	0.0035	656	75	11%
							060387-2-L	5	wet room	gross	-	585	320	0.0029			
							060387-1-H	5	wet room	gross	-	623	251	0.0033			
							060387-2-G	7	wet room	gross	-	691	603	0.0020	697	69	10%
							060387-2-M	7	wet room	gross	-	785	406	0.0029			
							060387-2-D	7	cure box	gross	-	616	260	0.0034			
							060387-2-F	62	wet room	gross	8.9	919	538	0.0023	891	28	3%
060387-2-B	62	cure box	gross	-	864	469	0.0028										
Batch ID	CF	ben	w/c	SL	G	%air	cylinder ID	age	storage	strain	water	qu	E	eu	AVG	STD	%STD
061687-1	413	0	0.91	7.75	142	1.8	061687-1-B	3	cure box	gross	8.3	1379	586	0.0035	1379		
							061687-1-H	7	wet room	gross	8.8	1786	954	0.0024	1722	133	8%
							061687-1-L	7	wet room	gross	-	1536	1097	0.0020			

(Continued)

(Sheet 1 of 7)

Table D1 (Continued)

						061687-1-A	7	cure box	gross	-	1842	966	0.0031					
						061687-1-I	28	wet room	neop	8	2169			2215	34	2%		
						061687-1-G	28	wet room	neop	9.8	2229							
						061687-1-J	28	wet room	neop	-	2248							
						061687-1-H	52	wet room	gross	-	2105	1034	0.0027	2291	132	6%		
						061687-1-K	52	wet room	gross	-	2385	984	0.0029					
						061687-1-O	52	wet room	gross	-	2383	1114	0.0029					
						061687-1	627	wet room	comp	8.3	2342	3120	0.0018	2371	67	3%		
						061687-1-C	660	wet room	comp	0	2307	2914	0.0018					
						061687-1-?	660	wet room	comp	0	2464	3051	0.0017					
Batch ID	CF	ben	w/c	SL	G	air cylinder ID	age	storage	strain	water	qu	K	eu					
071387-1	242	0	1.61	7.5	140	1.8 071387-1-A	3	cure box	neop	-	328			312	11	4%		
						071387-1-O	3	wet room	neop	9.2	309							
						071387-1-P	3	wet room	neop	-	301							
						071387-1-G	7	wet room	gross	9.1	558	627	0.0018	555	3	0%		
						071387-1-H	7	wet room	gross	-	553	528	0.0021					
						071387-1-M	30	wet room	gross	-	783	533	0.0023	753	21	3%		
						071387-1-K	30	wet room	gross	7.4	738	405	0.0024					
						071387-1-B	30	cure box	gross	-	737	459	0.0021					
						071387-1-C	91	wet room	gross	9.9	661	566	0.0023	661				
						071387-1-H	633	wet room	comp	0	780	1319	0.0016	767	13	2%		
						071387-1-K	500	wet room	comp	8.6	754	1853	0.0010					
Batch ID	CF	ben	w/c	SL	G	air cylinder ID	age	storage	strain	water	qu	K	eu					
102387-1	269	0	1.6	8.75	140	- 102387-1-A	7	wet room	comp	9.6	731	1207	0.0024	717	66	9%		
						102387-1-C	7	wet room	comp	-	631	396	0.0033					
						102387-1-B	7	wet room	gross	9.7	790	707	0.0031					
						102387-1-I	28	wet room	comp	8.4	918	1428	0.0024	1003	61	6%		
						102387-1-F	28	wet room	gross	-	1032	622	0.0031					
						102387-1-G	28	wet room	gross	-	1058	573	0.0029					
						102387-1-J	55	wet room	gross	10.2	763	440	0.0047	905	113	13%		
						102387-1-P	55	wet room	gross	-	911	662	0.0024					
						102387-1-M	55	wet room	gross	-	1040	578	0.0028					
						102387-1-K	91	wet room	comp	-	891	848	0.0034	905	90	10%		
						102387-1-H	91	wet room	gross	-	1022	618	0.0028					
						102387-1-L	91	wet room	gross	-	802	473	0.0030					
						102387-1-P	498	wet room	comp	8.1	943	2063	0.0020	865	54	6%		
						102387-1-N	540	wet room	comp	0	796	2350	0.0019					
						102387-1-Q	540	wet room	comp	0	841	2313	0.0017					
						102387-1-R	540	wet room	comp	0	882	2131	0.0019					
Batch ID	CF	ben	w/c	SL	G	air cylinder ID	age	storage	strain	water	qu	K	eu					
111387-1	321	0	1.26	7.75	142	- 111387-1-B	4	wet room	gross	10.8	931	298	0.0042	948	16	2%		
						111387-1-C	4	wet room	gross	-	943	534	0.0028					
						111387-1-A	4	wet room	comp	-	970	1031	0.0021					
						111387-1-J	7	wet room	gross	15.2	1065	618	0.0029	1094	47	4%		
						111387-1-I	7	wet room	gross	-	1160	676	0.0029					
						111387-1-L	7	wet room	comp	-	1057	1484	0.0020					
						111387-1-P	28	wet room	gross	-	1329	506	0.0033	1425	37	5%		
						111387-1-M	28	wet room	gross	-	1540	917	0.0029					
						111387-1-D	28	wet room	comp	-	1405	2171	0.0017					
						111387-1-K	91	wet room	comp	8.9	1492	1683	0.0018	1439	28	3%		

(Continued)

(Sheet 2 of 7)

Table D1 (Continued)

						110387-3-H	487	wet room	comp	10.4	711	1402	0.0015	635	87	14%
						110387-3-W	542	wet room	comp	0	681	1484	0.0017			
						110387-3-O	529	wet room	comp	0	514	1239	0.0006			
Batch ID	CF	ben	w/c	SL	G	%air cylinder ID	age	storage	strain	water	qu	K	eu			
111087-1	353	10	1.4	7.25	138	-										
						111087-1-A	3	wet room	gross	13.5	531	415	0.0034	552	19	3%
						111087-1-B	3	wet room	gross	-	547	518	0.0030			
						111087-1-C	3	wet room	comp	-	577	741	0.0028			
						111087-1-P	7	wet room	gross	14.3	764	566	0.0029	790	26	3%
						111087-1-D	7	wet room	comp	-	816	702	0.0024			
						111087-1-I	29	wet room	comp	-	978	1379	0.0017	962	16	2%
						111087-1-J	29	wet room	gross	14.3	967	1070	0.0019			
						111087-1-G	29	wet room	gross	-	941	932	0.0024			
						111087-1-L	94	wet room	comp	14.1	938	1289	0.0018	900	55	6%
						111087-1-K	94	wet room	comp	-	821	466	0.0021			
						111087-1-H	94	wet room	comp	-	939	1453	0.0016			
						111087-1	480	wet room	comp	11.3	997	1552	0.0021	976	22	2%
						111087-1-M	522	wet room	comp	0	984	1671	0.0018			
						111087-1-P	535	wet room	comp	0	946	1687	0.0016			
Batch ID	CF	ben	w/c	SL	G	%air cylinder ID	age	storage	strain	water	qu	K	eu			
060487-1	268	20	2.03	8.25	133	0.6										
						060487-1-A	4	cure box	gross	-	163	60	0.0042	160	3	2%
						060487-1-D	4	cure box	gross	-	158	67	0.0043			
						060487-1-B	33	cure box	neop	12.9	215			214	1	1%
						060487-1-C	33	cure box	neop	-	213					
Batch ID	CF	ben	w/c	SL	G	%air cylinder ID	age	storage	strain	water	qu	K	eu			
060587-1	300	20	2	9.25	130	0.2										
						060587-1-C	7	cure box	gross	-	160	43	0.0053	159	1	1%
						060587-1-A	7	cure box	gross	-	158	29	0.0055			
						060587-1-D	32	wet room	neop	-	176			176		
						060587-1-B	60	cure box	gross	16.5	171	82	0.0042	172	1	1%
						060587-1-P	60	cure box	gross	-	172	82	0.0033			
						060587-1-H	129	wet room	gross	19.3	182	96	0.0040	182		
Batch ID	CF	ben	w/c	SL	G	%air cylinder ID	age	storage	strain	water	qu	K	eu			
061887-1	369	20	1.53	6.75	132	0.7										
						061887-1-G	4	wet room	gross	13.8	366	199	0.0031	367	1	0%
						061887-1-D	4	wet room	gross	-	368	152	0.0032			
						061887-1-H	7	wet room	gross	14	441	257	0.0031	440	9	2%
						061887-1-A	7	wet room	gross	-	428	234	0.0031			
						061887-1-H	7	wet room	gross	-	450	243	0.0032			
						061887-1-B	28	wet room	neop	-	431			401	23	6%
						061887-1-O	28	wet room	neop	13.8	396					
						061887-1-W	28	wet room	neop	-	376					
						061887-1-N	50	wet room	gross	-	533	264	0.0030	540	5	1%
						061887-1-K	50	wet room	gross	12.7	545	420	0.0022			
						061887-1-L	50	wet room	gross	-	542	363	0.0026			
						061887-1	660	wet room	comp	0	528	1096	0.0024	529	15	3%
						061887-1-P	658	wet room	comp	0	512	1058	0.0013			
						061887-1-?	655	wet room	comp	13.4	548	1097	0.0018			
Batch ID	CF	ben	w/c	SL	G	%air cylinder ID	age	storage	strain	water	qu	K	eu			

(Continued)

(Sheet 4 of 7)

Table D1 (Continued)

071487-1	230	20	2.14	6.5	135	0.5	071487-1-B	3	cure box	neop	-	114		112	1	1%	
							071487-1-P	3	wet room	neop	12.2	111					
							071487-1-C	7	cure box	gross	12.3	184	249	0.0021	186	2	1%
							071487-1-O	7	wet room	gross	-	185	104	0.0030			
							071487-1-K	7	wet room	gross	11.7	189	260	0.0024			
							071487-1-H	29	wet room	gross	11.2	265	97	0.0046	257	6	2%
							071487-1-G	29	wet room	gross	-	256	109	0.0040			
							071487-1-A	29	cure box	gross	11	249	125	0.0043			
							071487-1-D	632	wet room	comp	0	239	570	0.0011	261	14	6%
							071487-1-E	632	wet room	comp	0	265	660	0.0014			
							071487-1-F	599	wet room	comp	12.4	261	656	0.0018			
							071487-1-J	632	wet room	comp	0	279	629	0.0013			
Batch ID	CF	ben	w/c	SL	G	hair	cylinder ID	age	storage	strain	water	qu	K	eu			
102687-1	294	20	1.85	8	136	0.5	102687-1-C	7	wet room	comp	19.1	311	529	0.0019	301	9	3%
							102687-1-B	7	wet room	comp	-	302	585	0.0022			
							102687-1-A	7	wet room	gross	-	290	413	0.0038			
							102687-1-I	28	wet room	gross	-	362	234	0.0031	367	6	2%
							102687-1-P	28	wet room	comp	16.4	373	570	0.0020			
							102687-1-G	51	wet room	gross	-	359	423	0.0030	370	8	2%
							102687-1-M	51	wet room	gross	-	373	224	0.0037			
							102687-1-J	51	wet room	gross	16.7	378	279	0.0025			
							102687-1-D	92	wet room	gross	-	360	525	0.0031	369	8	2%
							102687-1-L	92	wet room	gross	15.2	368	264	0.0029			
							102687-1-K	92	wet room	gross	-	379	257	0.0028			
							102687-1-K	495	wet room	comp	12.7	370	566	0.0030	358	10	3%
							102687-1-N	550	wet room	comp	0	343	401	0.0021			
							102687-1-O	537	wet room	comp	0	358	1019	0.0021			
							102687-1-X	537	wet room	comp	0	361	941	0.0021			
Batch ID	CF	ben	w/c	SL	G	hair	cylinder ID	age	storage	strain	water	qu	K	eu			
111387-2	257	20	2.04	7.5	136	-	111387-2-A	4	wet room	gross	-	193	207	0.0042	194	4	2%
							111387-2-C	4	wet room	gross	15.1	199	196	0.0037			
							111387-2-B	4	wet room	gross	-	189	156	0.0048			
							111387-2-H	7	wet room	gross	-	218	267	0.0035	215	3	2%
							111387-2-K	7	wet room	gross	9.5	211	235	0.0034			
							111387-2-F	7	wet room	comp	-	217	315	0.0031			
							111387-2-G	28	wet room	gross	-	260	196	0.0030	256	9	4%
							111387-2-D	28	wet room	gross	-	243	230	0.0028			
							111387-2-J	28	wet room	comp	-	264	559	0.0019			
							111387-2-M	91	wet room	comp	-	263	416	0.0028	260	3	1%
							111387-2-N	91	wet room	comp	15	257	333	0.0019			
							111387-2-I	532	wet room	comp	0	283	528	0.0033	277	6	2%
							111387-2-P	519	wet room	comp	0	271	664	0.0015			
Batch ID	CF	ben	w/c	SL	G	hair	cylinder ID	age	storage	strain	water	qu	K	eu			
061087-1	266	40	2.4	8.75	128	0.2	061087-1-B	5	wet room	gross	-	61	22	0.0070	64	3	5%
							061087-1-K	5	cure box	gross	-	68	5	0.0146			
							061087-1-D	7	wet room	gross	16.7	67	25	0.0366	69	3	4%
							061087-1-G	7	cure box	gross	-	67	35	0.0060			
							061087-1-C	7	cure box	gross	-	73	28	0.0074			
							061087-1-H	56	wet room	gross	16.4	74	26	0.0057	77	3	4%

(Continued)

(Sheet 5 of 7)

Table D1 (Continued)

						061007-1-J	56	cure box	gross	-	80	28	0.0070				
						061007-1-L	124	wet room	gross	19.4	85	31	0.0076	85			
Batch ID	CF	ben	w/c	SL	G	air cylinder ID	age	storage	strain	water	qu	K	eu				
061007-2	446	40	1.56	8.5	125	0.3	061007-2-A	4	wet room	gross	-	125	34	0.0066	126	2	1%
							061007-2-D	4	wet room	gross	21.3	128	36	0.0071			
							061007-2-L	7	wet room	gross	19.6	175	79	0.0088	168	8	5%
							061007-2-P	7	wet room	gross	-	172	44	0.0071			
							061007-2-G	7	wet room	gross	-	156	53	0.0057			
							061007-2-E	28	wet room	neop	-	136			138	7	5%
							061007-2-C	28	wet room	neop	17.5	148					
							061007-2-B	28	wet room	neop	-	130					
							061007-2-J	50	wet room	gross	21.7	192	134	0.0030	200	6	3%
							061007-2-H	50	wet room	gross	-	206	104	0.0043			
							061007-2-I	50	wet room	gross	-	203	116	0.0044			
							061007-2-K	625	wet room	comp	21.7	253	534	0.0025	253		
Batch ID	CF	ben	w/c	SL	G	air cylinder ID	age	storage	strain	water	qu	K	eu				
072107-1	244	40	2.35	7.25	131	0.5	072107-1-A	3	cure box	gross	-	77	37	0.0093	71	4	5%
							072107-1-D	3	wet room	gross	-	69	42	0.0080			
							072107-1-C	3	wet room	gross	14.3	69	31	0.0101			
							072107-1-M	7	cure box	gross	13.3	96	32	0.0084	95	3	3%
							072107-1-O	7	wet room	gross	-	91	32	0.0071			
							072107-1-L	7	wet room	gross	13.9	98	35	0.0070			
							072107-1-B	83	wet room	gross	16.4	127	70	0.0068	127		
							072107-1-N	592	WET ROOM	comp	17.2	139	263	0.0046	144	4	3%
							072107-1-X	625	wet room	comp	0	148	245	0.0062			
Batch ID	CF	ben	w/c	SL	G	air cylinder ID	age	storage	strain	water	qu	K	eu				
061207-1	321	60	2.28	7.75	122	0.8	061207-1-B	3	cure box	gross	20.1	37	18	0.0091	35	3	8%
							061207-1-P	3	wet room	gross	-	32	15	0.0117			
							061207-1-A	7	cure box	gross	22	45	12	0.0098	40	5	12%
							061207-1-J	7	wet room	gross	-	35	11	0.0098			
							061207-1-D	28	cure box	neop	19.8	37			35	1	4%
							061207-1-E	28	wet room	neop	20	35					
							061207-1-KS	28	wet room	neop	-	33					
							061207-1-G	54	wet room	gross	-	50	19	0.0085	50	1	2%
							061207-1-H	54	wet room	gross	20.5	49	16	0.0082			
							061207-1-I	54	wet room	gross	-	51	26	0.0074			
							061207-1-C	122	wet room	gross	28.1	73	20	0.0094	73		
Batch ID	CF	ben	w/c	SL	G	air cylinder ID	age	storage	strain	water	qu	K	eu				
062307-1	323	60	2.95	8	106	1.2	062307-1-C	3	cure box	gross	34.7	22	6	0.0095	20	1	5%
							062307-1-J	3	wet room	gross	33.5	19	6	0.0078			
							062307-1-G	3	wet room	gross	-	20	6	0.0103			
							062307-1-D	28	wet room	gross	-	31	9	0.0073	29	2	6%
							062307-1-K	28	wet room	gross	-	28	7	0.0078			
							062307-1-I	45	wet room	gross	34.8	29	7	0.0090	29	0	1%
							062307-1-W	45	wet room	gross	-	29	6	0.0088			
							062307-1-B	111	wet room	gross	50.1	44	13	0.0100	43	1	3%
							062307-1-A	111	wet room	gross	46.9	41	7	0.0111			

(Continued)

(Sheet 6 of 7)

Table D1 (Concluded)

Batch ID	CF	ben	w/c	SL	G	air	cylinder ID	age	storage	strain water	qu	z	eu			
072787-1	231	60	2.69	6.5	127	0.9	072787-1-B	3	cure box	gross 17.4	25	6	0.0108	25	0	1%
							072787-1-B	3	wet room	gross -	25	7	0.0090			
							072787-1-O	3	wet room	gross 14.8	25	7	0.0088			
							072787-1-I	7	wet room	gross -	25	13	0.0077	26	1	
							072787-1-D	7	cure box	gross 17.9	26	9	0.0084			
							072787-1-W	7	wet room	gross 16.7	28	13	0.0077			
							072787-1-A	77	wet room	gross 22.2	53	13	0.0092	56	3	5%
							072787-1-C	77	wet room	gross 21.1	59	12	0.0096			
							072787-1-J	94	wet room	gross -	52	35	0.0065	49	2	4%
							072787-1-Y	94	wet room	gross 21.2	49	39	0.0053			
							072787-1-M	94	wet room	gross -	48	29	0.0067			
							072787-1-K	586	wet room	comp 21.5	85	147	0.0044	85		

Total Number of Test Groups 100

Number of Test Groups With Only 1 Test 13

Average Standard Deviation Within Test Groups With More Than 1 Test 4% +/- 3%

Number of Test Groups With Standard Deviation >10% 4

Maximum Standard Deviation Within a Test Group 14%

Table D2

Summary of Phase II Unconfined Compression Test Program

EXPLANATION ON TABLE HEADINGS

CF cement factor, pounds of cement+bentonite per cubic yard of concrete
 %BN percent of cement factor, by weight, which is bentonite
 Age curing age, days
 SLUMP wet slump, inches
 W/C ratio of water to cement+bentonite, by weight
 Unit Wt. theoretical unit weight, pounds per cubic foot
 qu ultimate compressive strength, psi
 E Young's modulus, kips (1000 pounds) per square inch (ksi)
 eu strain at qu, %

Test ID	CF	%Ben	Age	SLUMP	W/C	Unit Wt.	Sample 1			Sample 2		
							qu	E	eu	qu	E	eu
							psi.	ksi.	%	psi.	ksi.	%
	pcy		days	inches		pcf						
080288-1	290	0	3	8	1.5	144.6	442	642	0.33	391	975	0.28
091488-1	302	0	3	7 1/2	1.4	146.5	793	-	-	759	1042	0.27
030189-1	299	0	7	7	1.4	145.2	760	1627	0.19	717	1477	0.23
102688-1	295	0	14	8	1.5	143.9	979	1750	0.15	945	1688	0.16
082688-1	304	20	3	8 1/2	1.8	133.4	282	467	0.32	276	446	0.33
080588-1	297	20	3	8	1.9	128.8	295	695	0.38	302	672	0.39
091088-1	302	20	3	8	1.9	139.7	290	446	0.41	297	446	0.44
081088-1	306	20	8	8 1/2	1.8	139.2	375	464	0.26	342	464	0.29
082388-1	289	20	7	8 1/4	1.9	138.8	-	-	-	345	466	0.35
090188-1	299	20	7	8 1/2	1.9	138.1	336	512	0.27	340	519	0.28
111688-1	300	20	14	8	1.9	138.8	408	619	0.33	397	565	0.38
091588-1	305	40	3	8 1/4	2.1	133.2	117	199	0.78	117	215	0.9
090988-1	306	40	3	8	2.1	133.3	127	114	0.78	127	108	0.61
091988-1	305	40	3	8 1/2	2.1	132.9	116	162	0.88	116	137	1.02
101488-1	302	40	3	8 1/4	2.2	134.3	124	179	0.92	121	161	0.7
083188-1	305	40	7	8 1/4	2.1	129.5	146	159	0.67	144	180	0.76
092888-1	296	40	7	8	2.3	133.6	134	241	0.64	128	255	0.73
102888-1	301	40	14	8 1/2	2.2	135.0	152	209	0.66	150	214	0.74
022289-1	308	40	14	7 1/2	2.1	132.9	155	190	0.72	153	223	0.49
100688-1	300	40	14	8	2.2	129.7	157	277	0.73	164	279	0.77

Table D3

Summary of Phase I Brazilian Splitting Tensile Test Program

CF	Cement factor, pounds of cement+bentonite per cubic yard
tben	Bentonite content as percent of cement factor
W/CF	Ratio of water to cement+bentonite, by weight
Tensile strength	From the equation:

$$T = 2P / \pi ld$$

T = splitting tensile strength, psi

P = peak load, lbs.

π = the number pi

l = cylinder length, inches

d = cylinder diameter, inches

Slump = 8 inches

test ID	tben	age	CF	W/CF	length	diameter	Load	tensile strength
		days	lbs/cu. yd.		in.	in.	lbs.	psi
053088-1-C	0	3	261	1.56	12.136	6.016	8850	77
053088-1-B	0	3	261	1.56	12.034	6.039	9050	79
053088-1-A	0	3	261	1.56	12.074	6.022	9775	86
053088-1-M	0	7	261	1.56	12.153	6.040	14550	126
053088-1-K	0	7	261	1.56	11.987	6.048	14800	130
053088-1-J	0	7	261	1.56	11.987	6.037	16600	146
053088-1-G	0	28	261	1.56	12.020	6.000	17850	158
053088-1-L	0	28	261	1.56	12.120	6.051	17100	148
053088-1-P	0	28	261	1.56	11.980	6.051	19150	168
053088-1-H	0	92	261	1.56	12.078	6.031	17700	155
053088-1-W	0	92	261	1.56	12.094	6.047	17200	150
053088-1-I	0	92	261	1.56	12.016	6.000	17500	155
060288-1-B	0	7	346	1.18	12.104	6.029	23950	209
060288-1-A	0	7	346	1.18	11.973	6.034	21650	191
060288-1-F	0	7	346	1.18	11.903	6.040	19950	177
060288-1-D	0	28	346	1.18	12.094	6.022	26200	229
060288-1-J	0	28	346	1.18	11.938	6.042	26800	237
060288-1-M	0	28	346	1.18	11.969	6.034	23750	209
060288-2-J	20	7	255	2.22	12.093	6.042	5475	48
060288-2-I	20	7	255	2.22	11.835	6.062	5125	45
060288-2-M	20	7	255	2.22	12.094	6.058	4650	40
060288-2-D	20	28	255	2.22	12.188	6.037	6050	52
060288-2-R	20	28	255	2.22	12.250	6.064	5625	48
060288-2-L	20	28	255	2.22	12.047	6.051	6725	59
060288-2-B	20	92	255	2.22	12.156	6.036	5400	47
060288-2-C	20	92	255	2.22	12.156	6.052	6275	54
060288-2-G	20	92	255	2.22	12.125	6.063	6300	55
061988-1-A	20	3	362	1.44	12.036	6.076	9600	84
061988-1-B	20	3	362	1.44	12.073	6.057	7450	65
061988-1-F	20	7	362	1.44	12.170	6.045	11250	97
061988-1-L	20	7	362	1.44	12.120	6.044	11575	101

(Continued)

Table D3 (Concluded)

061988-1-R	20	7	362	1.44	12.100	6.060	13250	115
061988-1-K	20	30	362	1.44	12.050	6.042	13875	121
061988-1-J	20	30	362	1.44	12.080	6.056	14900	130
061988-1-D	20	30	362	1.44	12.000	6.052	13375	117
062288-2-A	60	3	330	2.34	12.136	6.046	430	4
062288-2-B	60	3	330	2.34	12.083	6.049	590	5
062288-2-C	60	3	330	2.34	11.996	6.051	625	5
062288-2-H	60	8	330	2.34	12.156	6.046	670	6
062288-2-J	60	8	330	2.34	12.125	6.054	800	7
062288-2-P	60	28	330	2.34	11.940	6.047	750	7
062288-2-K	60	28	330	2.34	12.125	6.048	755	7
062288-2-D	60	28	330	2.34	12.000	6.048	810	7
062288-2-X	60	90	330	2.34	12.219	6.042	1020	9
062288-2-J	60	90	330	2.34	12.094	6.047	900	8

Table D4

Summary of Phase II Brazilian Splitting Tensile Test Results

EXPLANATION ON TABLE HEADINGS

CF cement factor, pounds of cement+bentonite per cubic yard of concrete
 %BEN percent of cement factor, by weight, which is bentonite
 Age curing age, days
 SLUMP wet slump, inches
 W/C ratio of water to cement+bentonite, by weight
 Unit Wt. theoretical unit weight, pounds per cubic foot
 T splitting tensile strength, psi
 T/US splitting tensile strength divided by average unconfined shear strength ($qu/2$)
 from same batch and age

Test ID	CF	%Ben	Age	SLUMP	W/C	Unit Wt.	T	T/US
	pcy		days	inches		pcf	psi.	
080288-1	290	0	3	8	1.5	144.6	56	0.27
091488-1	302	0	3	7 1/2	1.4	146.5	123	0.32
030189-1	299	0	7	7	1.4	145.2	88	0.24
102688-1	295	0	14	8	1.5	143.9	127	0.26
082688-1	304	20	3	8 1/2	1.8	133.4	42	0.30
080588-1	297	20	3	8	1.9	128.8	39	0.26
091088-1	302	20	3	8	1.9	139.7	35	0.24
081088-1	306	20	8	8 1/2	1.8	139.2	55	0.31
082388-1	289	20	7	8 1/4	1.9	138.8	46	0.26
090188-1	299	20	7	8 1/2	1.9	138.1	46	0.28
111688-1	300	20	14	8	1.9	138.8	45	0.22
091588-1	305	40	3	8 1/4	2.1	133.2	13	0.23
090988-1	306	40	3	8	2.1	133.3	19	0.30
091988-1	305	40	3	8 1/2	2.1	132.9	14	0.25
101488-1	302	40	3	8 1/4	2.2	134.3	14	0.23
083188-1	305	40	7	8 1/4	2.1	129.5	17	0.23
092888-1	296	40	7	8	2.3	133.6	20	0.31
102888-1	301	40	14	8 1/2	2.2	135.0	17	0.22
022289-1	308	40	14	7 1/2	2.1	132.9	19	0.24
100688-1	300	40	14	8	2.2	129.7	22	0.27

Table D5

Summary of Flexural Beam Test Program

CF Cement factor, lbs of cement+bentointe per cubic yard of concrete
 %BEN Bentonite content as a percent of cement factor
 W/C Ratio of water to cement+bentonite, by weight
 Modulus of Rupture:

$$R=3Pl/2bd^2$$

P= peak load, pounds

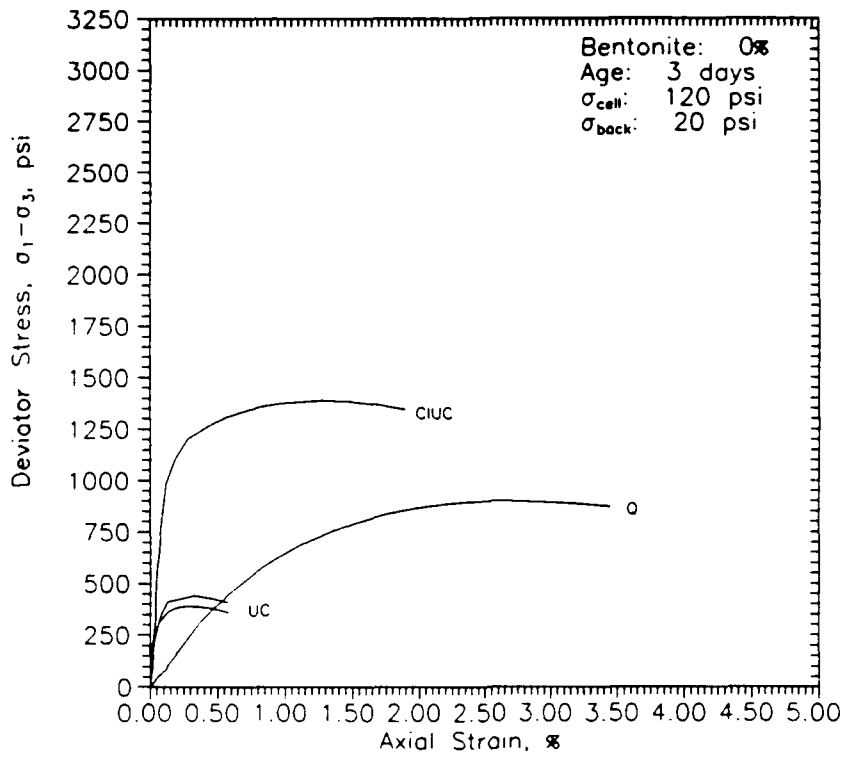
l= length of beam, inches

b= width of beam at point of rupture, inches (average 3 measurements)

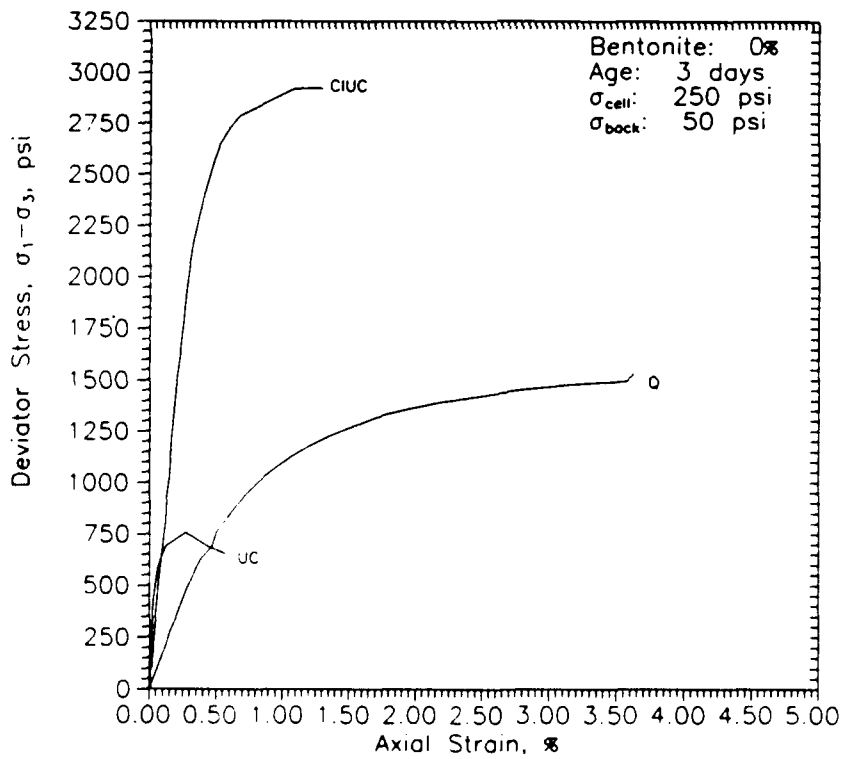
d= depth of beam at point of rupture, inches (average 3 measurements)

Batch ID	BEN %	CF pcy	W/C	Age days	Average		Length in.	Load at Modulus of	
					Width in.	Depth in.		Failure lbs.	Rupture psi
060288-1	0	346	1.18	28	6.18	6.06	18.0	3100	369
053088-1	0	261	1.56	28	6.09	6.00	18.0	2850	351
061988-1	20	362	1.44	32	6.02	6.04	18.0	2175	267
060288-2	20	255	2.22	28	6.08	6.15	18.0	1005	118
062288-1	60	330	2.34	29	5.99	6.06	18.0	235	29
060288-2	60	246	2.62	29	6.00	6.02	18.0	185	23

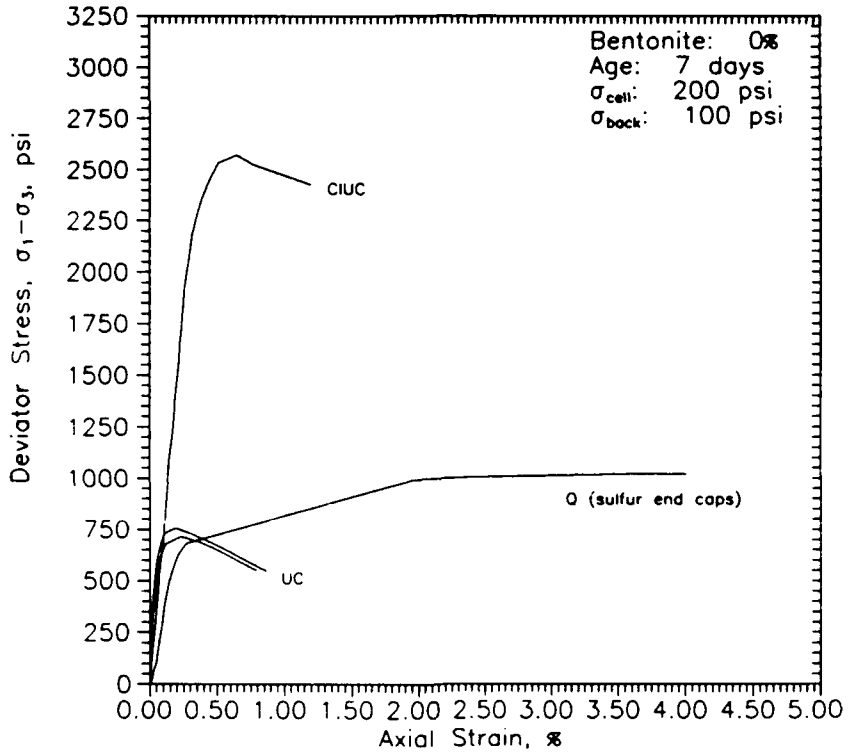
APPENDIX E: PHASE II CIUC, Q, AND UC STRESS-STRAIN CURVES BY BATCH



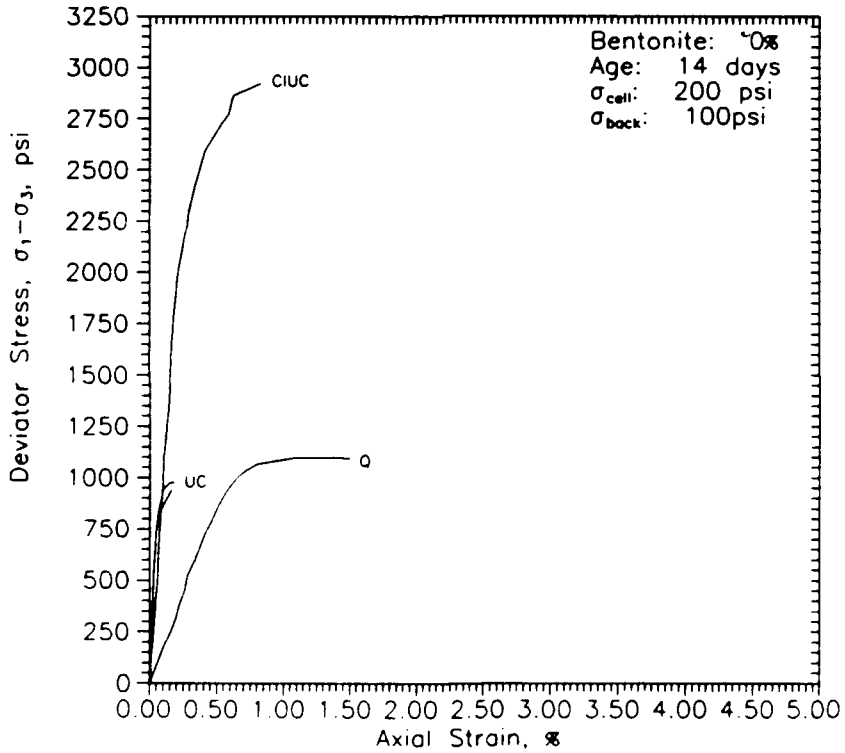
Deviator Stress vs. Axial Strain
 Batch: 080288-1



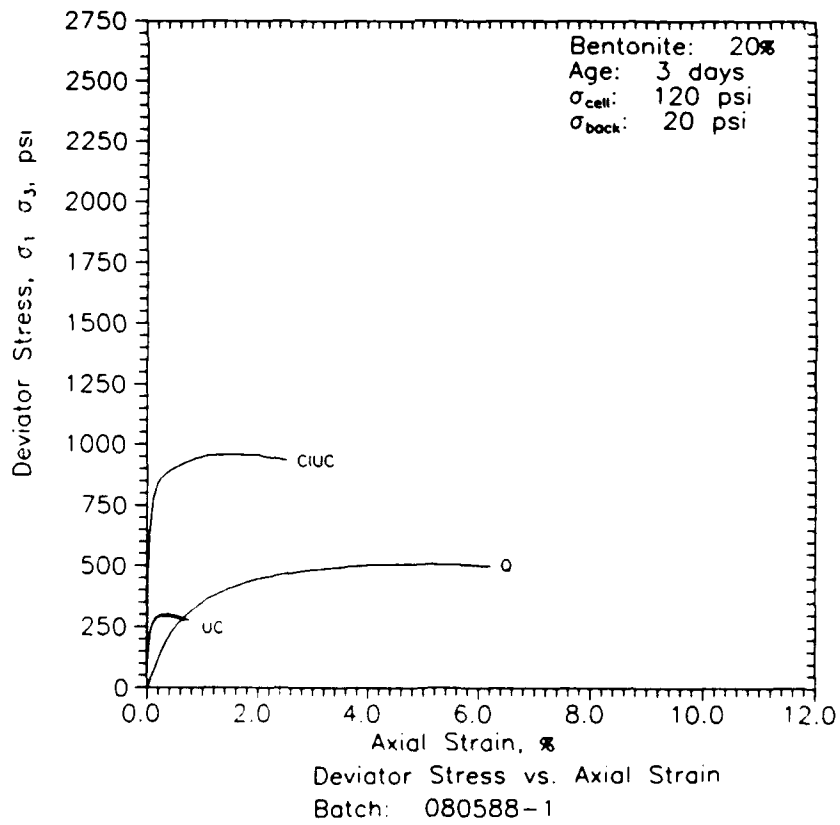
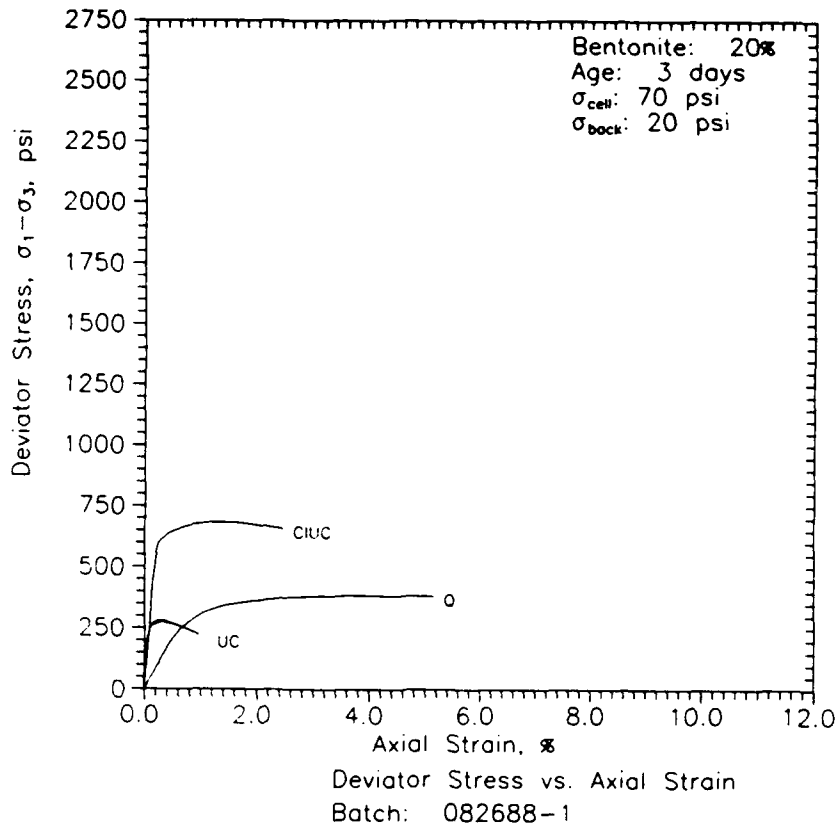
Deviator Stress vs. Axial Strain
 Batch: 091488-1

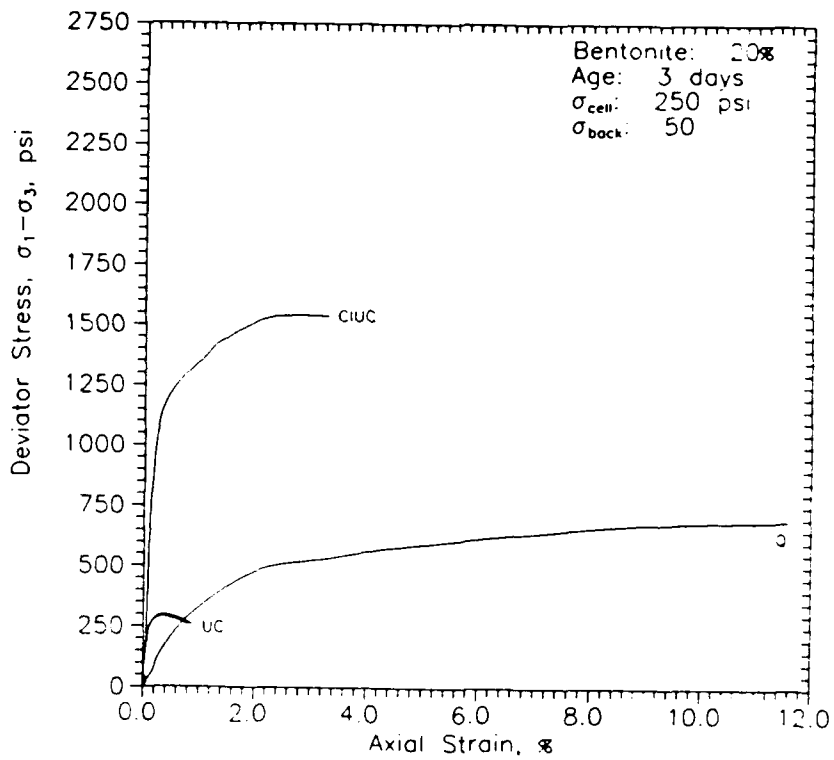


Deviator Stress vs. Axial Strain
 Batch: 030189-1

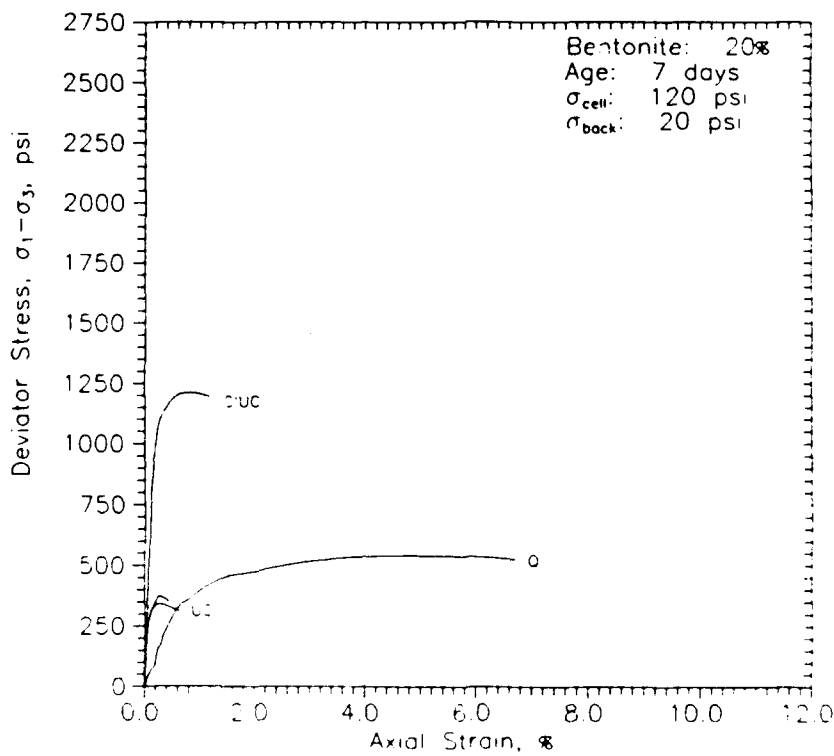


Deviator Stress vs. Axial Strain
 Batch: 102688-1

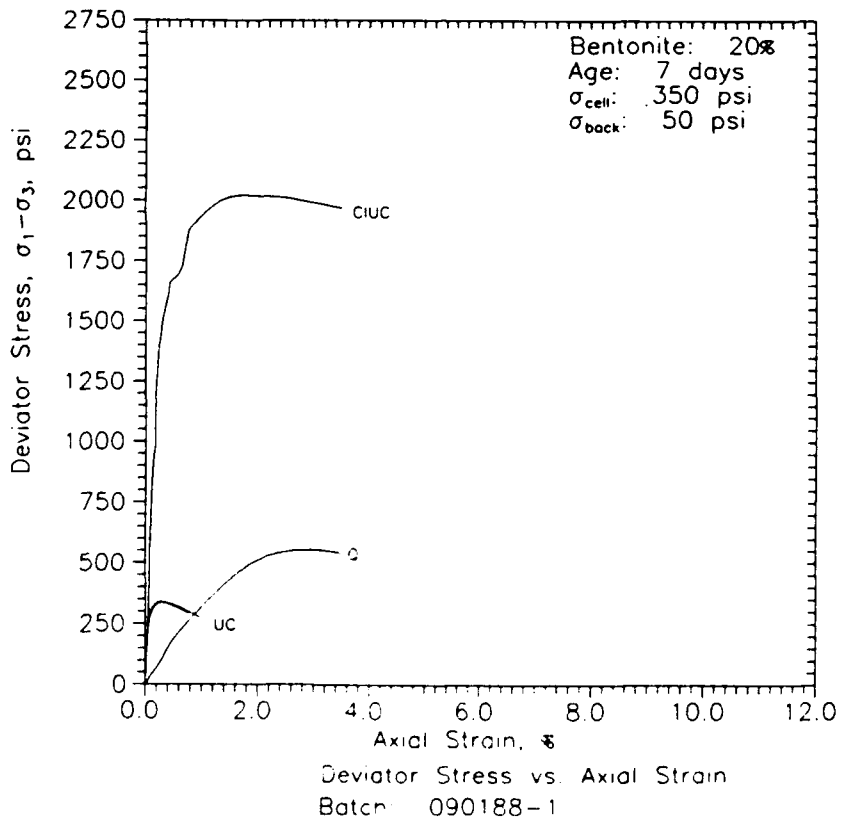
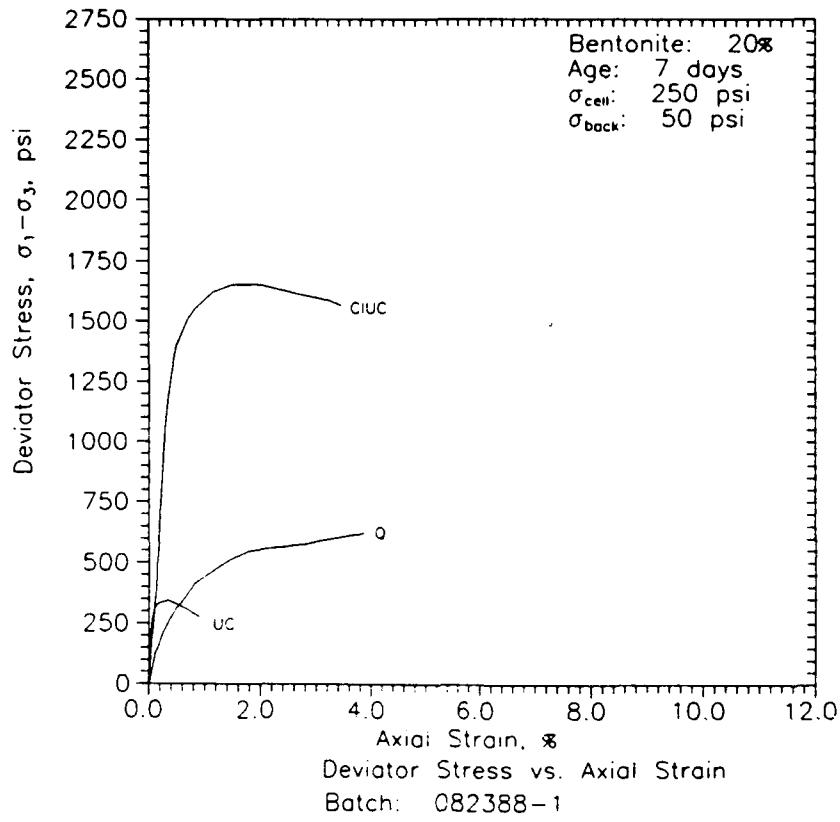


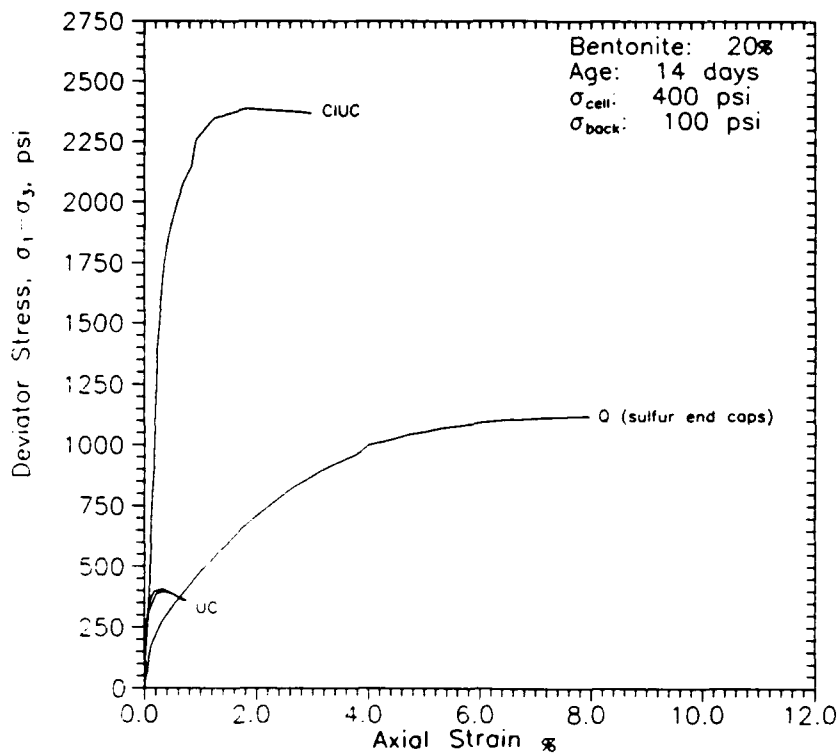


Deviator Stress vs. Axial Strain
Batch: 091088-1

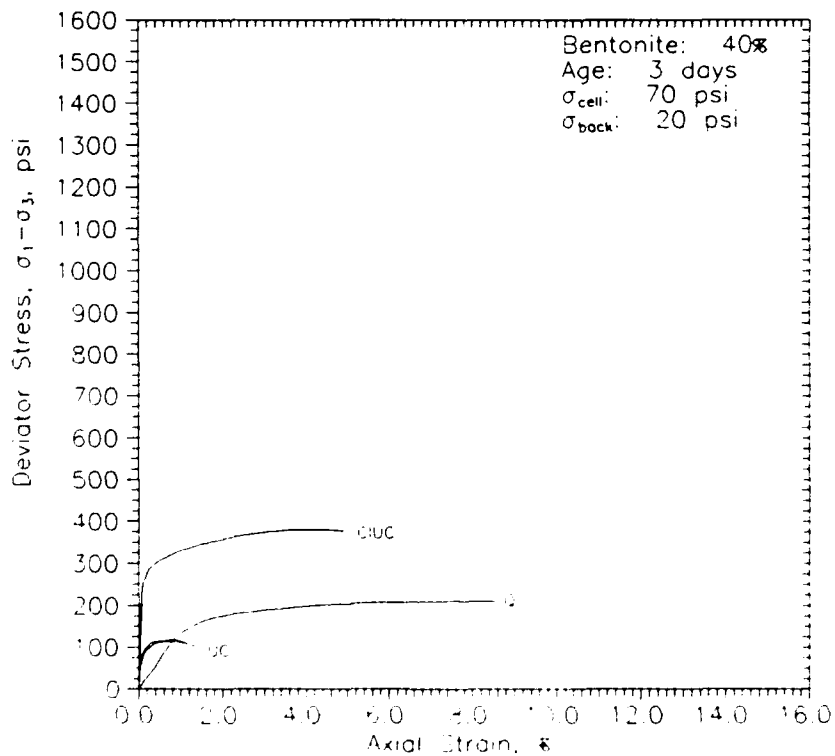


Deviator Stress vs. Axial Strain
Batch: 081088-1

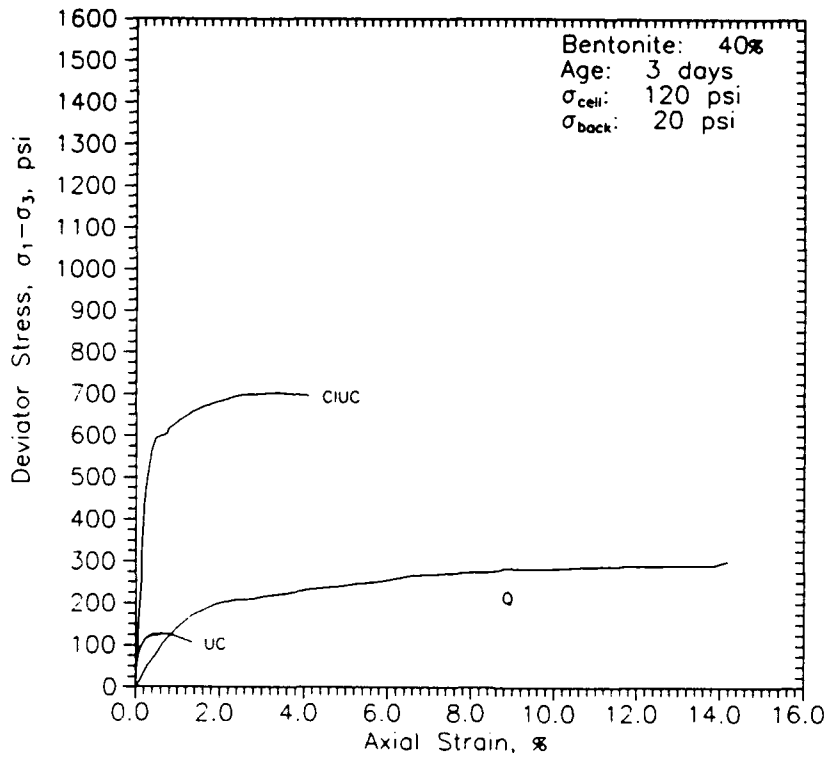




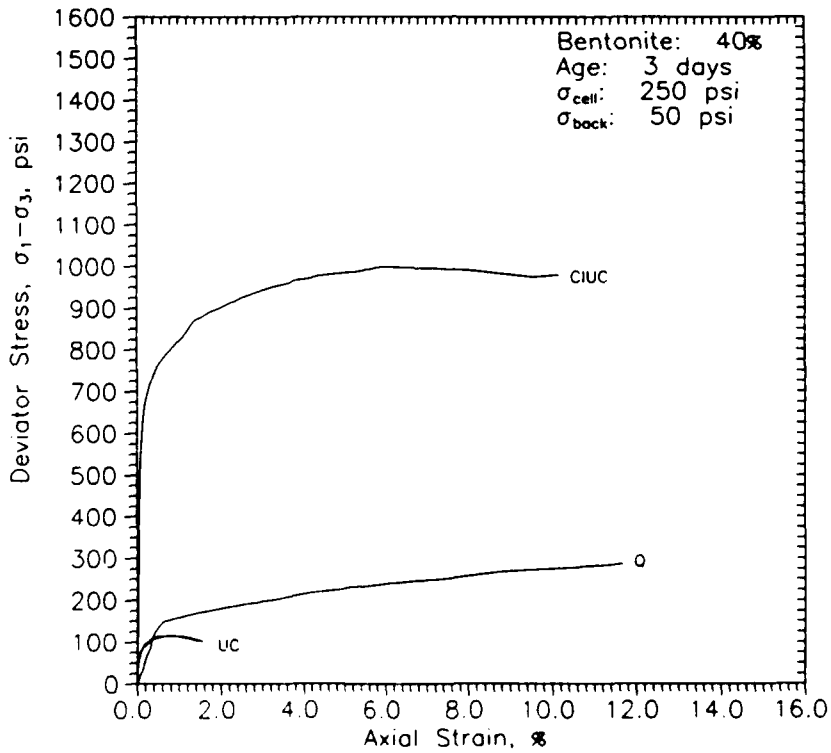
Deviator Stress vs. Axial Strain
 Batch: 111688-1



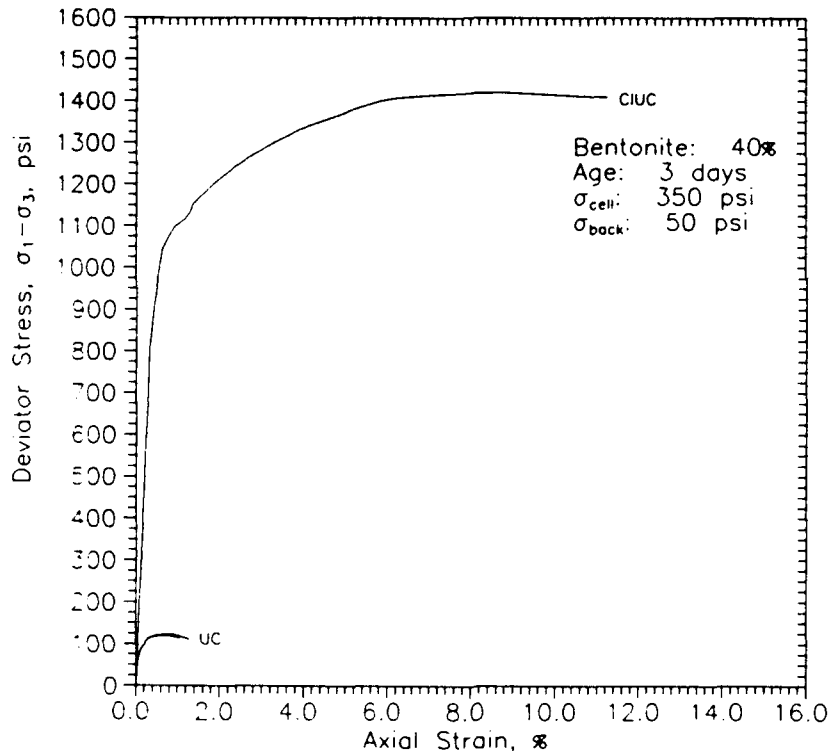
Deviator Stress vs. Axial Strain
 Batch: 091588-1



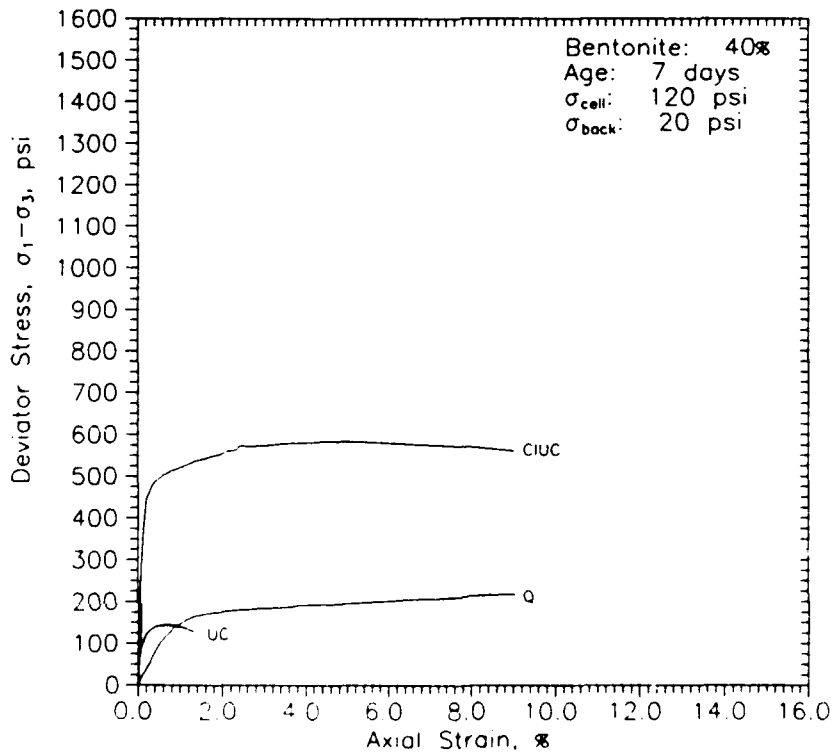
Deviator Stress vs. Axial Strain
Batch: 090988-1



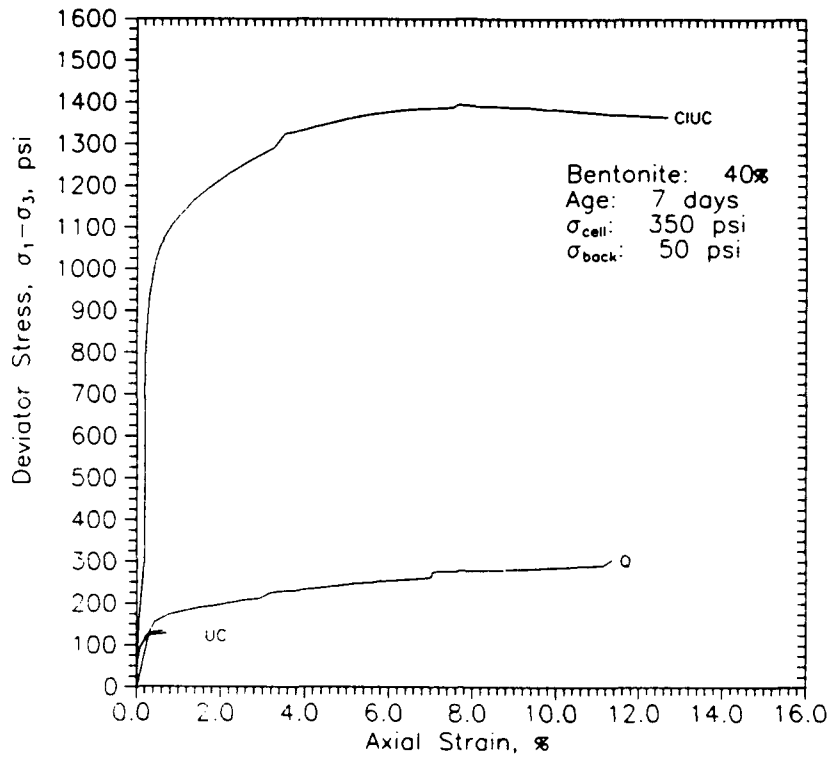
Deviator Stress vs. Axial Strain
Batch: 091988-1



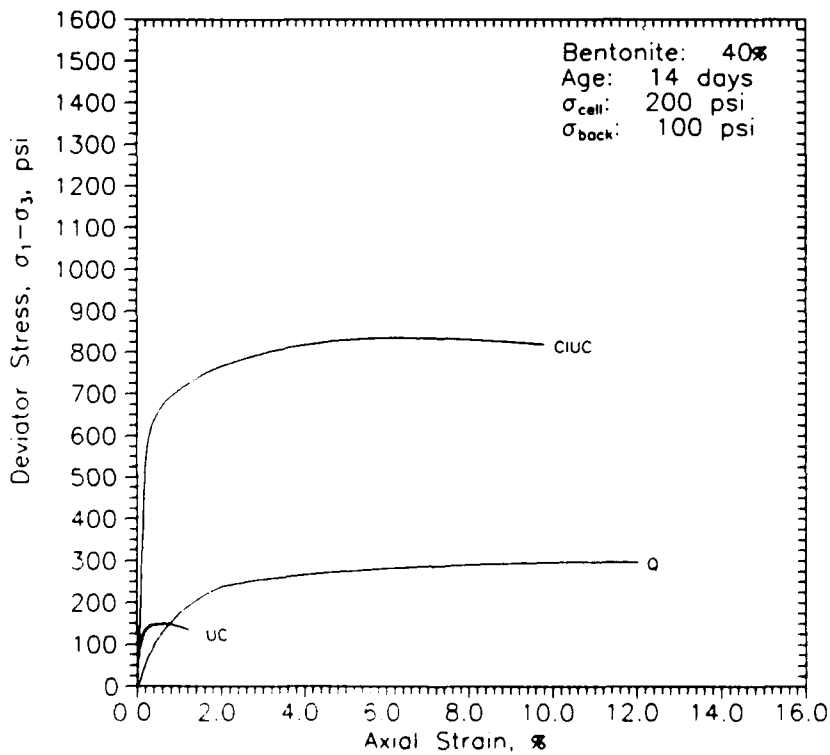
Deviator Stress vs. Axial Strain
Batch: 101488-1



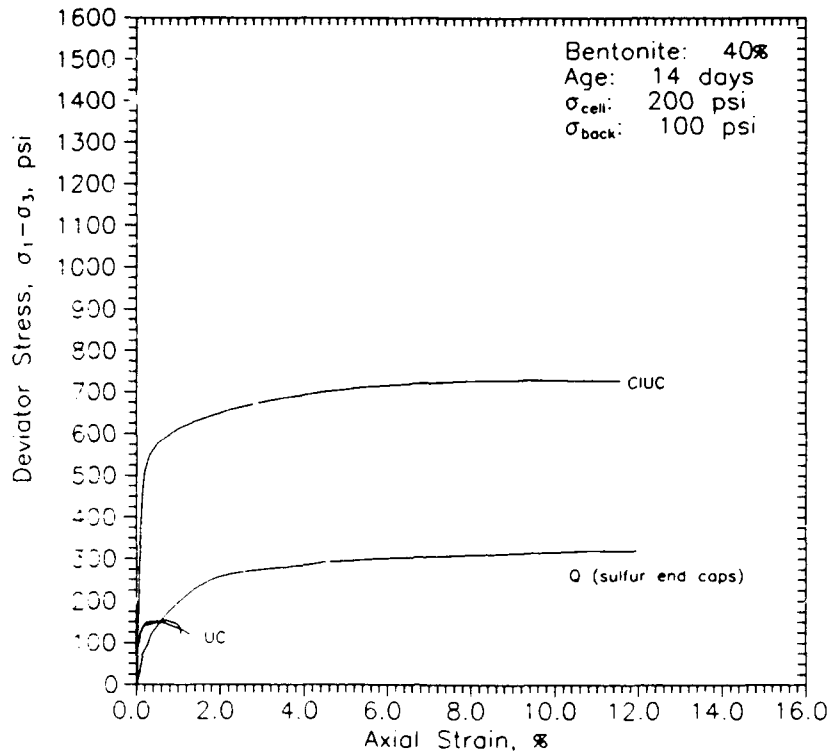
Deviator Stress vs. Axial Strain
Batch 083188-1



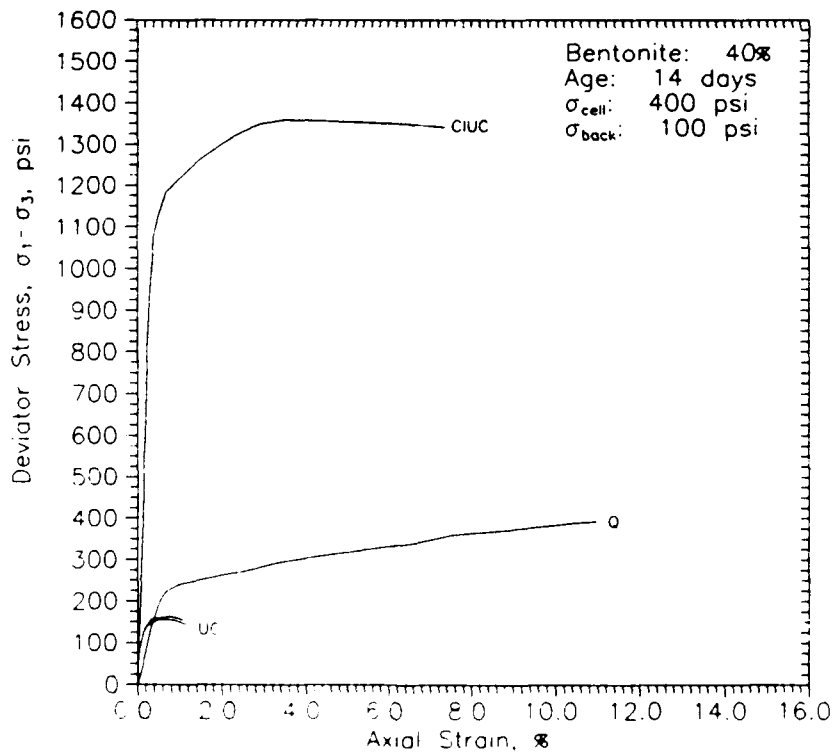
Deviator Stress vs. Axial Strain
 Batch: 092888-1



Deviator Stress vs. Axial Strain
 Batch: 102888-1



Deviator Stress vs. Axial Strain
 Batch: 022289-1



Deviator Stress vs. Axial Strain
 Batch: 100688-1

APPENDIX F: SUMMARY TABLES OF PERMEABILITY TESTS

(Project: Plastic Concrete Research
Waterways Experiment Station)

Batch ID: 080288-1
 Cement Factor: 317 lbs./cu.yd.
 Bentonite: 0 %
 Fabrication Da 8/2/88

Specimen Dimensions:
 Height, ft.: 0.96
 Area, sq. cm.: 176.4

Date	Time	Elapsed Time sec.	Cell Press. psi.	Gage Press. Ped. psi.	Gage Press. Top Cap psi.	Diff. Press. psi.	Head loss across sample ft	Grad. across sample	Flow thru sample ml.	Perm. cm/sec
8/3/88	15:54	0	118	19.9	10.1	9.8	22.6	23.4	0.0	
8/3/88	16:04	600	119	19.9	10.1	9.8	22.6	23.4	3.9	1.6E-06
8/3/88	16:16	1320	119	19.9	10.1	9.8	22.6	23.4	3.4	1.2E-06
8/3/88	16:39	2700	119	19.9	10.1	9.8	22.6	23.4	5.4	9.5E-07
8/3/88	17:18	5040	119	19.9	10.1	9.8	22.6	23.4	7.9	8.2E-07
8/4/88	14:53	0	119	20	10	9.8	22.5	23.4	0.0	
8/4/88	15:28	2100	119	20	10	9.6	22.2	23.0	1.8	2.1E-07
8/4/88	16:06	4380	119	20	10	9.5	22.0	22.8	2.1	2.3E-07
8/4/88	16:38	6300	119	19.9	9.9	9.5	21.9	22.7	1.6	2.0E-07
8/4/88	17:01	7680	119	20	9.9	9.5	21.9	22.7	1.1	1.9E-07
8/4/88	18:22	12540	119	19.9	9.9	9.4	21.6	22.4	3.4	1.7E-07
8/5/88	13:19	0	119	20	10	9.9	23.0	23.8	0.0	
8/5/88	15:06	6420	120	19.9	9.8	10.0	23.0	23.8	1.6	5.7E-08

Batch ID: 091488-1
 Cement Factor: 328 lbs./cu.yd.
 Bentonite: 0 %
 Fabrication Dat 9/14/88
 In Pipette #: 5
 Out Pipette #: 6

Specimen Dimensions:
 Height, ft.: 0.98
 Area, sq. cm.: 174.5

Date	Time	Elapsed Time sec.	Cell Press. psi.	Gage Press. Ped. psi.	Gage Press. Top Cap psi.	Diff. Press. psi.	Head loss across sample ft	Grad. across sample	Flow thru sample ml.	Perm. cm/sec
9/16/88	11:34	0	251	50	25	24	56.3	57.1	0.0	
9/16/88	15:50	15360	250	50	25	25	57.7	58.6	0.8	5.1E-09
9/16/88	19:00	26760	250	50	25	25	57.7	58.6	0.6	5.2E-09
9/16/88	23:00	41160	250	50	25	25	57.7	58.6	1.0	6.8E-09
9/17/88	8:20	74760	250	50	25	25	57.7	58.6	1.6	4.7E-09
9/17/88	16:59	105900	250	50	25	25	57.7	58.6	1.0	3.1E-09
9/17/88	17:05	106260	245	50	25	23	54.1	54.9	0.2	5.8E-08

Batch ID: 030189-1
 Cement Factor: 325 lbs./cu.yd.
 Bentonite: 0 %
 Fabrica. Date: 3/1/89
 In Pipette #: 5
 Out Pipette #: 6

Specimen Dimensions:
 Height, ft.: 0.95
 Area, sq. cm.: 183.6

Date	Time	Elapsed Time sec.	Cell Press. psi.	Gage Press. Ped. psi.	Gage Press. Top Cap psi.	Diff. Press. psi.	Head loss across sample ft	Grad. across sample	Flow thru sample ml.	Perm. cm/sec
3/4/89	11:45	0	198	100	50	49.5	114.2	120.4	0.0	
3/4/89	16:30	17100	200	99.7	49.9	48.8	112.5	118.6	4.8	1.3E-08
3/5/89	21:00	0	204	100	50	49.8	114.9	121.1	0.0	
3/6/89	17:55	75300	203	100.3	50.2	49.1	113.3	119.4	12.6	7.6E-09
3/6/89	17:58	0	203	100.3	50.2	49.1	113.3	119.4	0.5	
3/7/89	8:55	53820	202	100.5	50.4	49.1	113.2	119.3	6.6	5.6E-09
3/7/89	21:07	97740	205	100.4	50.4	49.0	113.2	119.3	4.1	4.2E-09
3/8/89	8:09	137460	203	100.5	50.4	48.9	112.8	118.9	3.8	4.4E-09

Batch ID: 102688-1
 Cement Factor: 317 lbs./cu.yd.
 Bentonite: 0 %
 Fabrica. Date: 10/26/88

Specimen Dimensions:
 Height, ft.: 1.01
 Area, sq. cm.: 173.2

Date	Time	Elapsed Time sec.	Cell Press. psi.	Gage Press. Ped. psi.	Gage Press. Top Cap psi.	Diff. Press. psi.	Head loss across sample ft	Grad. across sample	Flow thru sample ml.	Perm. cm/sec
11/2/88	16:20	0	201	100	50	50	114.6	113.8	0.0	
11/3/88	10:30	65400	200	100	50	50	115.3	114.6	2.2	1.7E-09
11/4/88	14:54	167640	201	100	50	50	115.8	115.0	3.1	1.5E-09
11/6/88	15:03	340980	203	100	50	50	116.2	115.4	4.9	1.4E-09

Batch ID: 080888-1
 Cement Factor: 313 lbs./cu.yd.
 Bentonite: 20 %
 Fabrication Dat 8/5/88

Specimen Dimensions:
 Height, ft.: 0.98
 Area, sq. cm.: 183.1

Date	Time	Elapsed Time sec.	Cell Press. psi.	Gage Press. Ped. psi.	Gage Press. Top Cap psi.	Diff. Press. psi.	Head loss across sample ft	Grad. across sample	Flow thru sample ml.	Perm. cm/sec
8/6/88	6:01	0	120	20	10	9.5	21.8	22.3	0.0	
8/6/88	6:21	1200	120	20.1	10	9.5	21.9	22.4	0.1	2.0E-08
8/6/88	6:40	2340	120	20.1	10	9.5	21.9	22.4	0.1	2.1E-08
8/8/88	14:02	0	120	40	10	29.7	68.6	70.1	0.0	
8/8/88	17:27	12300	120	39.8	10	29.6	68.4	69.9	1.1	7.0E-09

Batch ID: 091088-1
 Cement Factor: 348 lbs./cu.yd.
 Bentonite: 20 %
 Fabrica. Date: 9/10/88

Specimen Dimensions:
 Height, ft.: 0.96
 Area, sq. cm.: 167.8

Date	Time	Elapsed Time sec.	Cell Press. psi.	Gage Press. Ped. psi.	Gage Press. Top Cap psi.	Diff. Press. psi.	Head loss across sample ft	Grad. across sample	Flow thru sample ml.	Perm. cm/sec
9/12/88	11:52	0	251	50	25	24.2	55.8	57.9	0.0	
9/12/88	14:27	9300	252	50	25	23.7	54.7	56.8	1.2	1.4E-08
9/12/88	15:32	13200	252	50	25	23.6	54.4	56.4	0.4	1.1E-08
9/12/88	23:41	42540	253	49.9	25	24.3	56.1	58.1	2.2	7.5E-09
9/13/88	10:08	80160	252	50	25	23.3	53.7	55.7	2.3	6.4E-09
9/13/88	20:15	116580	249	50	25	23.3	53.9	55.8	1.7	5.0E-09

Batch ID: 081088-1
 Cement Factor: 351 lbs./cu.yd.
 Bentonite: 20 %
 Fabrication Dat 8/10/88

Specimen Dimensions:
 Height, ft.: 0.98
 Area, sq. cm.: 169.8

Date	Time	Elapsed Time sec.	Cell Press. psi.	Gage Press. Ped. psi.	Gage Press. Top Cap psi.	Diff. Press. psi.	Head loss across sample ft	Grad. across sample	Flow thru sample ml.	Perm. cm/sec
8/12/88	13:30	0	119	20.2	9.8	11.0	25.5	25.9	0.0	
8/12/88	14:45	4500	119	20.2	9.8	11.1	25.7	26.1	0.1	7.5E-09
8/12/88	22:32	32520	119	20.1	9.8	11.0	25.5	25.9	1.5	1.2E-08
8/13/88	19:56	109560	119	20	9.6	11.0	25.4	25.8	2.8	8.3E-09
8/15/88	00:59	214140	119	20	9.6	11.0	25.3	25.8	1.7	3.7E-09

Batch ID: 082388-1
 Cement Factor: 340 lbs./cu.yd.
 Bentonite: 20 %
 Fabrication Dat 8/23/88

Specimen Dimensions:
 Height, ft.: 0.96
 Area, sq. cm.: 164.8

Date	Time	Elapsed Time sec.	Cell Press. psi.	Gage Press. Ped. psi.	Gage Press. Top Cap psi.	Diff. Press. psi.	Head loss across sample ft	Grad. across sample	Flow thru sample ml.	Perm. cm/sec
8/25/88	12:16	0	249	50.1	30	19.1	44.0	46.0	0.0	
8/25/88	22:20	36240	248	50	30	19.0	43.8	45.8	3.3	1.2E-08
8/26/88	10:31	80100	249	50	29.9	19.0	43.8	45.8	3.0	9.1E-09
8/26/88	12:13	86220	249	49.9	20	28.9	66.7	69.7	0.6	8.5E-09
8/26/88	16:49	102780	249	49.7	20	29.2	67.4	70.5	1.9	9.9E-09
8/26/88	20:20	115440	250	49.7	19.9	28.4	65.6	68.6	7.1	
8/27/88	19:16	198000	250	49.9	20	28.2	65.1	68.1	4.4	4.7E-09
8/28/88	18:35	281940	250	49.8	20	28.3	65.3	68.3	3.4	3.6E-09
8/29/88	16:43	361620	250	49.7	19.8	29.9	69.0	72.2	2.4	2.6E-09
8/30/88	10:30	425640	250	50	20	28.4	65.4	68.4	1.8	2.5E-09

Batch ID: 090988-1
 Cement Factor: 365 lbs./cu.yd.
 Bentonite: 40 %
 Fabrica. Date: 9/9/88

Specimen Dimensions:
 Height, ft.: 0.95
 Area, sq. cm.: 165.1

Date	Time	Elapsed Time sec.	Cell Press. psi.	Gage Press. Ped. psi.	Gage Press. Top Cap psi.	Diff. Press. psi.	Head loss across sample ft	Grad. across sample	Flow thru sample ml.	Perm. cm/sec
9/11/88	10:25	0	121	19.9	10	9.7	22.4	23.6	0.0	
9/11/88	14:26	14460	122	19.9	9.9	9.7	22.5	23.6	0.8	1.3E-08
9/11/88	15:40	18900	120	20	9.9	10.1	23.3	24.5	0.3	1.7E-08
9/11/88	15:45	0	120	20	10	10.0	23.1	24.3	0.0	
9/11/88	20:13	16080	120	20	10	10.0	23.1	24.3	0.8	1.2E-08

Batch ID: 101488-1
 Cement Factor: 370 lbs./cu.yd.
 Bentonite: 40 %
 Fabrica. Date: 10/14/88

Specimen Dimensions:
 Height, ft.: 0.94
 Area, sq. cm.: 165.0

Date	Time	Elapsed Time sec.	Cell Press. psi.	Gage Press. Ped. psi.	Gage Press. Top Cap psi.	Diff. Press. psi.	Head loss across sample ft	Grad. across sample	Flow thru sample ml.	Perm. cm/sec
10/16/88	15:59	0	350	50	20	31.0	71.5	75.7	0.0	
10/16/88	16:05	360	350	50	20	30.0	69.2	73.3	0.2	3.4E-08
10/17/88	11:42	70980	354	50	20	30.8	71.1	75.3	12.5	1.4E-08
10/17/88	17:18	91140	354	50	20	30.7	70.9	75.1	2.9	1.2E-08

Batch ID: 092888-1
 Cement Factor: 364 lbs./cu.yd.
 Bentonite: 40 %
 Fabrica. Date: 9/28/88

Specimen Dimensions:
 Height, ft.: 0.95
 Area, sq. cm.: 164.1

Date	Time	Elapsed Time sec.	Cell Press. psi.	Gage Press. Ped. psi.	Gage Press. Top Cap psi.	Diff. Press. psi.	Head loss across sample ft	Grad. across sample	Flow thru sample ml.	Perm. cm/sec
10/1/88	20:57	0	340	50	24.9	25.1	57.9	61.1	0.0	
10/3/88	17:18	159660	340	50	24.9	25.1	57.9	61.1	2.2	1.4E-09
10/3/88	17:37	0	349	50	25	25.0	57.7	60.9	0.0	
10/4/88	10:07	59400	350	50	25.1	23.5	54.2	57.2	2.3	4.1E-09
10/5/88	13:17	318000	350	49.8	25	23.4	54.1	57.0	2.3	9.5E-10

Batch ID: 102888
 Cement Factor: 357 lbs./cu.yd.
 Bentonite: 40 %
 Fabrica. Date: 10/28/88

Specimen Dimensions:
 Height, ft.: 0.96
 Area, sq. cm.: 168.9

Date	Time	Elapsed Time sec.	Cell Press. psi.	Gage Press. Ped. psi.	Gage Press. Top Cap psi.	Diff. Press. psi.	Head loss across sample ft	Grad. across sample	Flow thru sample ml.	Perm. cm/sec
11/2/88	16:08	0	199	100	50	50.0	115.3	119.9	0.0	
11/3/88	10:30	66120	200	100	50	50.0	115.4	120.0	14.1	1.1E-08
11/4/88	14:53	168300	199	100	50	49.9	115.2	119.8	20.5	9.9E-09
11/6/88	14:40	340320	203	100	50	50.3	116.1	120.7	32.8	9.3E-09
11/6/88	15:00	0	200	100	50	49.4	114.0	118.6	0.0	
11/7/88	14:28	84480	201	99.4	50.5	50.0	115.4	119.9	16.0	9.4E-09
11/7/88	14:54	0	200	100	50	50.6	116.8	121.4	0.0	
11/7/88	18:38	13440	200	100	50	50.0	115.4	120.0	3.4	1.2E-08
11/8/88	9:07	65580	200	100	50	50.0	115.4	120.0	10.0	9.5E-09
11/8/88	16:55	93660	200	100	50	50.0	115.4	120.0	6.0	1.1E-08